NTNU – Trondheim
Norwegian University of
Science and Technology

Adapting the Design Procedures of Heat Pump Systems to nZEB

Mikkel Ytterhus

Norwegian University of Science and Technology
Department of Energy and Process Engineering

NTNU

Norwegian University
of Science and Technology

Department of Energy
and Process Engineering

EPT-M-2015-104

MASTER THESIS

for

Mikkel Ytterhus

Spring 2015

Adapting the design procedures of heat pump systems to nZEB

Tilpasning av design prosedyrer for varmepumpesystemer til nZEB

Background

The goal for the project work is to analyse the change in design procedures of heat pump systems when the building energy performance is progressively improved, i.e. starting from the standard performance of today, to the passive house standard and, finally, to the nearly-zero energy (nZEB) level. This is done using a simple modelling approach implemented in Matlab/Simulink using the Carnot blockset combined with Modelica.

This proposal is the continuation of a Master thesis of Thomas Murer during fall 2014 as well as of the project work of Mikkel Ytterhus. The present contribution will further improve the system modelling and the analysis of results. The project work is connected to the NTNU-SINTEF Zero Emission Building (ZEB) activity on development of an early-stage design tool for the selection of renewable thermal energy supply systems for nZEB (nearly Zero Emission Buildings) as well as the IEA HPP Annex 40 on heat pumps for nZEB.

Objectives:
- Improvement of the existing modelling procedure:
    1. Critical analysis of the *borehole model* based on the previous project work
    2. Improvement of the heat pump model to account for *part load operation*
- Sensitivity analysis to determine how the model quality and the uncertainty of inputs influence the design process.

The following tasks are to be considered:
1. **Critical analysis** of the previous Master thesis of Thomas Murer (from fall 2014).
2. **Improvement** of the decision tool as regards the model quality and simulation time.
3. Perform **sensitivity analysis** to determine the best trade-off between the modelling accuracy, the computational time and the uncertainty on inputs in the context of a heat pump design.

-- ” --

Within 14 days of receiving the written text on the master thesis, the candidate shall submit a research plan for his project to the department.

When the thesis is evaluated, emphasis is put on processing of the results, and that they are presented in tabular and/or graphic form in a clear manner, and that they are analyzed carefully.

The thesis should be formulated as a research report with summary both in English and Norwegian, conclusion, literature references, table of contents etc. During the preparation of the text, the candidate should make an effort to produce a well-structured and easily readable report. In order to ease the evaluation of the thesis, it is important that the cross-references are correct. In the making of the report, strong emphasis should be placed on both a thorough discussion of the results and an orderly presentation.

The candidate is requested to initiate and keep close contact with his/her academic supervisor(s) throughout the working period. The candidate must follow the rules and regulations of NTNU as well as passive directions given by the Department of Energy and Process Engineering.

Risk assessment of the candidate's work shall be carried out according to the department's procedures. The risk assessment must be documented and included as part of the final report. Events related to the candidate's work adversely affecting the health, safety or security, must be documented and included as part of the final report. If the documentation on risk assessment represents a large number of pages, the full version is to be submitted electronically to the supervisor and an excerpt is included in the report.

Pursuant to "Regulations concerning the supplementary provisions to the technology study program/Master of Science" at NTNU §20, the Department reserves the permission to utilize all the results and data for teaching and research purposes as well as in future publications.

The final report is to be submitted digitally in DAIM. An executive summary of the thesis including title, student's name, supervisor's name, year, department name, and NTNU's logo and name, shall be submitted to the department as a separate pdf file. Based on an agreement with the supervisor, the final report and other material and documents may be given to the supervisor in digital format.

☐ Work to be done in lab (Water power lab, Fluids engineering lab, Thermal engineering lab)
☐ Field work

Department of Energy and Process Engineering, 14. January 2015

Olav Bolland
Department Head

Asc. Prof. Laurent Georges
Academic Supervisor
laurent.georges@ntnu.no

Research Advisor:
Prof. Trygve Eikevik, EPT/NTNU, trygve.m.eikevik@ntnu.no
Maria Justo Alonso, SINTEF Byggforsk

Preface

My master thesis is written as the final work of the study Energy and Environment at the Department of Energy and Process Engineering at the Norwegian University of Science and Technology (NTNU).

The main objective of the thesis is further development and improvement of an early decision tool for energy systems based on heat pump technology in passive houses and nearly zero energy buildings (nZEB) focusing on office buildings. The development of the early decision tool is connected to the International Energy Agency Heat Pump Program (IEA HPP) under Annex 40 "Heat Pumps for Zero-Energy Buildings" and to the activity of NTNU-SINTEF on zero emission buildings. My project thesis from fall 2014, which mainly focused on the modelling of the ground, was a preparation for the master thesis. In collaboration with the supervisors, I have put a lot of effort into reducing the computation time and making the graphical interface more user friendly. As this and other tasks have been time consuming, it has not been possible to implement a variable heat pump in the tool. Part load operation of heat pumps are included in the literature review.

I want to thank my supervisors Laurent Georges and Maria Justo Alonso for great support throughout the working process. Special thanks to supervisor Laurent Georges for his contribution on improving the Carnot ground source model. I also want to thank Randi Ramstad and Jørn Stene for their help on relevant topics. Fellow student Simon Aldebert has, for the second half of the semester, worked at the development of the same tool. Simon has contributed positively on several aspects of the tool development. I feel the working process of the master thesis has been rewarding as it has given me a lot of new insight on both heat pump systems and system modelling.

Trondheim June 2015

Mikkel Ytterhus

Summary

This thesis is a continuation of the master thesis of Leif Småland conducted in spring 2013 and the master thesis of Thomas Murer from 2014/15 on the development of an early decision tool for heat pump systems. Focus is on office passive houses and nZEB. One important question is how optimal design of the heating and cooling system changes with improved building standards. The current development of the tool is developed in Matlab/Simulink in connection with the Carnot library developed at "Solar Institut Jülich".

Several aspects of the decision tool has been greatly improved during the thesis. The thesis is focusing on ground source heat pump (GSHP) systems using vertical borehole heat exchangers (BHEs). A more realistic dimensioning, modelling and control of the ground source system have been implemented in the tool. The work on the ground source system has partly been based on findings from the project thesis. Other changes in the system are the introduction of a cooling tank in order to account for the thermal mass of the building and a change in the dimensioning of the peak load units. The graphical interphase of the model has been completely changed in order to make the system more user friendly. Computation time has been dramatically reduced as a result of the changes in the system. All the different changes in the tool conducted during the thesis are presented in this report.

Simulations have been performed for five different heat pump sizes. The building loads, taken as an input for the simulations, are based on previously calculated data for a benchmark office building. The loads include the demand for space heating and cooling and domestic hot water (DHW). Zero Energy Buildings (ZEBs) using photovoltaic (PV) panels to counterbalance for the energy consumption of the heating system are also evaluated. Results are given for annual energy consumption, CO_2 emissions and costs. Cost curves are used to find optimal power coverage factor (OCF) for different systems. Simulations are further used to verify if the system is able to deliver the energy demands of the building for a given heat pump size. With the new version, it has also been possible to evaluate results of several years.

Summary (Norwegian)

Denne masteroppgaven er en videreføring av masteroppgaven til Leif Småland fra høsten 2013 og masteroppgaven til Thomas Murer gjennomført i 2014/15 og omhandler utviklingen av et tidligfase beslutningsverktøy for varmepumpesystemer. Fokuset er rettet mot kontorbygg av passivhusstandard og nær nullenergibygg. Et viktig spørsmål er i hvilken grad optimal design av oppvarmings og kjølingssystemer endres med forbedrede bygningsstandarder. Utviklingen av beslutningsverktøyet er basert på simuleringsprogrammet Matlab/Simulink i tilknytning til Carnot biblioteket utviklet ved "Solar Institut Jülich".

Flere deler av beslutningsverktøyet har blitt betydelig forbedret gjennom arbeidet med denne masteroppgaven. Oppgaven fokuserer på bruk av bergvarmepumper med vertikale borehullsbrønner. Både dimensjoneringen, modelleringen og kontrollsystemet av grunnvarmesystemet har blitt forbedret. Arbeidet med grunnvarmesystemet er delvis basert på funn fra prosjektoppgaven. Andre endringer i simuleringsverktøyet er blant annet introduksjon av en kjøletank for å ta hensyn til den termiske massen til bygget og en endret dimensjonering av spisslastene. Store endringer av det grafiske brukergrensesnittet til modellen har blitt gjennomført for å forbedre brukervennligheten til system. Simuleringenes tidsbruk har blitt dramatisk redusert som en følge av flere forskjellige endringer i systemet. All de viktigste endringene som har blitt gjennomført i løpet av denne masteroppgaven er presenterte i rapporten.

Simuleringer har blitt gjennomført for fem forskjellige varmepumpstørrelser. Energibehovene til bygget, som er en input til verktøyet, er basert på et tidligere definert referanse kontorbygg. Dette inkluderer behov for romoppvarming, kjøling og oppvarming av varmt tappevann. Nullenergibygg med installerte solcellepaneler for å veie opp for energibruket til bygget, er også analysert. Resultater er blitt presenteres for årlig energibruk, CO_2 utslipp og kostnader. Kostnadskurver er brukt til å finne optimal effektdekningsgrad til varmepumpen. Resultater fra simuleringer er videre blitt brukt til å sjekke om systemet er i stand til å dekke bygget energibehov for forskjellige varmepumpsstørrelser. Det har med den nye versjonen av beslutningsverktøyet også blitt mulig å kjøre simuleringer over flere år.

Table of content

Table of figures

Table of tables

Nomenclature

Abbreviations:

BHE: Borehole Heat Exchanger

COP: Coefficient of Performance

DHW: Domestic Hot Water

DOT: Dimensional Outdoor Temperature

GHG: Green House Gas Emissions

GSHP: Ground Source Heat Pump

HVAC: Heating Ventilation and Air Conditioning

NS: Norwegian Standard

OCF: Optimal coverage factor

PLF: Part load factor

PLR: Part load ratio

PV: Photovoltaic (solar panels)

SP: Technical Research Institute of Sweden

SPF: Seasonal Performance Factor

TEK: Technical regulation for Norwegian buildings

THB: Thermo-Hydraulic Bus

TMY: Typical Metrological Year

nZEB: Nearly Zero Energy Building

ZEB: Zero Energy Building (can also mean Zero Emission Building)

Symbols:

A: Area [m^2]

B: Disctance between boreholes [m]

C: Annual cost [NOK/yr]

c: Energy price [NOK/kWh]

E: Energy consumption [kWh]

e: Power consumption [kW]

I: Investment cost [NOK]

ir: interest rate [-]

N: lifetime [yr]

Q: Thermal energy [kWh]

q: Thermal power [kW]

U: Overall heat transfer coefficient [W/m^{2}K]

Subscript:

ctr: control signal (on/off)

FoC: forced cooling

FrC: forced cooling

hp: heat pump

nom: nominal conditions

pl: peak load

sc: space cooling

sh: space heating

1. Introduction

A large focus on global warming as well as energy security has led to increased interest for energy efficient solutions. In 2004, the energy consumption from buildings accounted for 37% of the total energy consumption in the EU, which was larger than both the transport sector and the industry sector (Pérez-Lombarda, 2007). The total energy consumption of residential and commercial buildings in Norway in 2009 was 83 TWh, 37% of the total energy consumption in mainland Norway (Magnussen, 2011). Reducing the energy consumption of the building sector will therefore represent an important contribution to reducing the overall energy consumption both nationally and in the EU. As the technical regulations of buildings in Norway becomes increasingly stricter in their requirements, the demand for space heating has steadily decreased. At the same time, it is still important that future buildings have energy efficient design for space heating and cooling and domestic hot water (DHW) heating. Heat pumps represent an energy efficient technology for heating and cooling of buildings and have a much lower energy consumption than conventional energy systems such as electric heaters and combustion boilers.

One important question is how the optimum design of future highly insulated buildings will change compared to buildings based on earlier building standards. Software programs can be used to evaluate and optimize the performance of heating, ventilation and air conditioning (HVAC) systems. This master thesis is a contribution to an ongoing research in which the final aim is to create an early decision tool for HVAC systems using heat pump technology. The decision tool focus on optimum design of office buildings with passive house standard and nZEB. Energy loads accounted for in the tool includes space heating and cooling and DHW. The base load for heating and cooling system evaluated in this thesis is ground source heat pump. The tool is developed in Matlab/Simulink. The main objective of this thesis has been to further develop and improve the previous version of the tool developed by Murer in 2014/15 and investigate results from the new system.

Results from yearly simulations can be used to calculate annual energy consumption, annual costs and annual green house gas (GHG) emissions. The tool can further be used to evaluate whether or not the system is able to meet the buildings heating and cooling demands. It is also

possible to run simulations over several years to evaluate if the results changes over time (e.g. decreasing temperatures in the ground). These types of results may be used in an early decision phase of a building project. The optimal power coverage factor (OCF) is one example of a parameter that can be investigated by the tool. In this report, OCF always refers to the relationship between nominal capacity of the heat pump and the maximum power demand for space heating. The table below shows a list of possible topics that the tool can be used to investigate. For future versions of the tool, this list may be extended to several new areas of investigation.

Table 1 – Possible areas of investigation for the decision tool.

- **Choice of heat source for the heat pump**
- **OCF for the heat pump**
- **Dimensioning of the source system**
- **Choice of type and dimensioning of peak load units**
- **Storage tank design**
- **Heat exchanger design**
- **Effects of changing various system parameters**
- **Control strategy**

For the tool to be useful, it is necessary that it is able to model the heating system with a sufficient accuracy and that the system is according to state of the art. Other requirements for the tool is that it has a reasonable computation time and that it has a user-friendly graphical interface. A lot of effort has therefore been put into this.

1.1 Method

Some overall goals were set at the beginning of the master thesis according to the assignment text. The goals have however been changing somewhat throughout the working process. Guidance has mainly been given through regular meetings with the supervisors. Due to the nature of developing a simulation tool, adjustments often have to be done in the working plan in order to fix unexpected computer and modelling problems that occur. The main tasks conducted during this thesis are a result of a continuous contact with the supervisors. For the

second part of the semester, fellow student Simon Aldebert has also contributed greatly in various discussions regarding the tool development.

The thesis is heavily relaying on previously work of Murer and Småland (Murer, 2015) (Småland, 2013). The Simien-files developed by Murer have been used as a starting point for the tool development conducted in this thesis. In this report, all the important changes from the previous model and results from simulations with the new version of the tool are presented. Some of the main improvements include the changes performed in the ground source system, reduced computation time and better graphical user phase

1.2 Thesis structure

- *Chapter 2:* This chapter aims to give a theoretical background for some relevant topics related to the tool development.
- *Chapter 3:* The status of the tool is described here. This includes the scope of the tool, the software used and the building demand used as input for the simulation tool.
- *Chapter 4:* The various improvements and changes from the previous version of the tool are described here. A general description of the functionality of the system is also given. The dimensioning of different system parameters for five different heat pump sizes has been conducted. The dimensioning is used as a basis for the simulations shown in chapter 5.
- *Chapter 5:* In this chapter results from simulations are shown and described. Both results over shorter periods of a few days, yearly results and results over several years are given. Results are used to evaluate the performance of the new version of the simulation tool.
- *Chapter 6:* This chapter gives suggestions for future improvements of the decision tool.
- *Chapter 7:* In the conclusion, the most important findings and results are gathered.

2. Background

2.1 Nearly Zero Emission Buildings and Passive Houses

The Energy Performance of Buildings Directive has given the following definition of nZEB (Maldonado, 2013):

"A building that has a very high energy performance… The nearly zero or very low amount of energy required should be covered to a very significant extent by energy from renewable sources, including energy from renewable sources produced on-site or nearby".

Possible base load energy solutions for nZEBs are cogeneration, district heating, solar energy, heat pumps and bio energy or a combination of these alternatives. Currently there is not one exact mathematical definition of the nZEB concept. nZEBs are likely to be buildings with passive house standard or better. Passive houses are characterised by a thigh building envelope, small air leakages and highly efficient heat recovery. This results in a significant reduction in space heating demand. The Norwegian government has announced that the upcoming building regulation directive for 2015 (TEK15) will approach a passive house requirements and that new buildings should fulfil nZEB requirements by 2020 (Stene and Smedegård, 2013). Building owners can reduce the net energy consumption by generating energy on site. Surplus electricity can be exported to the grid. Subtracting the energy supplied to the grid from the used energy will give lower total energy consumption. In this way it can be possible to achieve zero energy buildings or even plus houses (export more energy than imported).

Figure 1 shows the development of typical energy demands of office buildings for different building standards. The energy demands are dramatically reduced, starting from the technical standard of 1987 (TEK87) to a passive house standard. The largest reduction comes from the demand for room heating and heating of ventilation air is dramatically reduced. There may however also be significant deviations in the heating and cooling demand of different buildings of the same standard, as a result of local climate, amount of solar shading and the thermal mass of the building. Although the electricity specific demand has been reduced, figure 1 shows that electric specific demands contributes to a larger share of the total energy demand with improved

building standard. The DHW depends on the user pattern of the building. As the demand for space heating and cooling decreases, the total share of DHW heating is increased, making this a more significant part of the overall energy performance.
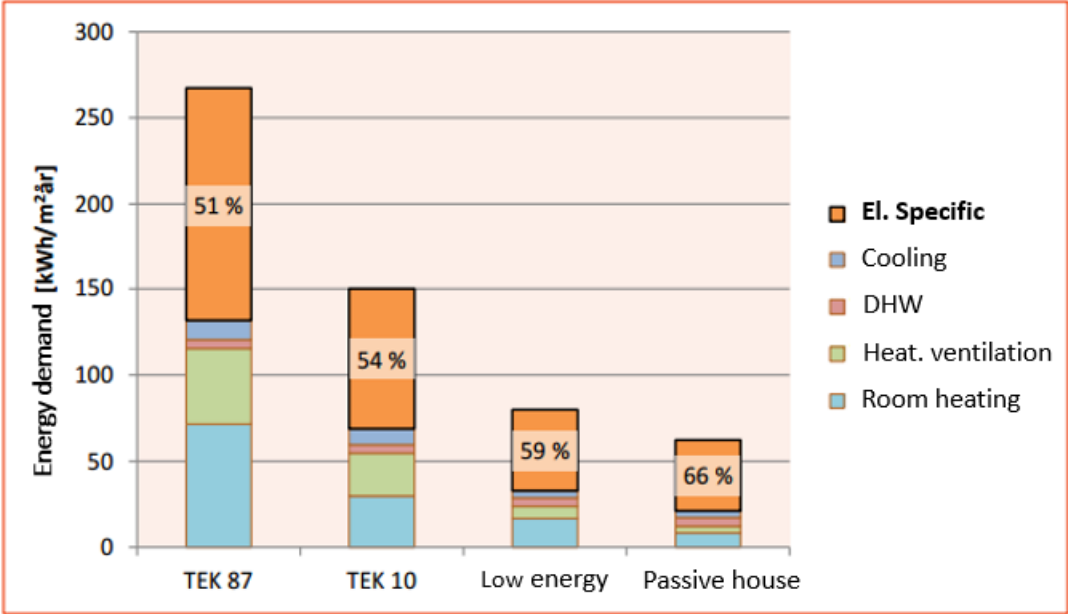
Figure 1 – Typical heating demands with different building standards (Stene and Smedegård, 2013).

Power consumption for space heating and cooling and DHW through the year can be described with a power duration curve. Figure 2 shows a power duration curve for passive house office house building located in Oslo. The duration curve for space heating is very steep, with only a short duration above 50% of the maximum power demand for space heating. Both space heating and cooling demand follows the outdoor temperature closely. Dimensional outdoor temperature (DOT) is here about -25 °C in the winter and 30 °C in the summer. The grey dashed line can be used to estimate the annual energy coverage for a given power coverage factor of the heating demand. Figure 2 indicates that a relative power coverage factor of 20 % will give an annual energy coverage factor of about 80%.
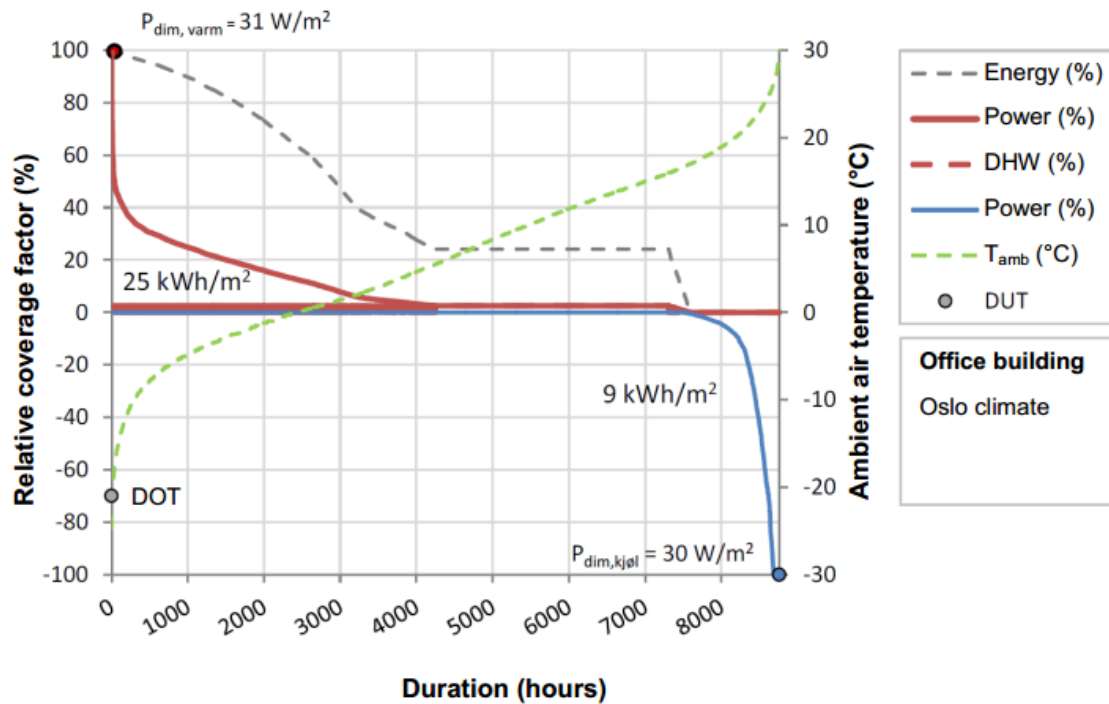
Figure 2 – Power duration curve of a 3600 m² office building of passive house standard located in Oslo (Stene and Smedegård, 2013).

2.2 Heat pumps

Heat pump technology represents an energy efficient solution for heating and cooling of buildings. Compared with a system based solely on direct electric heating, heat pump systems have typically an annual energy saving in the range of 50 – 80 % (Stene, 2014 C). Figure 3 shows a highly simplified sketch of a heat pump system for heating and cooling of buildings. Heat pumps can use a number of different heat sources, where ambient air, ground source and seawater are the most interesting. Ambient air is the most common heat source for heat pumps in smaller residential buildings in Norway. For heat pump systems in large non-residential buildings, ground source and seawater are the most common heat sources (Stene, 2014 B). Only the performance of GSHP systems is investigated in this thesis.
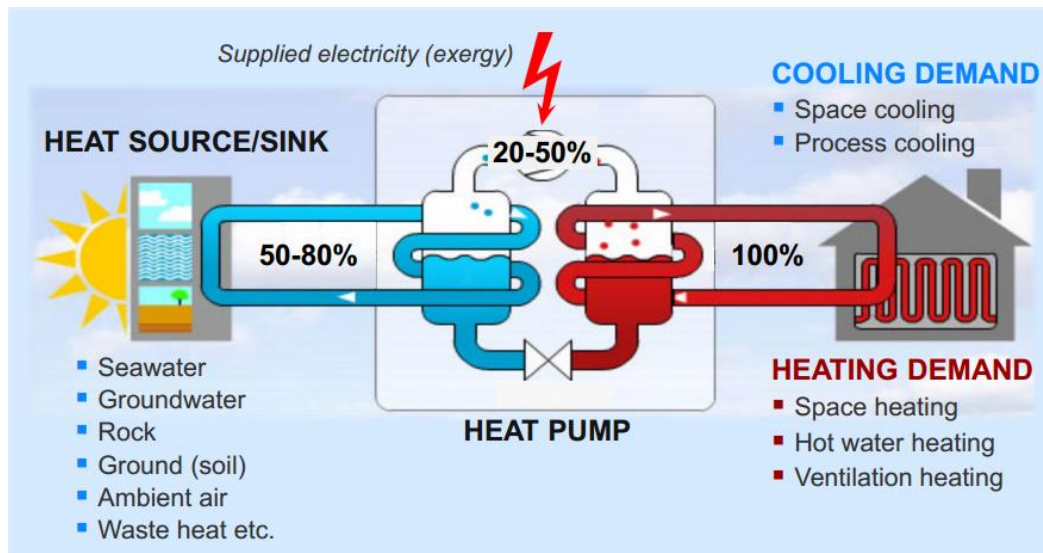
Figure 3 – Principle sketch of a simple heat pump, source/sink and heating/ cooling system (Stene, 2014).

Section 2.2 gives an overview on some topics related to heat pumps. Focus is mainly on topics that is found to be of relevance for the rest of the thesis. Section 2.2.1 and 2.2.2 give a basic introduction to the principles of the heat pump cycle and the energy performance of the heat pump. The literature review on part load heat pump operation given in section 2.2.3 may be used as a starting point for later investigations on this topic. The last section on GSHPs will be used as a background for dimensioning and analysis of results later in the report.

2.2.1 Heat pump cycle

The thermodynamic cycle of a heat pump process can be described by a pressure–enthalpy diagram. Figure 4 shows a pressure-enthalpy diagram for the most simple heat pump design, consisting of one compressor, one evaporator, one condenser and one expansion valve. A working fluid is circulating inside the heat pump and changing phase throughout the cycle. At the inlet of the compressor (point 1 in figure 4) the working fluid has to be in fully vapour state as liquid cause damage and potential failure of the compressor. When the heat pump is turned on, an electric input is given to the compressor as it compresses the gas to a higher pressure and temperature level (from state 1 to state 2 in figure 4) at the same time as it causes the working fluid to circulate. The heat removed from the condenser (from state 2 to 3) first occurs with a decreasing temperature until the gas reaches a saturated state where at heat removal is in the form of condensation at constant temperature. The heat given from the condenser is either used

to heat up the heating distribution system or to dump heat to a heat sink when the heat pump is used for cooling purposes. Through the expansion valve (state 3 to 4 in figure 4), the pressure and temperature of the working fluid decreases. In the evaporator, the enthalpy is increasing as heat is absorbed from a heat source or from surplus heat of the building during cooling. The heat transfer from the condenser and the heat transfer to the evaporator are determined by the product of the change in specific enthalpy and the mass flow rate of the working fluid. The mass flow rate is determined by the volumetric flow from the compressor and the density of the vapour at the compressor inlet. Increasing the evaporation temperature causes an increase in vapour density and thereby also higher mass flow and heat transfer rate. The higher the pressure ratio and thereby the temperature difference between the cold and hot side of the heat pump, the higher the required electric consumption of the compressor (Stene, 2014 C).
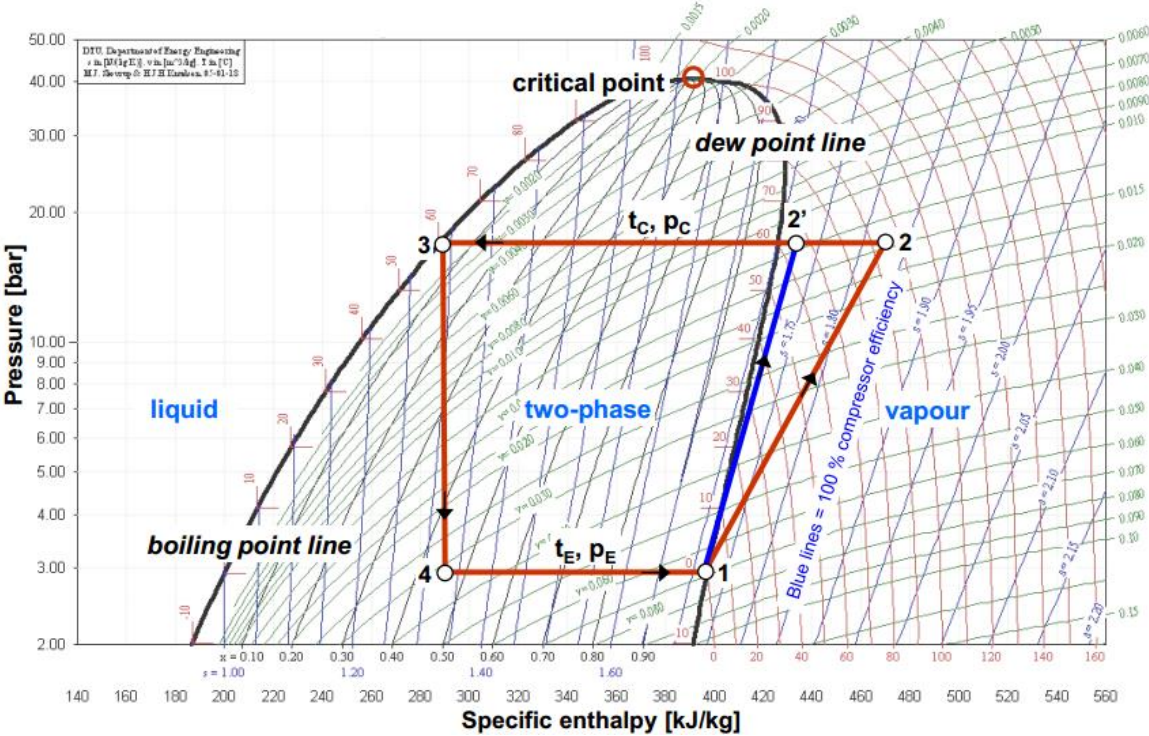
Figure 4 – log p-h diagram of a simple one-stage heat pump cycle (Stene, 2014).

2.2.2 Heat pump performance

The coefficient of performance (COP) is an instantaneously value that describes the relationship between the power delivered by the heat pump and the electric power consumption of the compressor (eq. 2.1 and 2.2). When the heat pump is used for heating, the energy delivered is

the heat from the condenser side. Delivered energy in cooling mode is the energy absorbed by the evaporator.

$$COP_{heating} = \frac{q_{condenser}}{e_{compressor}}$$

(eq. 2.1)

$$COP_{cooling} = \frac{q_{evaporator}}{e_{compressor}}$$

(eq. 2.2)

COP has both yearly and daily fluctuations due to changes in operational conditions. The COP of the heat pump is to a large degree determined by the temperature lift between the cold and hot side of the heat pump. Table 1 shows typical values of how COP and heating power are affected by changes in the evaporation and condensation temperature.

Table 2 – Effects of changing condenser and evaporator temperature on COP and heating power (Stene, 2014 C).

	Decrease in condensation temperature [K]	Increase in evaporation temperature [K]
Relative change in COP	+2- 3 %	+2- 3 %
Relative change in heating power	+0.5 %	+3- 4 %

With increasing COPs, the required electric input to the compressor for a given energy demand decreases. By lowering the temperature of the heating distribution system and utilizing a heat source with a high/moderate temperature, the energy consumption of the heat pump will reduce. When the heat pump is used for cooling purposes, a cold source temperature is desirable. The COP also varies with several other factors such as system design, the thermo-physical properties of the working fluid and the choice of components. Heat pump design can be improved by introducing extra heat exchangers and/ or using several compressors. Different types of compressors are piston, scroll, screw and turbo compressors, where scroll compressors are the most commonly used type for small and medium sized heat pumps (Stene A, 2014).

The seasonal performance factor (SPF) describes the average performance over the year. The SPF of the heat pump is defined as the total heating and cooling delivered divided by the total consumption over the year (eq. 2.3). Forced cooled is the term for the cooling that is delivered to the building by the heat pump. The total energy consumption of the heating system does however not only depend on the performance of the heat pump. Other factors that have an influence on the overall performance are the total annual energy coverage of the heat pump, the type of peak load units, energy consumption of auxiliary and heat losses from storage tanks and other parts of the system. Equation 2.4 shows the overall SPF factor of the heating system. Free cooling, meaning cooling without the use of a heat pump (e.g. from water or ground source), increase the overall SPF. Auxiliary includes electric consumption of pumps and fans.

$$SPF_{hp} = \frac{Q_{hp}}{E_{hp}} = \frac{Q_{heating} + Q_{forced\ cooling}}{E_{hp}}$$

(eq. 2.3)

$$SPF_{total} = \frac{Q_{hp} + Q_{free\ coling} - Q_{losses}}{E_{hp} + E_{pl} + E_{auxilary}}$$

(eq. 2.4)

2.2.3 Part load operation

As the load from the building is varying greatly over time, the heat pump system needs to have a strategy for part load operation. The most commonly used practice has been intermittent on/off control. Due to losses during the on/off cycles, the heat pump should not be turned on and off too rapidly. Scroll compressors with intermittent control should not be turn on/off more than approximately six times per hour (Stene A, 2014). Other control strategies are however available depending on the type of compressor. The most efficient part load control is inverter control of the compressor. Variable speed heat pumps vary the volumetric flow of the working fluid during operation, which thereby varies the heating power from the heat pump. The heating power of the heat pump can then be controlled in order to meet the instantaneous load of the building. There is a minimum capacity at which the heat pump can operate, depending on the type of compressor. For part loads below this level, on/off control is necessary.

There are several reasons why variable speed heat pumps have the potential to increase the COP compared with constant speed on/off controlled heat pumps. The energy balance of the condenser determines the temperature at which the working fluid is condensing. During one on/off cycle at part load operation, the condenser will have to deliver the whole energy demand in the period that the heat pump is turned on. Required outlet water temperature and condensation temperature of the working fluid are therefore higher than it would have been if the heat pump were constantly delivering the given heating demand of the building. Figure 6 shows an example of the water heating temperature during one on/off cycle. It shows that the average heating temperature when the heat pump is turned on is 5.7 °C higher than what is necessary during the whole on/off cycle. The efficiency of the compressor will also change for the variable speed heat pump. This is a function of several factors such as the type of compressor, compressor motor and frequency converter technique. The optimal mass flow rate of the ground may also change as a result of switching from on/off control to variable speed controlled heat pump (Karlsson, 2006).
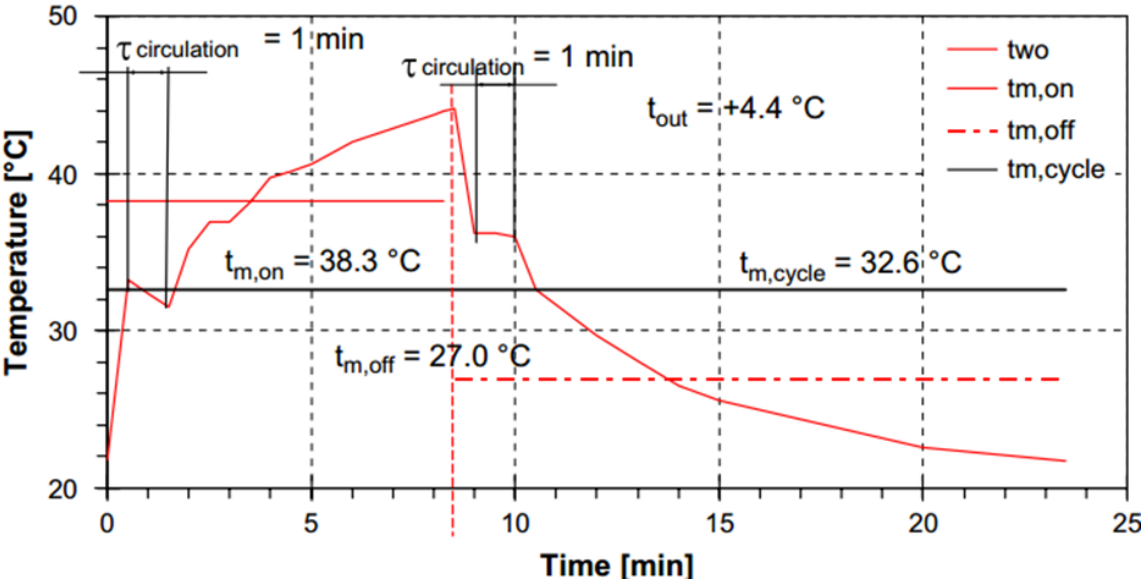
Figure 5 – Heating temperature during one on/ off cycle for intermittent on/ off heat pump (Karlsson, 2006).

The efficiency of the heat pump at part load can be described by plotting the part load factor (PLF) versus the part load ratio (PLR). PLF is the relationship between COP at a given part load and COP of the heat pump at full load at rated conditions. PLR is the relationship between the load of the building and the heating capacity of the heat pump at full load (Filliard, 2009).

Figure 7 shows PLF as a function of a PLR between 0 and 1.3 for both constant and variable controlled air-to-air heat pumps. The figure is based on results from laboratory tests performed at the Technical Research Institute of Sweden (SP). For PLRs below 30%, on/off control is used also for the variable speed heat pump case. The figure shows significantly better performance for the variable speed heat pumps than the on/off controlled heat pumps.
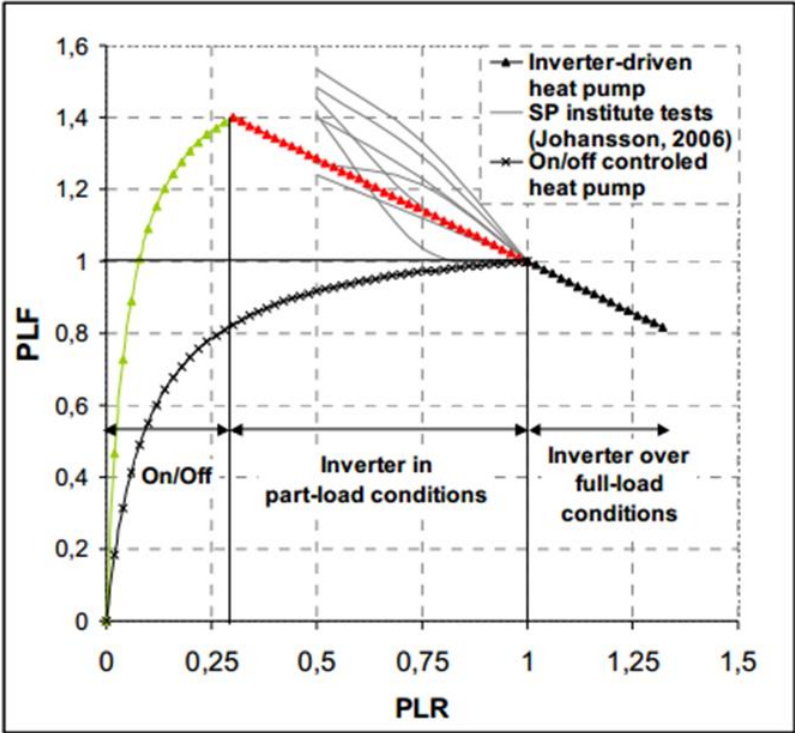
Figure 6 – Part load factor vs part load ratio for variable and constant air-to-air heat pump (Filliard, 2009).

SP published in 2006 test results for ground source heat pump systems using an inverter controlled variable speed heat pump and compared the results with an on/off heat pump system (Karlsson, 2006). They compared two variable speed ground source heat pump systems with one reference system based on an on/off controlled heat pump. One of the variable heat pumps used a scroll compressor specifically designed for part load operation. Despite having a higher COP at part load, the total SPF for the variable speed scroll compressor system were lower than for the on/off controlled heat pump. For a heating system of supply/ return temperature at DOT of 35/28 °C, the variable speed scroll compressor system had a total SPF of 3.5, whereas the reference system had a total SPF of 4.0. The reasons for this was that the variable speed heat pump had a lower COP at full load operation and that the total energy consumption for the

Side 12

pump increased due to longer run time of the heat pump. It is suggested that the variable speed heat pumps will get improved performance in the future by further improving the efficiencies of inverter compressors, compressor motors and pumps (Karlsson, 2006).

2.2.4 Ground source heat pump

GSHPs can by divided between open or closed loop systems and horizontal or vertical systems. The type of heat pump evaluated in this thesis is the closed looped vertical GSHP, also called bedrock heat pump. This is the most common type of GSHP. It consists of one or several borehole heat exchangers (BHEs) that are connected to the heat pump. In Norway, the boreholes are either single or double U-formed tubes (Stene, 2014 B). For larger buildings in Norway the depth of the boreholes are normally in the range of 200 to 250 meters. The boreholes can either be grouted with a filling material or filled with groundwater. All bedrock heat pumps in Norway are established with groundwater filled boreholes (Ramstad, 2015).

Inside the borehole tubes there are an antifreeze fluid, called brine, that circulates when the brine pump is turned on. When the heat pump is used to heat up the building or the DHW, heat are extracted from the ground to the circulating brine. When the system is used for cooling, heat is transferred in the opposite direction, from the BHEs to the ground. GSHPs can use both free and forced cooling. Surplus heat from the building is in free cooling mode transferred directly or through a heat exchanger to the ground. If it is not possible to deliver the whole cooling demand with free cooling, the heat pump can be used to cool down the water in the cooling circuit further and transfer additional heat to the ground.

The "undistributed ground temperature" means the temperature in the ground at different depth when there is no external heat extraction or injection. Below a depth of 15 meters the undistributed ground temperature is very stable throughout the year. Equation 2.5 shows a simplified approximation of the undistributed ground temperature.

$$T(z) \approx \overline{T_{amb}} + 1 + \frac{dT}{dz} z \ [°C],$$

for z > 15 meters

(eq. 2.5) (Stene, 2014)

Here, $\overline{T_{amb}}$ is the annual average outdoor temperature and z the depth below ground level. Although the ground temperature gradient can vary on different locations, a typical value is 0.02 Km^{-1}.

Typical possible heat extraction from vertical BHEs is 45 W/m with a variation of 20 to 80 W/m (Stene, 1997). Borehole fields are normally dimensioned according to the annual heat extraction rate. Typical specific annual heat extraction rates for lines of boreholes for Norwegian conditions are in the range of 50 – 80 kWh per meter borehole per year (Ramstad, 2015). The amount of energy that can be extracted from the ground without causing drastic decrease in the ground temperature depends on several parameters including the climate, ground conditions, depth and type of BHEs and configuration of the field of boreholes. For a field with a of line boreholes, where there is a much larger annual heat extraction than heat injection, there should be a minimum distance between the boreholes of 15 meters (Ramstad, 2015).

Due to more stable source temperatures, GSHPs can achieve higher COPs and SPF than air source heat pumps. Test data shows that the average COP of brine coupled heat pumps has increased the last decades from an average, at a temperature level of 0°C inlet to the evaporator and 35°C outlet from condenser, of 3.82 in 1993 to an average of 4.45 in 2008 (Wemhöner, 2010). IEA HPP Annex 32 has conducted measurements of a large number of heat pump systems. Figure 8 shows monthly performance factors for different ground source systems in central Europe from 2008 and 2009 (Wemhöner, 2010). 32 systems were evaluated in the beginning of the period, while 62 systems were evaluated at the end of the period. Most of the systems are based on vertical BHEs, but there are also some systems based on horizontal collectors. The heat pump systems are connected to low energy buildings that mostly uses floor heating. SPF are based on space heating and DHW heating. The total average SPF is found to be 3.89. This includes the energy use of the back-up heaters and the brine pump. Energy use for back-up heaters is very small and contributes only to about 2 % of the total energy consumption. Electric consumption represents 6% of the total energy consumption. The monthly performance is lower in the summer than in the winter. The reason for this is the increased share of DHW heating which has a lower COP due to higher supply temperature.
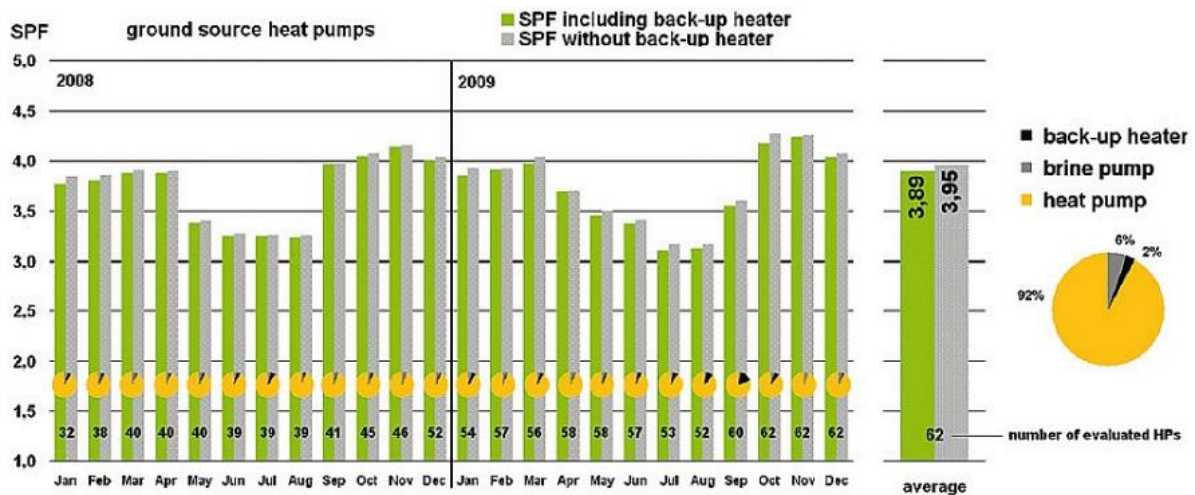
Figure 7 – Monthly SPF of different ground source heat pump system evaluated in 2008 and 2009 (Wemhöner, 2010).

2.3 Heat Exchangers

Heat exchangers transfer heat between two mediums separated by a solid wall. Heat transfer is caused by temperature differences of the two mediums. Heat exchangers have a large number of different applications in HVAC systems. The condenser and the evaporator in the heat pump are both examples of heat exchangers. Other examples are brine-water heat exchangers in indirect ground source heat pumps, heat exchangers used to up storage tanks and radiators in building distribution and emission systems. Equation 2.6 shows a general equation for heat exchanges.

$$q = UA * \Delta T_m$$

(eq. 2.6)

A is the total heat transfer area and U is the overall heat transfer coefficient which varies with several factors including the efficiency of the heat exchanger and the flow rates. A common way to calculate the efficiency of the heat exchanger is by using the so called NTU method. ΔT_m is the mean temperature difference between the fluids. Equation 2.6 shows that the required temperature difference between the two sides of the heat exchanger is reduced by increasing heat exchanger coefficient or by increasing the overall heat transfer area. Reducing the temperature difference in heat exchangers are advantageously in heat pump systems as the

COP of the heat pump is increasing with a decreasing temperature lift. Heat exchangers can be classified according the flow arrangement. The most efficient flow arrangement is counterflow heat exchangers (Incropera, 2006).

3. Early decision tool

3.1 Scope

The simulation tool is used to simulate heat pump systems for space heating and cooling and DHW heating of buildings. The physical system has been implemented into Simulink-files. A number of different HVAC component are represented in the system. This includes the heat pump, the BHEs, pumps, valves, storage tanks, peak load units and heat exchangers. In addition to the physical components, the simulation tool includes the external input signals, the control system, and the calculation of output signals. While this thesis only focuses on GSHP systems, in parallel fellow student Simon Aldebert has investigated the use of air source heat pumps in the simulation tool.

The actual building is decoupled from the simulations tool. The demands of the building is a result of previously calculated values form the program SIMIEN. The SIMIEN-files includes the outdoor and indoor temperatures through the year. The temperatures of the distribution and emission systems are however not an output from SIMIEN simulations. These values have therefore been calculated in forehand of the simulations for the current version of the tool. Section 3.3 gives a description of the building loads. In section 4.2, the representation of the distribution and emission systems is given.

The simulation tool has so far been focusing mainly on thermal calculations. To avoid the system of getting to complex, pressure drop calculations in the pipes has been not yet been implemented. This is also due to the fact that the ground source model included in the Carnot library does not include any pressure calculations. As the energy consumption of pumps are depending on the pressure drops in the system, it was decided during this thesis to neglect the electric consumption of the pumps.

In order for the tool to be effective various criteria should be fulfilled. Below is a list of some of the most important criteria of the tool.

1. **System according to state of the art:** Design of the physical system and default values in the tool should up to date.
2. **Large flexibility of design and parameters:** The user should be able to test the effect of a large number of parameters in the system. It should be also be able to evaluate different system designs.
3. **Sufficient accuracy of results:** It is necessary that the tool have reliable results with sufficient precession in order for it to be useful.
4. **User-friendly interphase:** Having an easily understandable tool to work with for the user will greatly improve the power of the tool.
5. **Low/moderate computation time:** It is obvious that a reduced computation time without reducing accuracy is preferable. With decreased computation time, the user can test a much larger number of parameters and designs.

Some of the points listed above may be in conflict. Reducing the complexity of calculations can cause reduction in computation time at the expense of reduced accuracy. If however the reduction in accuracy is small while the reduction in computation time is very large, the reduced complexity may still be preferable. Having a large number of different possibilities in design and parameters may be in conflict with having a user friendly tool that is easy to use. This can to some degree be solved by having good default values. These are type of questions that often have to be considered in the tool development.

3.2 Choice of software

At the beginning of the project work of fall 2014, different software simulation programs were considered for the future development of the decision tool. Possible platforms that were discussed included Modelica and TRNSYS. In collaboration with supervisors and fellow student Murer, it was decided to use Simulink/Matlab in combination with the Carnot library. Simulink/Matlab has the advantage of a large flexibility in system design. Another reason was that program was considered the easiest to get into.

3.2.1 The Carnot library

The Carnot library has been developed at Solar-Institute Jülich as an extension to Simulink. The library includes models of many different components used in thermal energy systems. For this master thesis, the newest version of the Carnot library has been used (version 6.0 beta). Carnot is available for free at University of Applied Sciences Düsseldorf. The Carnot library has no guidance and does not offer any guaranty of its utility for any particular application (Carnot Version 6.0, 2014).
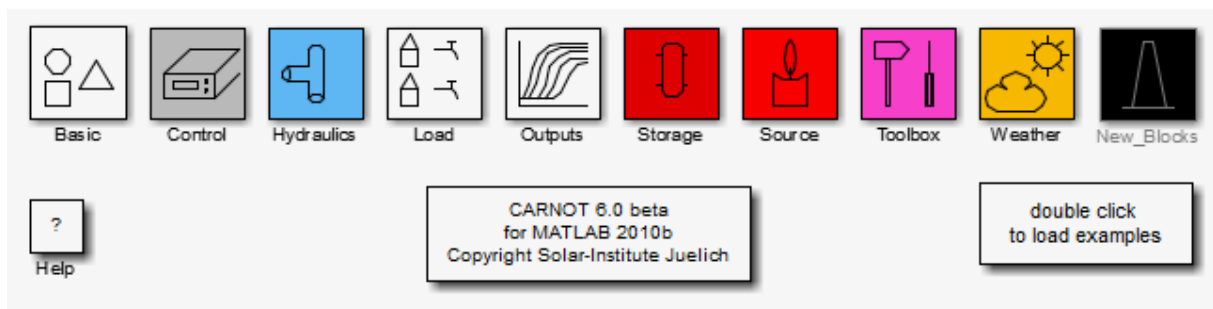
Figure 8 – The Carnot library (Carnot version 6.0, 2014).

Carnot uses a Thermo-Hydraulic Bus (THB) signal to describe the different properties and the state of the fluid circulating in the system. The THB consists of a total of 12 different parameters, including temperature, mass flow rate, pressure, fluid type and fluid mix. From the parameters in the THB, other fluid properties such as heat capacity and flow characteristics such as the Reynolds number, can be calculated by other blocks that are implemented in the library. The Carnot library includes blocks for a large range of different HVAC components. The most important Carnot blocks used for the simulation tool is described in this section.

3.2.1.1 Heat pump
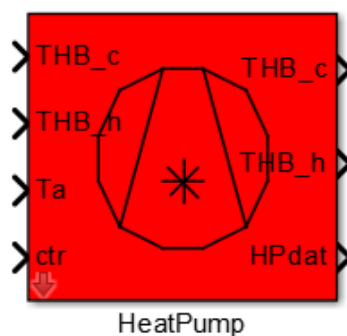
Figure 9 – Carnot heat pump block (Carnot Version 6.0, 2014).

The Carnot heat pump block is a simplified model where the heat pump cycle is treated as a "black box". This means that the model does not take into account the different heat pump parameters that effect the performance of the heat pump, such as the type of working fluid and type of components. Instead, the heat transfer on the condenser and evaporate side and the electric consumption of the compressor are found by interpolating between tabulated temperature dependent values defined by the user. The block is developed only for on/off control. Simon Aldebert has in his work made changes in the block so that it is also possible to run it as a reversible air source heat pump.

3.2.1.2 Ground source
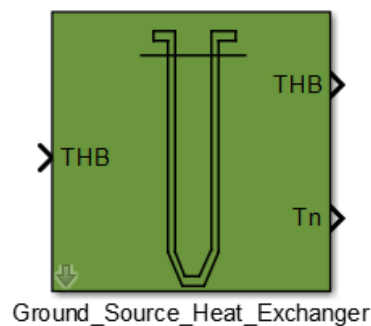
Figure 10 – Ground source block in Carnot (Carnot Version 6.0, 2014).

The ground source block in the Carnot library is based on the so called EWS model. The model is developed for double U-tubed and grouted vertical BHEs. Ground water flow is neglected in the model and it is assumed that all heat transfer outside the tubes is in the form of conduction. The model it not able to model freezing of the ground and pressure drop calculations are not included. The user can set a number of different parameters in the model, including the properties of the ground and grout, the geometry of the boreholes and the borehole configuration. Initial temperatures in the ground can either be set to undistributed ground temperatures (equations 2.5) or be based on a constant heat extraction/ injection rate over a given period. The ground is divided in a radial and an axial grid. Temperatures in the upward and downward flowing brine are calculated during simulation. The outer boundary temperature in the ground is changing less rapidly and is updated only once every week. This temperature is calculated according to a predefined function called "g-function". While the brine temperatures and the temperatures in the ground close to the borehole is calculated independently of the borehole configuration, the calculation of the outer boundary temperature

Side 19

takes into account the interaction between the different boreholes in a borehole field. Equation 3.1 shows the radius from the borehole of the outer boundary temperature.

$$r_{boundary} = \frac{B}{2}$$

<div align="right">(eq. 3.1)</div>

"B" is here the distance between the boreholes. The temperatures of the inner calculation grid is updated rapidly (determined by the step size in Simulink). Equation 3.2 shows the different radiuses from the boreholes in the calculation grid. "f" is a grid factor and "DimRad" is the number of radial nodes.

$$r_j = r_{j-1} + (r_{boundary} - r_{borehole}) \frac{1-f}{1-f^{DimRad-1}} f^{j-2}$$

<div align="right">(eq. 3.2)</div>

By combining equation 3.1 and 3.2 it is possible to find the radius for the different nodes. All the ground temperatures at different depths and radiuses are included in the "Tn" output of the block (see figure 12). A more comprehensive discussion of the Carnot EWS model was given in the project thesis (Ytterhus, 2014). It was during the project thesis found significant weaknesses in the Carnot EWS implementation. Section 4.7.2 describes the improvement of model which has been done in collaboration with supervisor.

3.2.1.3 Storage tank
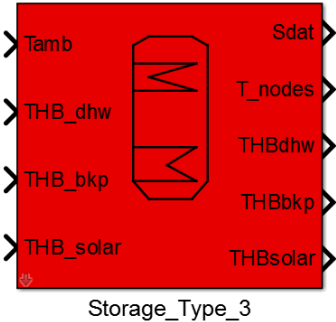
Figure 11 – Carnot storage tank block (type 3) (Carnot Version 6.0, 2014).

The Carnot library includes several different storage tank blocks. Figure 14 shows a storage tank with two heat exchangers. This block is used to represent the space heating and DHW tanks in the tool. By default settings, the temperature in the tank are calculated at ten different relative heights. The UA value is calculated according to the following equation.

$$UA = uac * \dot{m}^{uam} * \left(\frac{T_{heat\ exchanger} + T_{tank}}{2}\right)^{uat}$$

(eq. 3.3)

"uac" is a constant specific heat transfer coefficient, while "uam" and "uat" are dimensionless confidents used mass flow and temperature dependent heat transfer respectively.

3.2.1.4 Other Carnot blocks

The pump block is used to set a given constant mass flow rate when the pump is turned on. The mass flow is controlled on/off by the control input signal which is either one or zero. Type of fluid and fluid mix is set in the pump block. The two types of valves used in the Simulink model are diverter and mixer valves. The diverter valve splits the flow between two possible directions according to a given control input signal. The mixer valve merges two fluid flows into one flow. For each diverter valve in the model, there are a corresponding mixer valve.

In addition to the heat exchangers inside the tanks, one additional heat brine to water heat exchanger is used in the system (see section 4.1). A counter flow is chosen as this is the most efficient type. The outlet temperatures are calculated with the NTU-method.

The two peak load units used for simulations in this thesis are an electric heat and a biomass boiler. The biomass boiler represented with is furnace model implemented in Carnot. Carnot also has a simple electric heater block with a 100% efficiency.

3.2.2 Matlab/ Simulink

In addition to the Carnot blocks that are used to model physical components, a large number of different Simulink blocks are used in order for the system to work properly. Results from simulations are exported to a file using the "to file" block. All input signal are imported with a

resolution of one hour into "signal builder" blocks in Simulink. It is possible to import data into a signal builder block from datasheets in excel. For simulations over several year, the "signal builder" blocks were replaced with "from workspace" blocks as they have the possibility of exceeding the input signal as a repeating sequence.

Simulations have been performed with the Matlab version R2014b. All simulations are performed with the solver ode45 and variable step size. Running simulations from Matlab-scripts, it has been possible to run two systems in parallel using parallel processors. The results of yearly simulations has been exported to excel where different values are calculated and graphs are plotted. Plots over shorter periods are created using the Simulation Data Inspector in Simulink.

3.3 Loads

The space heating and cooling demand used for the simulations in this thesis is based on previously calculated values in the program SIMIEN performed by Småland (Småland, 2013). The simulations in SIMIEN were based on a fictive benchmark building initially made in another thesis (Smedegård, 2012). The building is a free standing, four floor office building with a total heated area of 2400 m^2. The building is classified as heavy. A low cooling demand is ensured with the use of structural canopy and external solar shading. Heat loads are based on data for a typical metrological year (TMY) with Oslo climate. The user pattern is set to be at 100% during working hours, defined as 12 hours a day for five days a week. For a more comprehensive description of the benchmark building see (Småland, 2013) and (Smedegård, 2012).
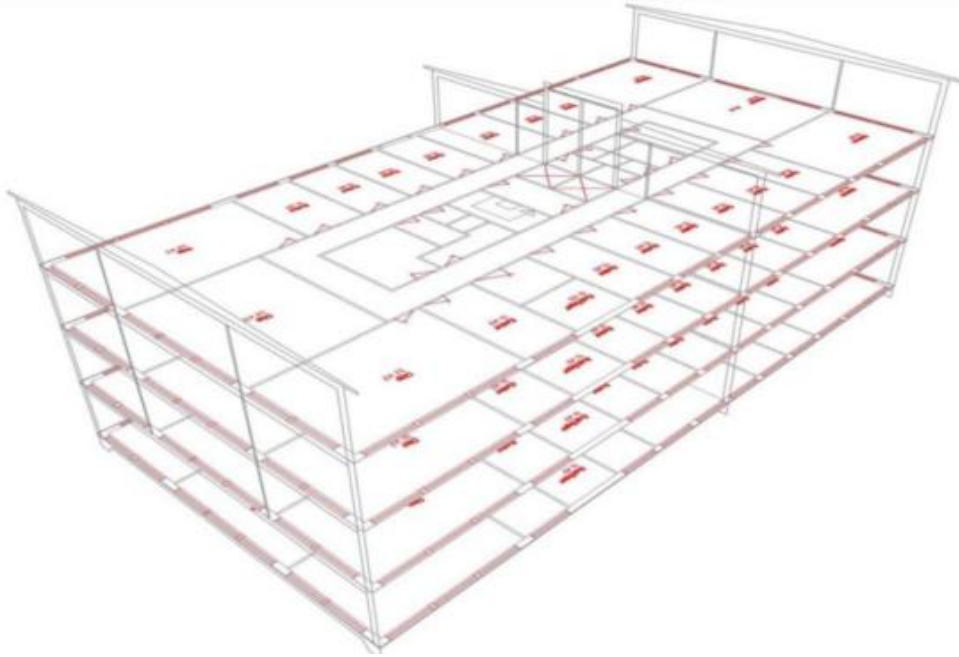
Figure 12 – Benchmark office building (Smedegård, 2012)

In the tool development by Murer, the space heating and cooling demand for the benchmark building with a TEK 10 and passive house standard were imported into a signal builder blocks in Simulink (Murer, 2015). Same was done for the indoor and outdoor temperatures. The resolution of all input signals is one hour. Heat demand for rom heating and heating of ventilation air was merged into one value. When referring to the space heating demand in this report, it always includes both room heating and heating of ventilation air. The same input signal for space heating and cooling used in the tool developed by Murer, is used for the simulations in this thesis. However, only simulations with the demand of the benchmark building with passive house standard is performed. Figure 15 shows the demand for space heating and cooling over the year. There is never a demand for space heating and cooling at the same time. The figure shows that the peaks of the cooling power demand are virtually flat. This may be caused by a limitation of the SIMIEN program.
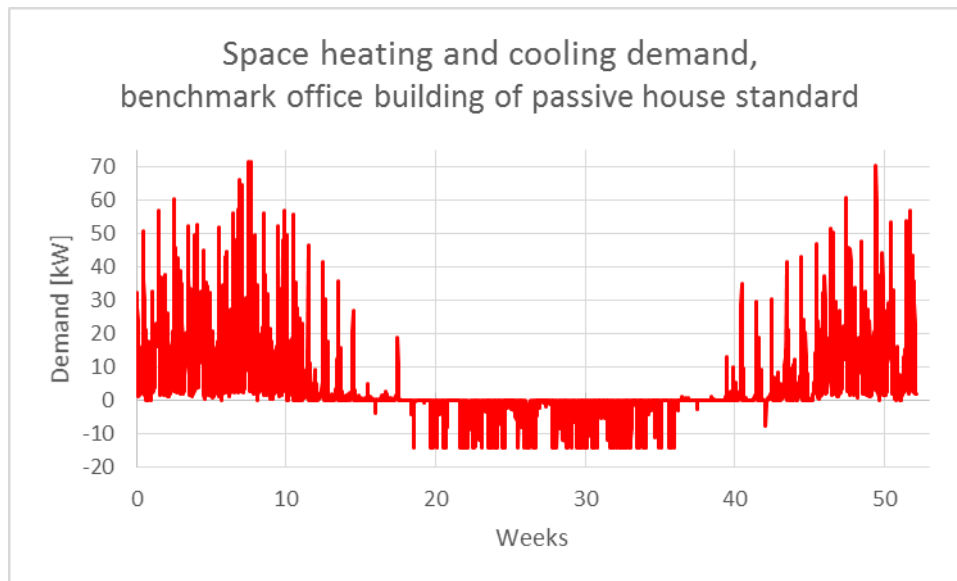
Figure 13 – Heating and cooling demand from Simien calculations over one year.

The demand for DHW in the previous tool was based on measured data from an office building (Murer, 2015). The data has daily and weekly fluctuations according to the user pattern of the building. A repeating sequence over one week with the resolution of one hour was used as an input to the Simulink model. The total DHW consumption was however much higher than what is typical for office buildings. According to the Norwegian standard NS 3031, a typical value for yearly DHW consumption for an office building is 5 kWh/m^{2}yr (NS 3031:2014). With a total heated area of 2400m^2 this gives a total DHW consumption of 12 MWh/yr. This is similar to the DHW consumptions used in the first version of the tool (Småland, 2013). In order to get this amount of yearly energy consumption, the DHW demand from the previous model has been scaled down with a factor of 6.2. For this reason, the total amount of energy used to heat up the DHW tank is dramatically reduced. Figure 16 shows the weekly power consumption of DHW used in the current version of the tool. It shows that the energy consumption is reduced during weekends.
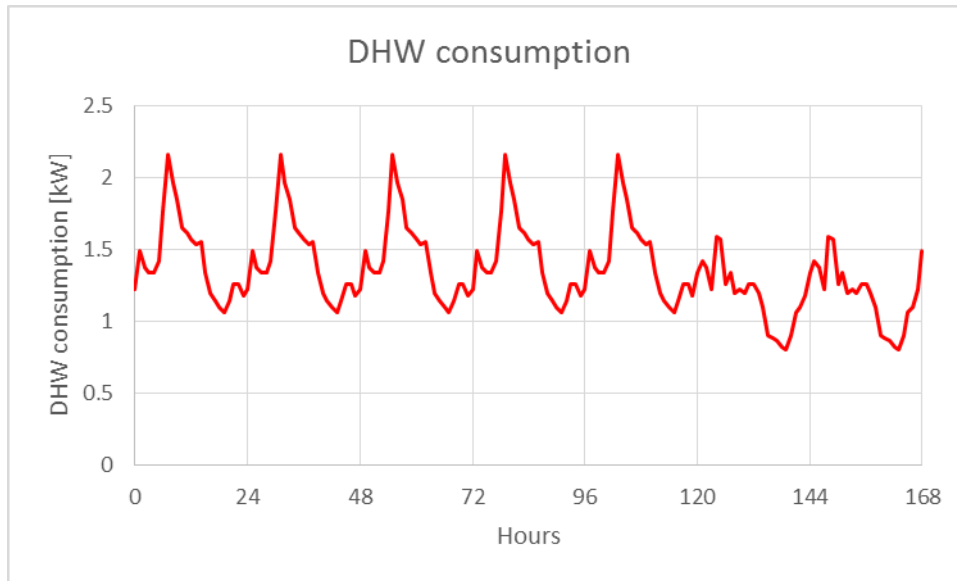
Figure 14 – DHW consumption over on week.

Figure 17 shows the power duration curve for space heating and cooling and DHW over the year. Comparing the curve with figure 2, the peak power for space heating is about the same, while the total energy consumption for space heating is significantly lower ($15kWh/m^2/yr$ versus $25kWh/m^2/yr$). This is also shown with a steeper power curve for space heating in the loads used in this thesis. The cooling demand is also much lower than what was found to be a typical value in the literature review. As already described, the benchmark buildings has a good solar shading and a high thermal mass, which give low cooling demand. However, the high duration in which the cooling demand is at its peak cooling power demand does not seem realistic. A complete overview of the different energy and power demands are shown in table 3. The temperature curve is similar as for figure 2, with a DOT in winter of - 25°C and a DOT of 30°C in summer.
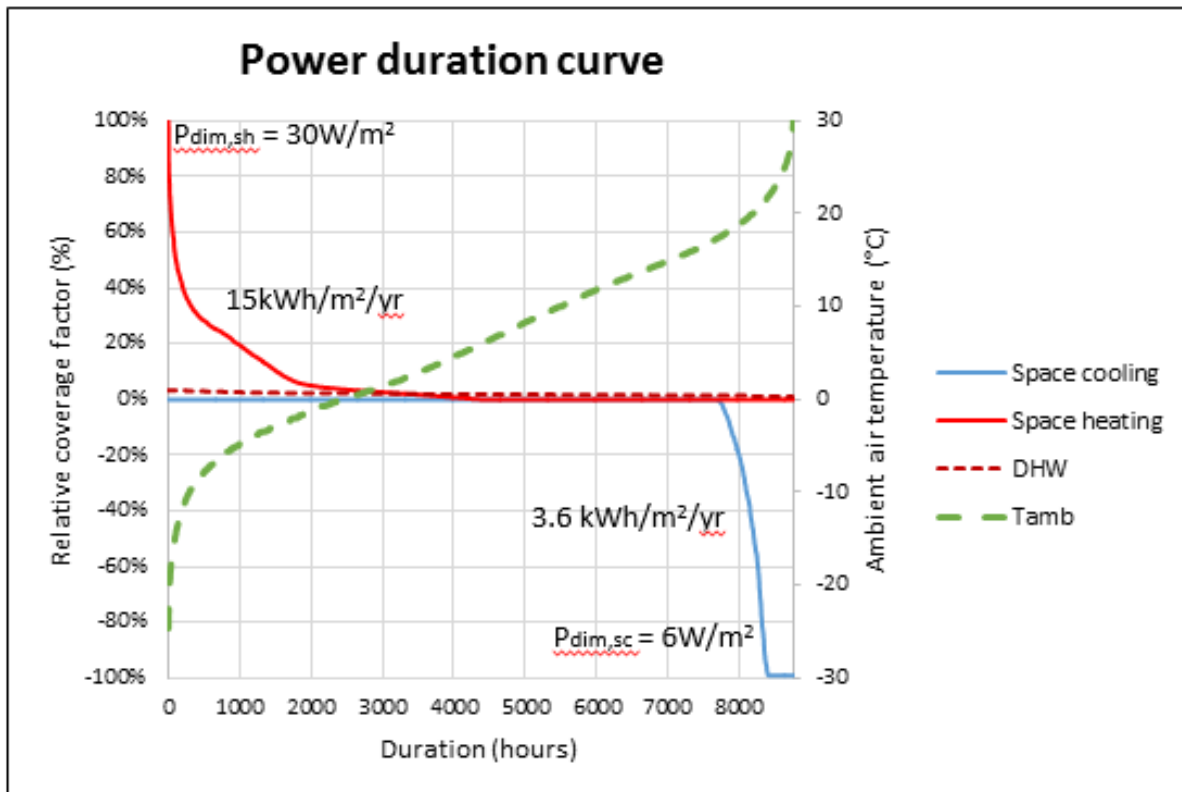
Figure 15 – Power duration curve for space heating and cooling and DHW.

Table 3 – Demands for passive house office building used for simulations.

	Space heating	Space cooling	DHW
Peak power [kW]	71.5	14.3	2
Specific peak power [W/ m²]	29.8	6	0.8
Annual energy demand [MWh/yr]	35.3	8.66	12
Specific energy demand [kWh/(m²yr)]	14.7	3.6	5
Relative share of energy demand [%]	63	15.5	21.5

3.4 Costs and emissions

The total annual costs are calculated as the sum of annual energy and maintenance cost and the discounted investment costs (eq 3.3). The annual capital cost for each component is calculated by the product of the investment cost and the annuity factor as described in equation 3.4. Investment costs include costs of the heat pump, BHEs, floor heating system, peak load units and storage tanks. For the ZEB, additional investment costs are included for the PV panels. When electric heaters are used as peak load units, all energy consumption is in the form of electricity. When biomass boilers are used, the energy costs are a combination of electricity costs and costs of bio fuel. All cost and emission parameters are given in appendix 4.

$$C_{Total} = \sum_i \left(C_{Capital}(i) + C_{Maintenace}(i) \right) + c_{el}P_{el} + c_{fuel}P_{fuel}$$

(eq. 3.3)

$$C_{Capital}(i) = I(i) * annuity = I(i) \left(\frac{ir}{1 - (1 - ir)^{N(i)}} - ir \right)$$

(eq. 3.4)

Annual emission are calculated as the product of the energy consumption and an emission factor. The CO_2 emission factor for the electricity is depending on the power mix of the grid. This CO_2 coefficient from the electric power grid in Norway is according to standard NS 3700, 395 g/kWh. The emission factor from the bio boiler depends on the type of bio mass being used. Energy price and emission factor for electricity and bio mass is shown in table. All the cost and emission factors used during this thesis is similar to the values used in the thesis of Murer.

Table 4 – Emission factor and energy price (Murer, 2015).

	Electricity	Bio mass
Emission factor [g CO_2-eq/ kWh]	0.8	0.74
Energy price [NOK/kWh]	395	42

3.5 ZEB and PV panels

Results for the ZEB are based on the simulations of the benchmark passive house building. For the ZEB, additional PV panels are included in the cost analysis. For the building to achieve net zero energy, the solar panels are dimensioned so that they are able to generate an annual electricity production equal to the total energy consumptions of the building for space heating and cooling and DHW. Higher performance of the heating system will therefore decrease the necessary installed capacity and investment costs of the PV panels. In collaboration with supervisors, it was decided to use a first assumption that all the energy produced by the PV panels is sold to the grid for the same price as energy is imported. With this assumption, the annual energy costs will also be zero. The panels are set to have an annual energy production of 781 kWh per installed kW of PV (Murer, 2015).

4. Tool development

During this thesis, several parts of the tool has been significantly changed. As a starting point it was necessary to get a good overview of the existing system implemented in the previous version. Murer build up the physical heating and cooling system in several different Simulink files for different types of source, emission and tank systems of passive house and TEK10 standard. The development of the tool during this master thesis is an extension of the previous Simulink system with GSHP, passive house standard and floor heating emission system. Although extensive work was conducted by Murer, there was also a large potential for improvements. Below is a list of the most important areas in which the Simulink system has been changed during this thesis.

1. Much more user friendly graphical interface
2. Dimensioning of BHEs and peak load units according to the heat pump size
3. Improved ground source model (Carnot EWS model)
4. Introduction of a cooling tank to represent the thermal mass of the building
5. Changed control strategy for the cooling system
6. Pre-calculation of temperatures and mass flow in the distribution and emission system
7. Improve the modelling of the cooling system

8. Made the system able to run several year simulations
9. Computation time reduced with a factor of about ten

In addition to the areas listed above, some bugs and inaccuracies in the Simulink system have been fixed. Further, the reduction in DHW consumption described in section 3.3, has caused large changes in the overall results. In this chapter, the functionality of the current simulation tool and its deviation from the previous tool is described.

4.1 System modes

The system layout is based on the layout of the previous version, but with some modifications. The system is now divided between the source system and storage system. Main components of the source system are the ground source system and the heat pump. In the storage system, energy is stored in buffer tanks. The peak load units connected to the heating tanks are also included in the storage system. A brine is circulating in the source system, while pure water is circulating in storage system. The mass flow rate on each side of the heat pump is a constant defined in the manufacturer data sheet (see 4.7.1). Several valves are used to control the direction of the flow in different system modes. Figure 19 shows an overview of the heating system.
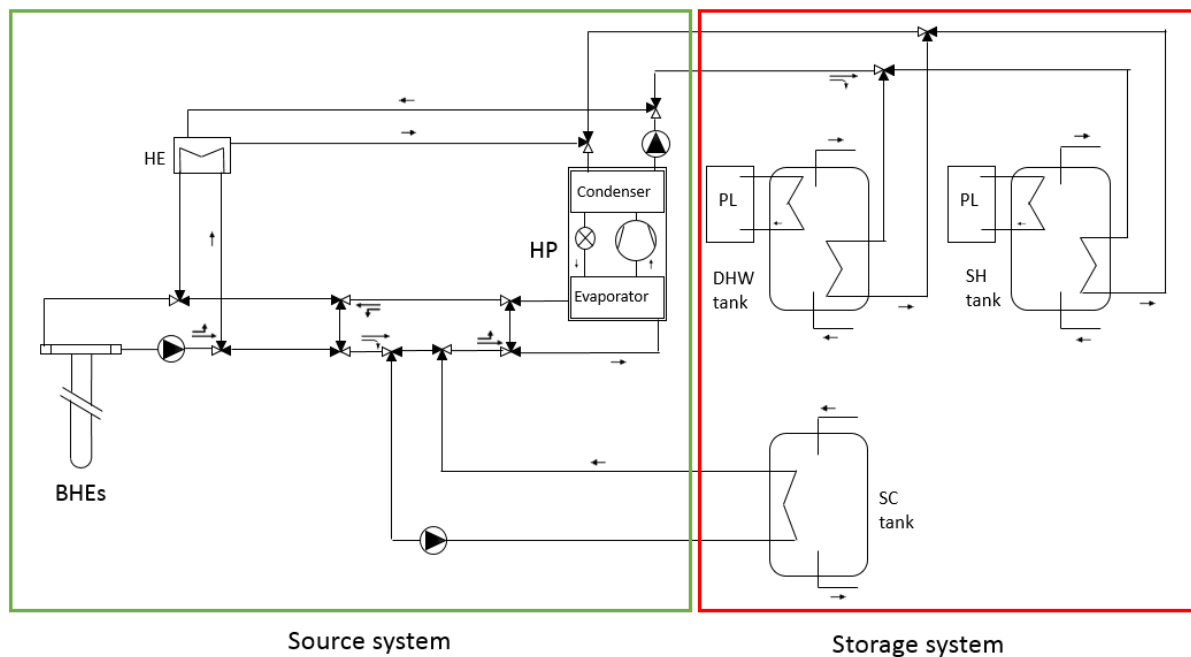
Figure 16 – System layout.

The system can operate in five different modes. Below is a list of the different system modes and the shortening of the control signal for each mode. The system cannot operate in more than one mode at the same time. The all times during the simulations, the control signals are either set to one when it is on or zero when it is turned off. DHW has priority in the system. This means that when there is a need to heat up the DHW tank, the heat pump is connected to the DHW tank regardless of whether or not there is a need for space heating or cooling. In addition to the system modes, the two peak load units can be turned either on or off. The peak load units are independent of the system mode. The control signal for peak load heating of the space heating and DHW tank are shortened to ctr_PL_SH and ctr_PL_DHW respectively.

1. **Space heating mode (ctr_HP_SH)**
2. **DHW mode (ctr_HP_DHW)**
3. **Forced cooling mode (ctr_FoC)**
4. **Free cooling mode (ctr_HP_FrC)**
5. **Off mode**

Figure 17 shows the system in space heating and DHW mode. In both cases the heat pump is connected to the BHEs on the evaporator side. Water is heated on the condenser side and further used to heat up the space heating or DHW tank.
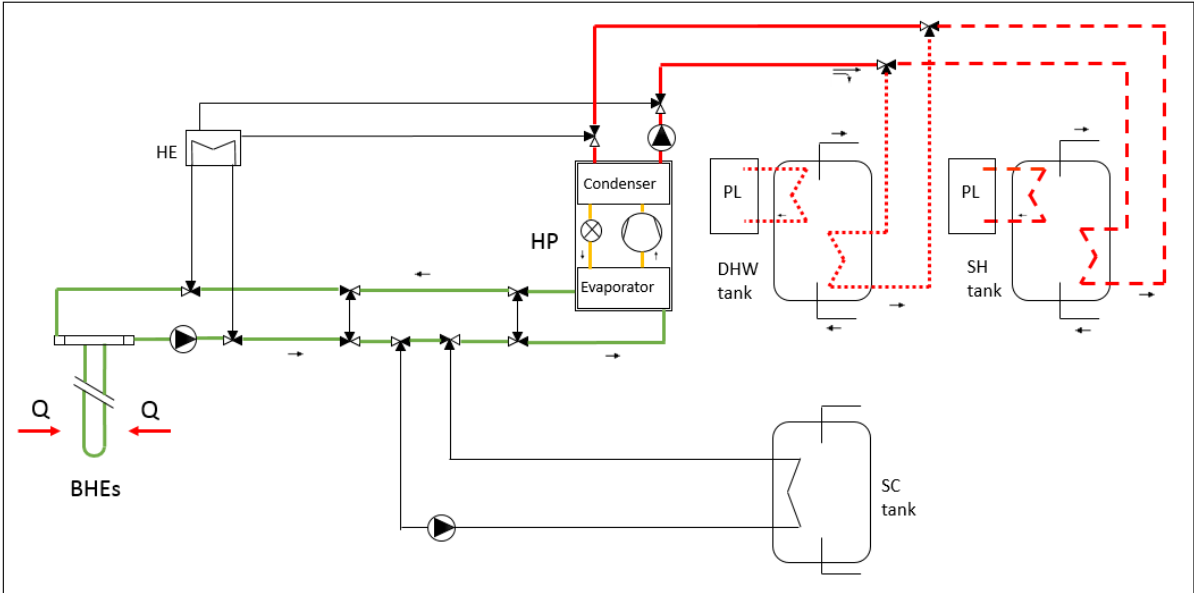
Figure 17 – System layout for space heating and DHW mode.

Figure 18 shows the system in free cooling mode. In free cooling mode, the BHEs are directly connected to the cooling system and the heat pump is not in use. In the new system it is introduced a cooling tank. The cooling system is discussed in section 4.2.3. Heat is injected to the ground both in free and forced cooling mode.
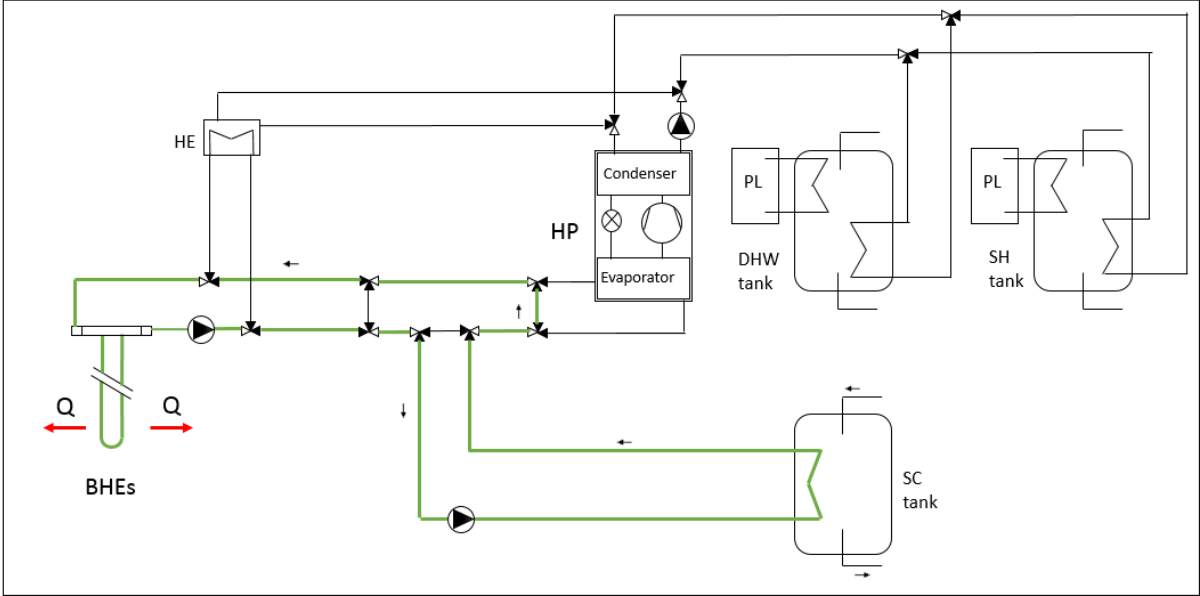
Figure 18 – System layout for free cooling mode.

Figure 19 shows the functionality of the system in forced cooling mode. Forced cooling is used when free cooling is not able to deliver sufficient amount of cooling to the building. The brine flowing from the ground is here connected to the condenser indirectly via a heat exchanger. The brine that is flowing in the heat exchanger inside the cooling tank is being cooled down by transferring heat to the evaporator. This causes a sufficiently higher temperature difference between the inlet and outlet of the heat exchanger in the cooling tank compared to free cooling. Forced cooling have thereby a larger potential for cooling than free cooling.
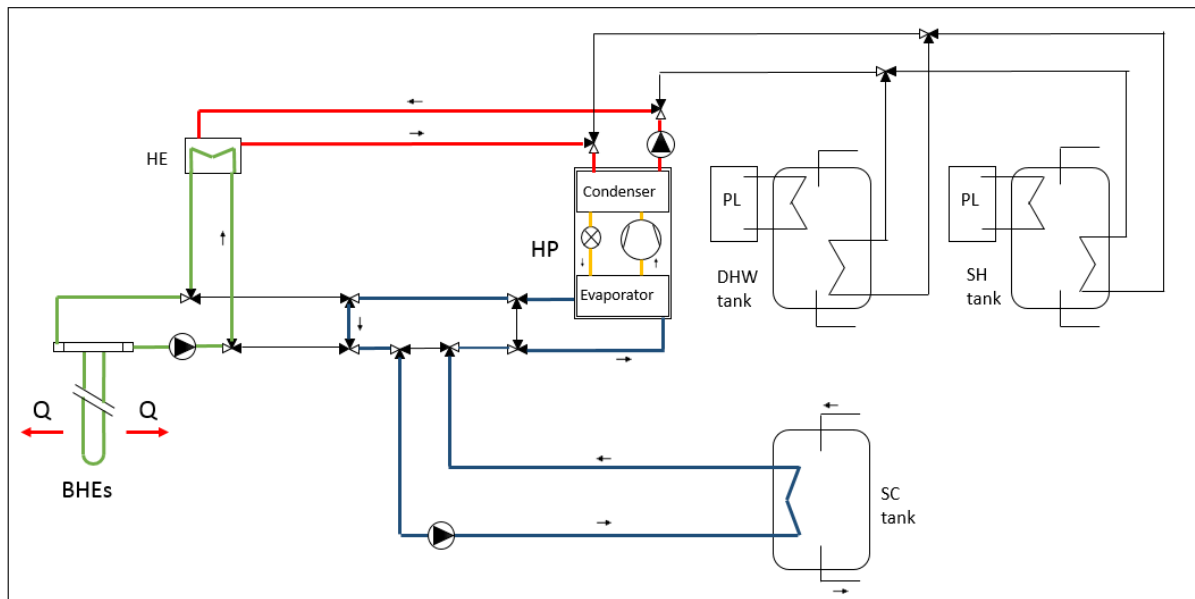
Figure 19 – System layout in forced cooling mode.

4.2 Distribution and emission system

As the SIMIEN-data does not include the temperatures and mass flow of the distribution system, these values had to be calculated during the thesis. By defining outdoor temperature compensation curves the distribution temperatures, it was possible to pre-calculate the temperatures and mass flow rates based on the SIMIEN-data and import the signals into signal builder blocks in Simulink.

4.2.1 Space heating system

The supply temperatures for space heating depends on the type of distribution and emission system used in the building. In this thesis, a low temperature floor heating systems is used. The same supply temperature curve as in the previous tool is used. At DOT, the supply and return temperature is set to 35 °C and 30° respectively. The return temperature is changed from the previous version so that it only varies with the outdoor temperature. Previously the return temperature was calculated as a function of both heating demand and indoor and outdoor temperature. The reason for the change is that the previous way of calculating the return temperature caused unreasonable return temperatures and additional restriction were used to

get reasonable values (Murer, 2015). The mass flow rates in all the distribution systems are now pre-calculated by the equation shown below. Figure 20 shows the compensation curve for supply and return temperature for the floor heating system.

$$\dot{m}_{distribution} = \frac{Q_{input}}{c_p * \Delta T_{distribution}}$$

(eq. 4.1)
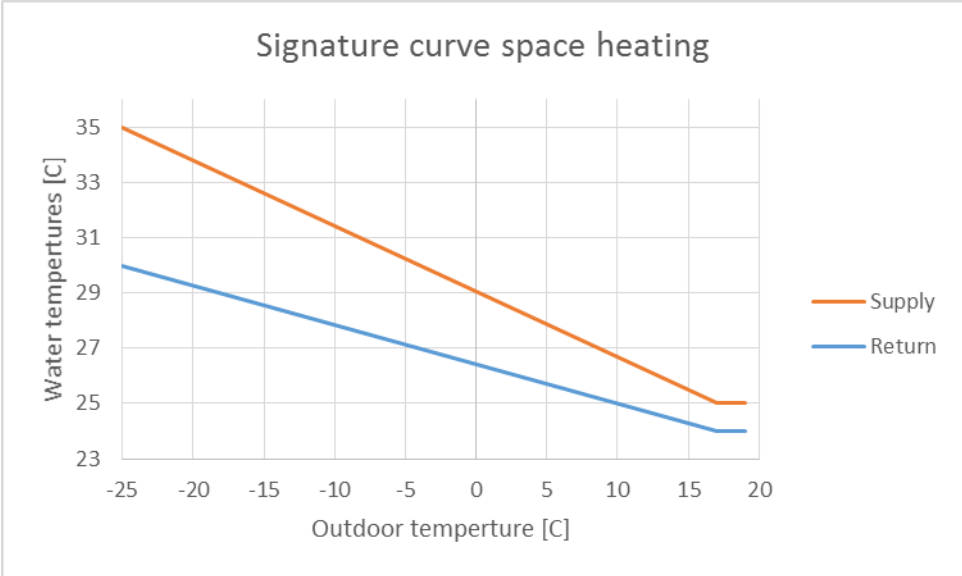
Figure 20 – Compensation curve for supply and return temperature in floor heating system.

The heat pump and peak load units are controlled to ensure that the temperature at the outlet of the tank is higher than the supply temperature. The water flow in the heat exchanger are in the opposite direction of the flow in the tank as this gives the highest efficiency. Water from the space heating tank is mixed with unheated return water to ensure that the supply temperature always match the desired supply temperature. The mass flow that flows into the space heating tank is calculated during simulation according to equation 6.2. Figure 24 shows the layout of the space heating system.

$$\dot{m}_{to\ tank} = \dot{m}_{distrbution} \frac{T_{supply} - T_{return}}{T_{tank} - T_{retun}}$$

(eq. 6.2)

Side 33
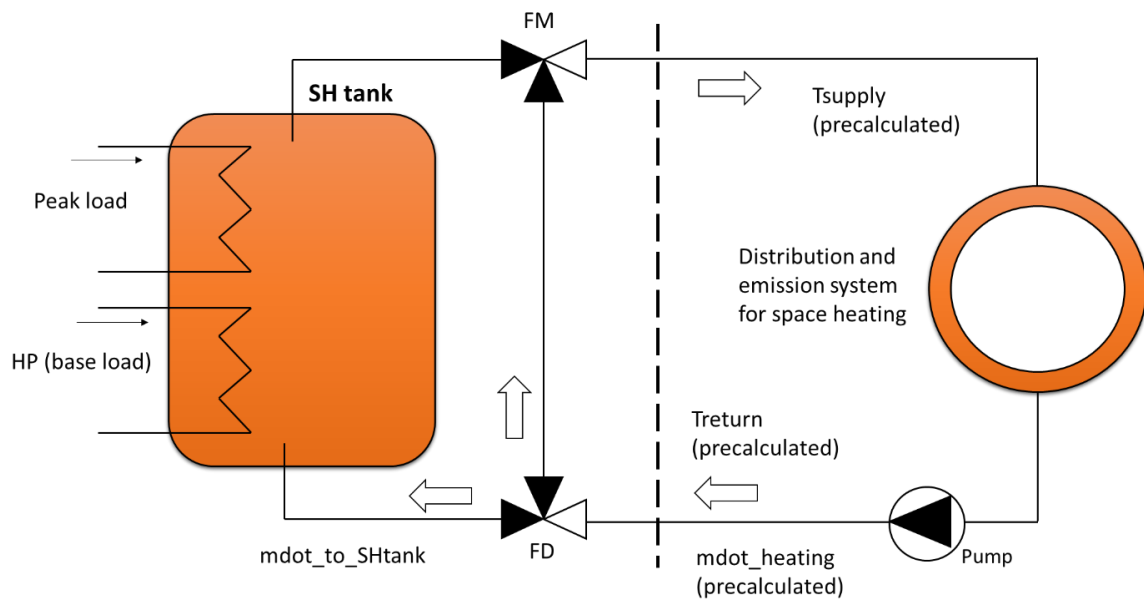
Figure 21 – Layout of SH system.

4.2.2 DHW system

The DHW system is an open system. It is assumed that the inlet temperature of the ground water is constant 5 °C over the whole year. It is further assumed that the supply temperature in the DHW distribution system is constant 45 °C though the year. The set temperature of the tank is increased by 10 °C one day of the week in order to avoid the spread of Legionella in the tank. Figure 25 shows a description of the DHW system.
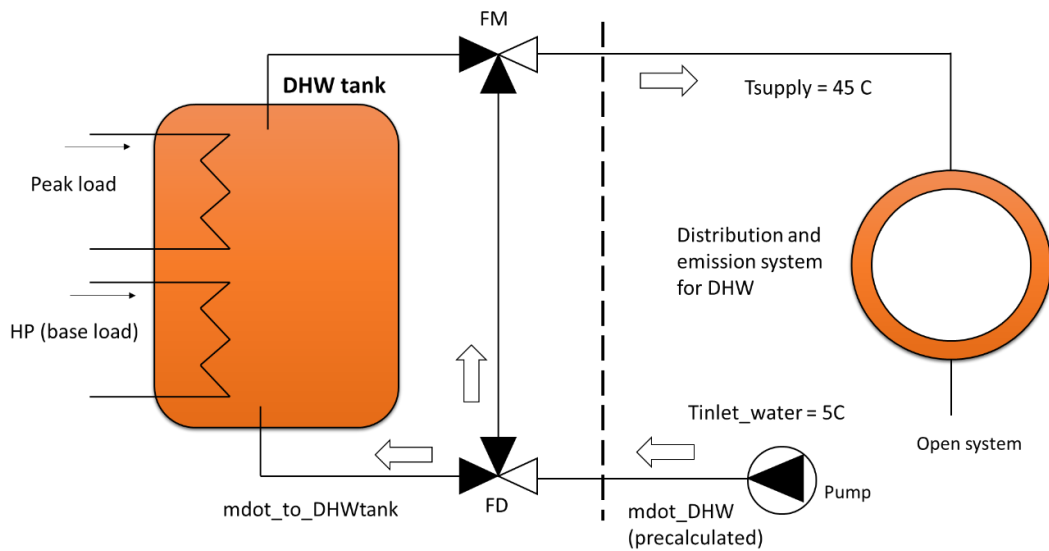
Figure 22 – Layout of the DHW system.

4.2.3 Space cooling system

The supply temperature curve of the cooling system is the same as for the previous version, based on a floor cooling system (Murer, 2015). Figure 26 shows the compensation curve for supply and return temperatures in the cooling system.
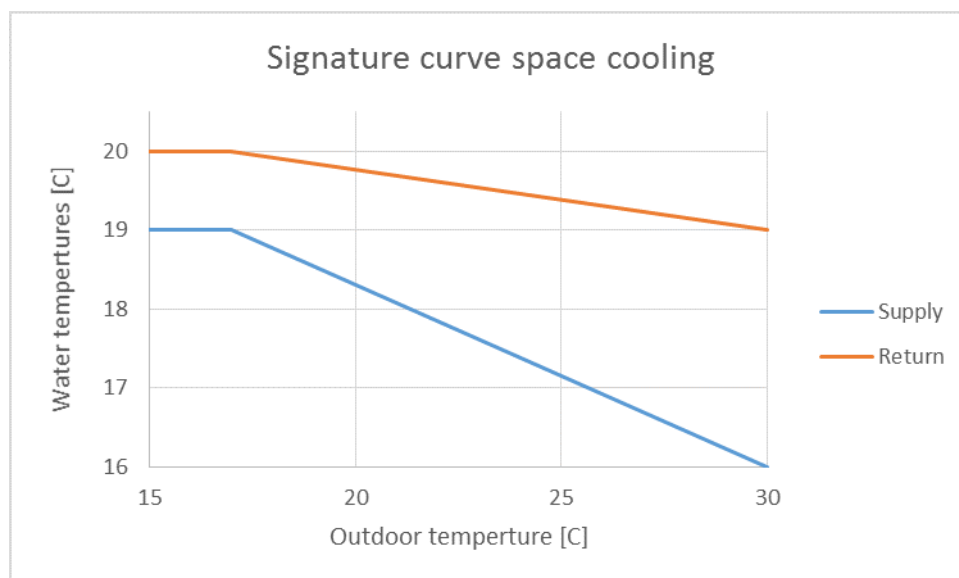
Figure 23 – Compensation curve for space cooling.

In the Simulink models developed by Murer, free and forced cooling were controlled only by the SIMIEN input and unaffected by the brine temperatures from the BHEs. As the simulation tool is decoupled from the building system, it is not able to model inertia in the system caused by the thermal mass of the building. In discussion with the supervisors it was found that the best way to solve this problem was to introduce a cooling tank and in this way include a thermal mass in the cooling system. The mass flow rate that flows into the cooling tank is calculated in the same way as for the heating tanks. The outlet from the cooling tank to the distribution system is however at the bottom of the tank as this is the coldest place in the tank.
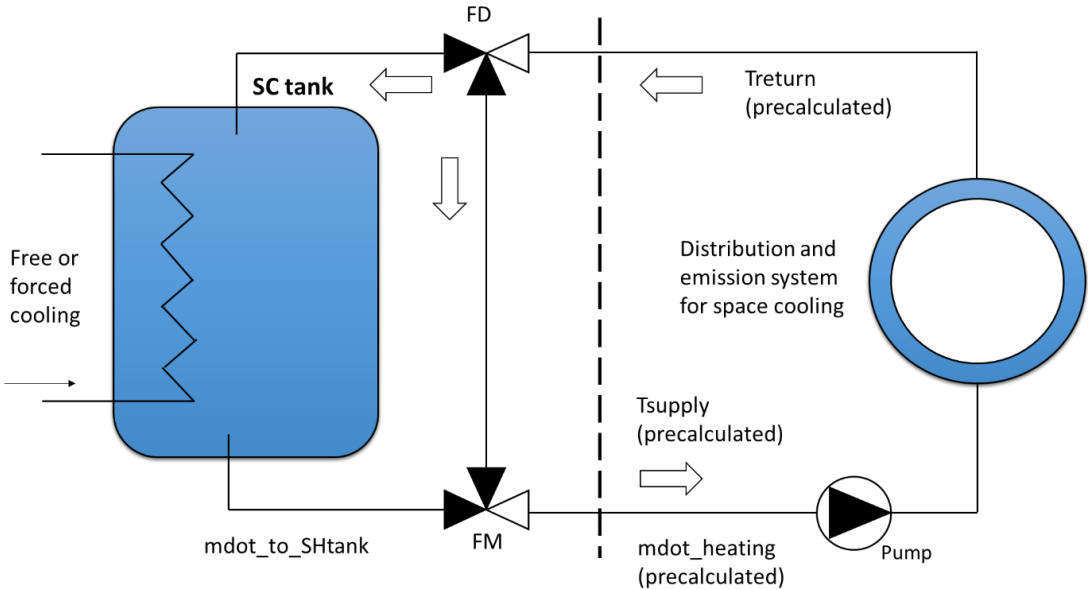
Figure 24 – Layout of cooling system.

4.3 Reordering the Simulink model

In order for the user of the tool to get a good understanding of the system, it is preferable that the Simulink model has a smart layout. The Simulink model is built up of different system blocks that perform various operations. Input and output signals are transferred between the blocks with arrow connections. In the previous version of the tool, an extensive use of arrows made the model somewhat incomprehensible. One Simulink system from the previous is shown in figure 25.
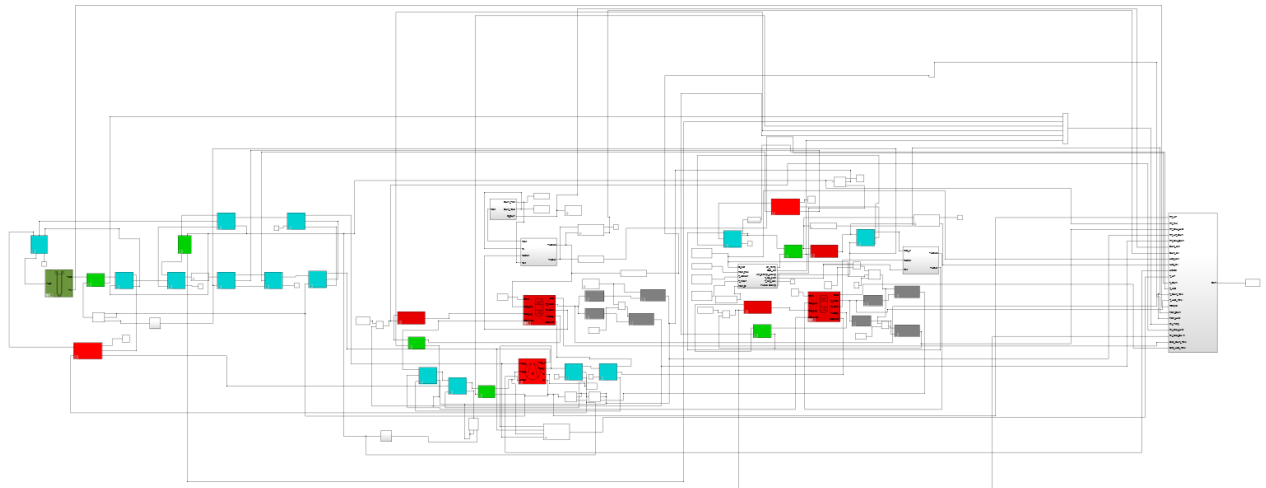
Figure 25 – Simulink model from previous version (Murer, 2015).

The system has been divided into several subsystems. Subsystems give the possibility of separating the tool into several layers. Firstly, the model is divided into four main subsystems: "Input_data", "Control_system", "Physical_system" and "Output_data". The physical system is future divided between the "Source_system" and the "Storage_system". In this way it is easier for the user of the program to look into a particular part of the system.
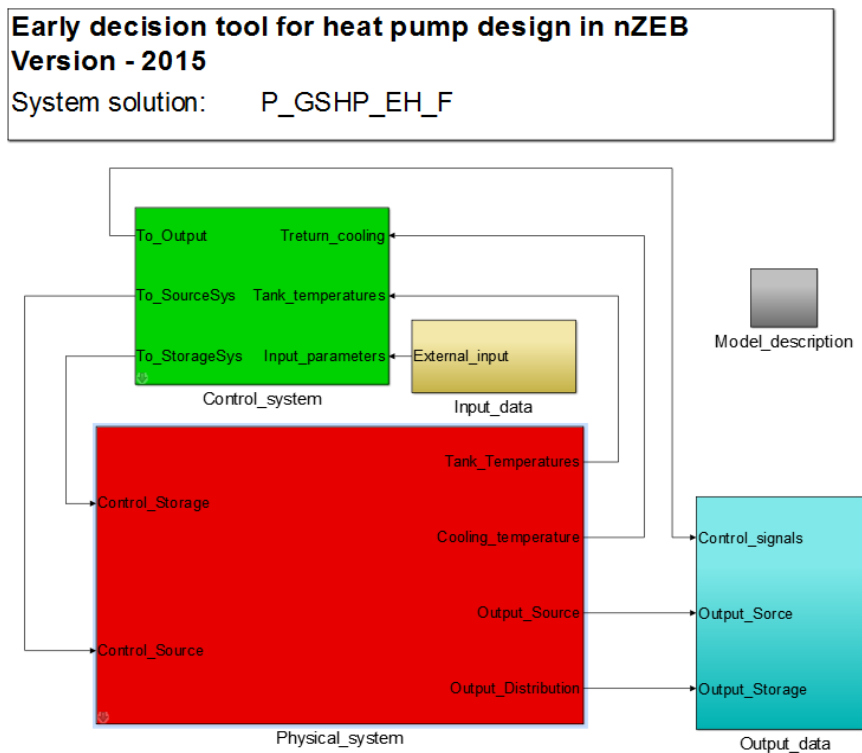
Figure 26 – Early decision tool.

Side 37

The physical subsystem is further divided between the source and the storage system. Figure 27 shows the source subsystem in Simulink. The main components are the ground source block and the heat pump. Data of the THB vector are transferred between the different components. THB signals from the heat pump and the heat exchanger used in forced cooling mode are being transferred to the storage subsystem. The light blue arrows are control signals from the control subsystem used to control the pumps, valves and the heat pump in different systems modes. Heat pump data, ground source temperatures and data from the cooling system are send to the output subsystem.
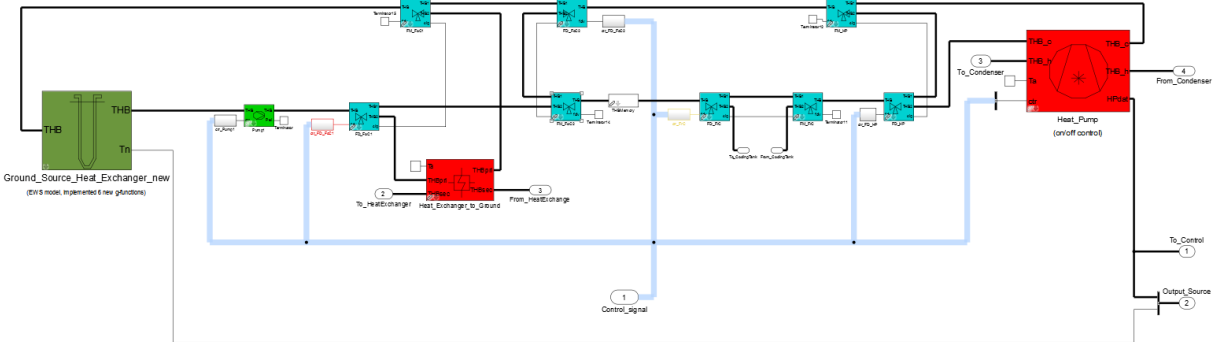
Figure 27 – Source subsystem in Simulink model.

Figure 28 shows the storage subsystem. The main components are the storage tanks and the peak load units. Emission and distribution systems of the space heating, space cooling and DHW are represented using Simulink blocks in separate subsystems. Peak load units are here electric heaters. Tank temperatures are sent to the control subsystem to evaluate whether the heat pump and/ or the peak loads should be turned on or off.
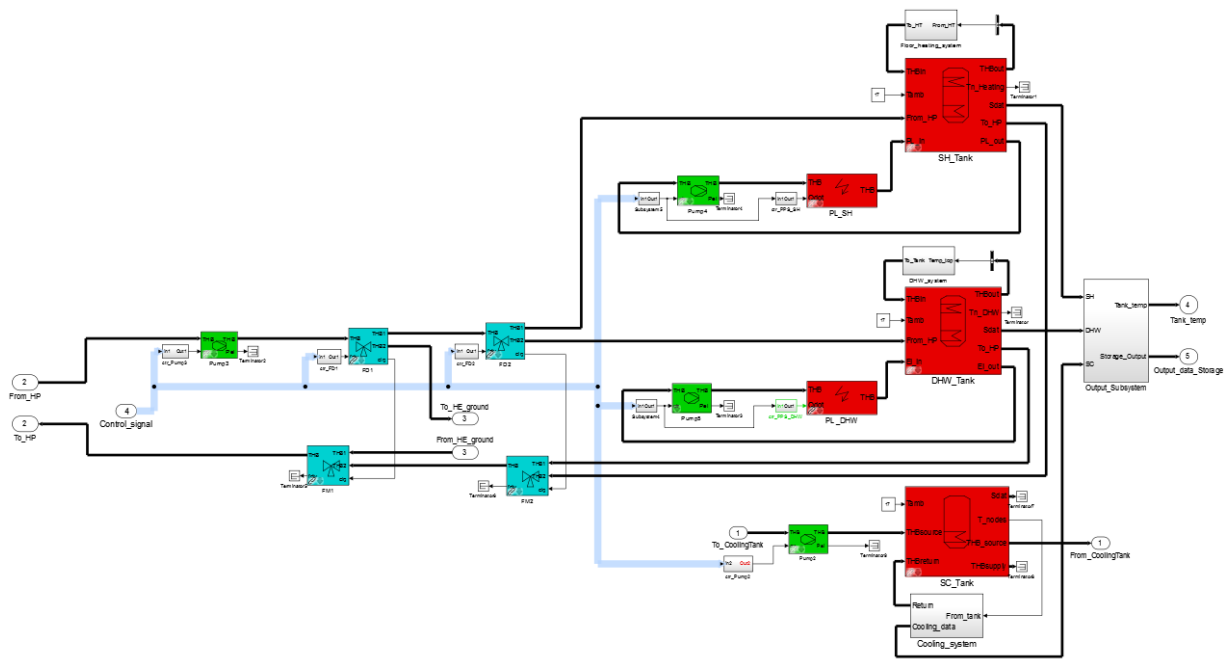
Figure 28 – Storage and peak load subsystem in Simulink model.

4.4 Improvement of ground source model

During the project work it was detected some errors in the original Carnot ground source mode. The outer boundary temperature changed too rapidly and was updated to the exact same temperature as its initial value at the beginning of each week. For this master work, supervisor Laurent Georges has help to solve this problem. He has made changes in the implementation of the g-functions in the Carnot EWS model. This has resulted in more realistic results of the ground source model. The changes have also significantly reduced the computation time of the block. One other improvement is that the mass flow rate of the brine used to calculated the convective heat transfer in the collectors is set as a block parameter, where it previous where hidden in the initialization script in the model.

In addition to the work of Georges, the author of this report has included additional g-functions into the block. This means that the ground source block is able to model more configurations of boreholes. The new g-functions have been read from figures in the doctoral thesis of

Miaomiao He (He, 2012). An overview of the different borehole configurations implemented in the new version of the block is found in appendix 5.

4.5 Control signals

In the control subsystem, the mode of the system is determined. The different control signals are merged into one bus signal and transferred to the source and storage subsystems. Control of the system modes is based on tank temperatures and supply temperature for the space heating and cooling and DHW system as explained in section 4.2.1 to 4.2.3. Three principles have been used when determining the control system. Firstly, the system should be able to deliver the given heating/ cooling demand through the whole year. For the heating tanks this means that the temperature at the top of the tank is higher than the supply temperature. For the cooling system the bottom tank temperate should be lower than the supply cooling temperature. Secondly, the tanks should not be heated/ cooled to unnecessary high/cold temperatures as this will decrease the COP of the heat pump and reduce performance. The third principle is that the system mode should not switched too rapidly as this will cause cycle losses to the heat pump and other components. This is solved by having a given range in which the tank temperature can vary before heating /cooling of the tank is turned on/off. In addition, a minimum time period for each system mode is set by a discrete sample time. This also serve the purpose of reducing the computation time (see section 4.6). The values used in the control system are also a result of a trial and error method based on system simulations. In collaboration with the supervisors it was decided to measure the heating tank temperatures on height one third from the top and the cooling tank one third from the bottom. A complete overview of the control system is given in appendix 1.

4.6 Sample time

When using a variable step size, the rate at which calculations are performed is determined by Simulink during simulaions base on the a maximum error tolerance. It is however also possible to set a fixed discrete sample time at individual Simulink block. In collaboration with supervisors, it was decided during this thesis to investigate the effects on computation time and accuracy when using discrete sample time at different places in the model. In the current version of the model it is set a sample time of 10 minutes for all the control signal in the system. This

is also because it is found in literature review that the heat pump should not be turned on/off more than six times per hour (scroll compressor). The use of discrete sample time of the control signals therefore serve two purposes. Firstly it ensures that the heat pump is not turned on and off too rapidly. Secondly, as seen in section 5.7, it causes a significant reduction in the computation time of the tool. A discrete sample time has also been set for a few other signals in the system.

4.7 Dimensioning

The simulation tool include a large number of parameters that can be defined by the user. This is one of the major strengths of the tool. In this way, sensitivity analysis on different parameters can be performed. At the same time, it can be challenging to find proper values of all the different parameters. This section aims to give an overview of the most important design parameters used for the simulations during this thesis. A combination of typical values from literature, discussions with supervisors and trial and error method have been conducted. In reality, the choice of parameter values will depend on a large number of factors and should be evaluated for each particular building project. The dimensioning conducted in this section is only used as a starting point in order to be able to run simulations and get results. In chapter 5, results from the simulation tool are presented.

4.7.1 Heat Pump

In his master thesis, Murer gathered manufacturer data for several different GSHPs from the company Tobler Haustechnik AG (Murer, 2015). Heating power and electric consumption read from figures were used to perform simulations with the Carnot heat pump model. These values are given for a constant mass flow rate on each side of the heat pump. Maximum outlet temperature of the condenser is 70 °C and minimum inlet temperature to the evaporator is -5 °C(Tobler, 2012). The same manufacturer data used by Murer has also been used in this thesis. Simulations have in this thesis been performed for five different heat pump sizes. As the 50kW heat pump used by Murer, had significantly higher COPs than the other heat pumps for the same temperature levels, this heat pump was not included in the results. The heat pumps have COPs in the range of 4.7 to 4.8 at a temperature level of 0 °C inlet to the evaporator and 35 °C outlet from the condenser, which gives a the heat pumps high performance. Heat pump

performance data for the 20kW heat pump are listed in appendix 2. The table below shows data for the different heat pump sizes used for simulations in this thesis.

Table 5 – Heat pump data used for this master thesis (Tobler, 2010).

Nominal heating power [kW]	Power coverage factor [%]	Mass flow evaporator side [m³/h]	Mass flow condenser side [m³/h]
6	8	1.3	0.5
11	15	2.45	1
20	28	5.1	1.9
40	56	11	3.2
75	104	14.3	7.3

4.7.2 Ground source

One of the main goals for this master thesis has been to improve the modelling of the ground source system. Due to the improvements in Carnot ground source block already described, it has been possible to perform a more realistic analysis of the temperature fluctuations in the ground. In order for the modelling of the ground to give proper results, it is important that the different design parameters are investigated. In the previous version by Murer, the GSHP where simulated with 50 BHEs for all heat pump sizes (Murer, 2015). This caused a large over dimensioning of the borehole field and unrealistically stable brine tempertures. Table 4 shows some of the main parameters of the ground source system used for simulations during this thesis. The type of collector and method of heat transfer calculations are given in the Carnot ground source model and cannot be changed by the user. The ground conductivity and temperature gradient in the ground are kept at default values from Carnot. Average outdoor temperature is to 6 °C, which can be found from the SIMIEN data. Borehole depth and distance between the boreholes are based on typical Norwegian conditions. The 25 % glycol concentration in the brine is given in the heat pump manufacturer data. This gives the brine a freezing temperature of – 13 °C (Tobler, 2012). Depth of boreholes and the distance between the boreholes are set to typical values for Norwegian conditions.

Table 6 – Main parameters of ground system used for simulations.

Parameter	Value	Description
Collector type	-	Double U-tubed (grouted)
Brine	75- 25 %	Water-glycol mixture
Borehole depth	200 m	
Multiple distance	20 m	Distance between boreholes
Ground conductivity	2 W/mK	
Temperature gradient	0.025 W/m	
Ground water flow considered	-	No. Only conduction.

When dimensioning the borehole filed, two different dimensioning principles are used. The required number of boreholes is firstly determined from a maximum specific annual heat extraction rate from the ground of 60 kWh/(m*yr). As the total yearly heat extraction depend on the result of simulations, additional assumptions had to be made. It is assumed that for the larger heat pump sizes the whole space heating and DHW demand is covered by the heat pump. Further, an annual average COP of the heat pump of 4 is assumed. This gives a total required borehole length of 583 meters, resulting in three 200 meters deep boreholes. For the 6kW and 11kW heat pumps, it has been assumed that a considerable amount of the total annual heat demand is covered by the peak loads and the number of boreholes is therefore reduced to two BHEs.

It is also set an additional restriction on the maximum specific power extraction of 45 W/m. This restriction is set to ensure that the brine temperatures does not get too low for the largest heat pump sizes. It is here assumed that the maximum heat extraction rate occurs at the temperatures levels of 5 °C into the evaporator and 35 °C out of the condenser. Table 7 shows the dimensioning of the five different heat pump sizes.

Table 7 – Dimensioning of BHEs.

Nominal power	Number of boreholes	Restriction
6	2	Energy [kW/(m*yr)]
11	2	Energy [kW/(m*yr)]
20	3	Energy [kW/(m*yr)]
40	4	Power [W/m]
75	7	Power [W/m]

4.7.3 Peak load system

The peak load systems evaluated in this thesis are electric heaters and biomass boilers. The biomass boilers are using wood pellets and has an efficiency of 74 %, while the efficiency of the electric heaters are set to 95%. The peak loads are connected to the heat exchangers of the space heating and DHW heating tank in the same manner as for heat pumps. The installed capacity of the peak loads was in the previous model set to 50 kW for all heat pump sizes with the passive house building. In collaboration with supervisors, it was decided to dimension the peak load unit connected to the space heating tank for each heat pump size. The nominal power of the peak load unit connected to the space heating tank is now the maximum power demand for space heating of 72kW minus the nominal capacity of the heat pump.

$$q_{pl\_sh,nom} = q_{sh,max} - q_{hp,nom}$$

(eq. 4.1)

Mass flow in the peak load heat exchanger in the space heating tank is set to give a temperature difference between inlet and outlet of 10 °C. Table 6 shows the installed capacity and mass flow rate from the peak load unit connected to space heating tank for the different heat pump sizes.

Table 8 – Dimensioning of peak load system for heating of SH tank for different heat pump sizes.

Heat pump size [kW]	Peak load power [kW]	Mass flow rate [kg/s]
6	66	1.6
11	61	1.5
20	52	1.3
40	32	0.8
75	0	0

The dimensioning of the peak load unit for the DHW tank is dimensioned to cover the maximum DHW power. Mass flow in the heat exchanger is set to give a temperature difference between inlet and outlet of 5 °C. This gives a peak load power of 2.2 kW and mass flow rate of 0.1 kg/s. The reason for the change in dimensioning strategy is small power needed for DHW.

4.7.4 Heat Exchanger

The heat exchangers have been idealized with high UA-values. Section 5.5.3 shows results from sensitivity analysis of the heat transfer efficiency of the heat exchanger in the space heating tank.

4.7.5 Storage tanks

The size of the space heating tank is set to the same value as in the previous version of 4 m³. For the cooling tank introduced in this thesis, the size of the tank is set to be equal to the space heating tank. As a result of the reduction in DHW consumption, the size of the DHW tank is reduced. As seen in the thesis of Murer, the best system performance is found when the heat pump is connected to the lower part of the heating tanks and the peak loads are connected to the upper part of the tank (Murer, 2015). This strategy is also chosen in this thesis. Figure 9 shows an overview of the parameters of the storage tanks.

Table 9 – Design of the different storage tanks.

	Space heating tank	DHW tank	Space cooling tank
Volume [m³]	4	1	4
Radius [m]	1.4	0.8	1.4
Relative inlet/outlet of heat pump	0 / 0.5	0 / 0.5	0/1 *
Relative inlet/outlet of peak load	0.5/ 0.7	0.5/ 0.7	-
Relative height of inlet/outlet of tank	0/ 1	0/ 1	1/ 0

* connected to the heat pump in forced cooling mode.

5. Results

This chapter shows and discusses results from simulations with the decision tool performed during the thesis. Results from simulations given in section 5.1 to 5.4 are based on the dimensioning shown in section 4.7. Simulations in section 5.1 to 5.3 uses electric heaters for peak loads, while section 5.4 look at the effects of using a biomass boiler. Different parameters are in section 5.5 changed in order to evaluate their influence on the overall performance. In section 5.6, the different results from simulations are compared with the results of Murer. The trade-off between accuracy and computation time is investigated in section 5.7.

5.1 Short term results

Section 5.1 shows results of short term simulations. It aims firstly to prove that the decision tool works properly and to detect possible weaknesses. Secondly, it shows how run times of the different system modes and temperatures in the system differ for the different heat pump sizes.

5.1.1 DHW

As described in section 3.3, the DHW consumption is based on a repeating sequence of one week and the set point temperature is increased by 10 °C one day of the week. Figure 29 shows the set point temperature and the temperature at the top and at one third from the top of the DHW tank for the eight first days of the year for the 20kW heat pump system. Control of the heat pump and peak load unit used to heat up the tank is also shown. According to the control strategy, the heat pump is turned on when the temperature at one-third from the top of the tank is three degrees above set point temperature and off when it is eight degrees above this temperature. The figure shows that the at the top of the tank is always higher than supply temperature which means that the system is able to deliver the given DHW demand. Over the course of one week the heat pump is used twelve times for heating the DHW tank. The peak load unit connected to the DHW tank is only used one time of the week when the set temperature is increased. Results for the other heat pump sizes are quite similar except that the run time of the heat pump increases with decreasing heat pump size.
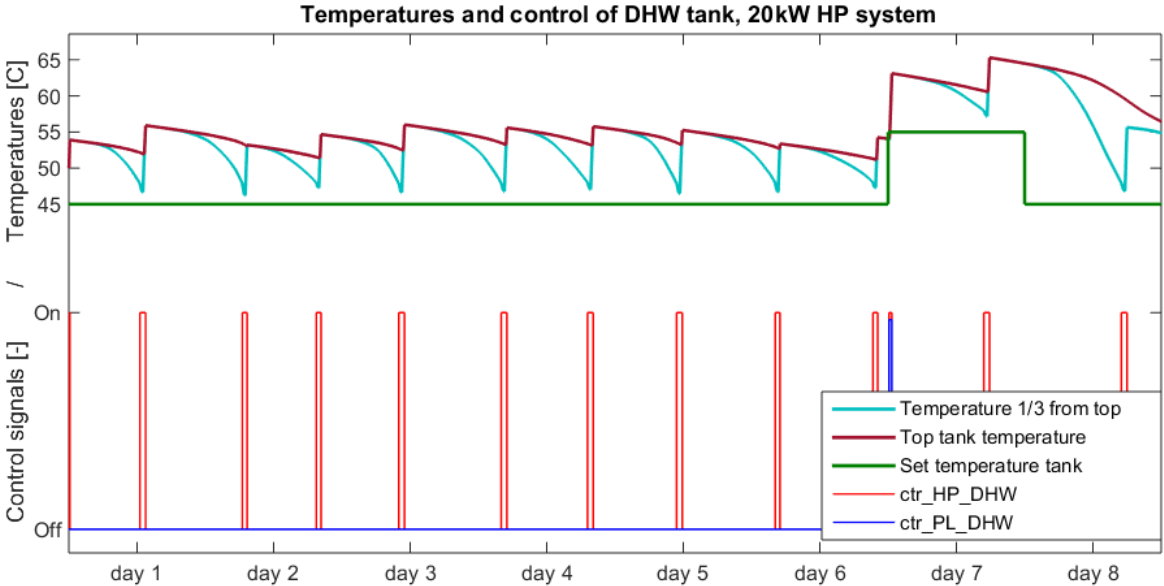
Figure 29 – Temperatures and control signals for the DHW system over one week for the 20kW heat pump system

.

5.1.2 Winter simulations

In order to evaluate the performance of the system in the winter, simulations have been performed over the coldest days of the year when the heating demand is at the highest. If the system is able to deliver sufficient amount of heat in this period, it is assumed that the system also will do so for the rest of the year. It should however be emphasised that the Simien data is based on a typical metrological year and some years will have a larger maximum space heating demand. Figure 30 shows the space heating demand and outdoor temperature from SIMIEN over three days in the winter. The two first days (day 52 and 53 of the year) have a peak space heating demand that is equal to the maximum space heating power demand through the year of 72kW. Day 53 also have the lowest yearly outdoor temperature with about - 25 °C. Simulations over this period are performed in order to evaluate the performance of the system in space heating mode.
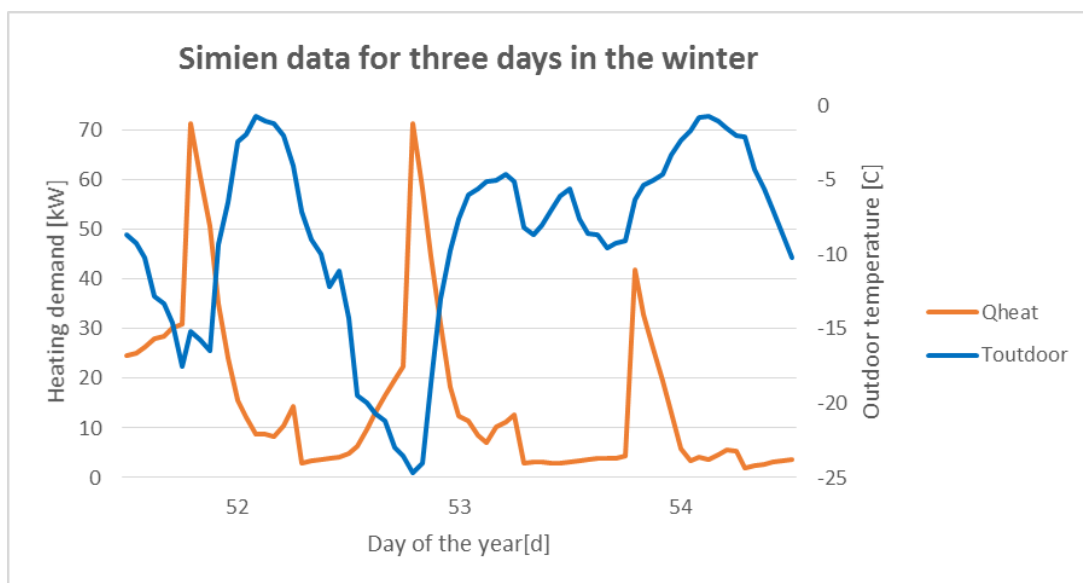
Figure 30 – SIMIEN space heating demand and outdoor temperature over three days in the winter.

Figure 31 shows the same type of graph as in section 5.1.1, but with temperatures and control of the space heating tank instead of the DHW tank. The outlet temperature of the space heating tank always stays above the supply temperature of the floor heating system. The run time of the heat pump during winter is much higher for the space heating tank than for the DHW tank. During the coldest periods, as for day 52 and 53, there is also significant use of the peak load unit.

Figure 31 – Temperatures and control signals of the space heating tank for the 20kW HP system over three days in the winter.

Figure 32 shows the inlet and outlet temperature of the evaporator and condenser over the same time period in winter. The temperature difference between inlet and outlet is much lower for the evaporator (cold side) than for the condenser side (hot side). The reason for this is that the mass flow rate of the brine in the ground is more than double of the mass flow rate of the water on the hot side (see table 5). The minimum inlet and outlet temperature of the evaporator is about 4 °C and 0.5 °C respectively. Outlet temperature from the condenser in space heating mode is in the range of 40 to 45 °C. During the three days period of simulation, the heat pump is used four times to heat up the DHW tank. When the system is switched to heating up the DHW tank, the inlet and outlet temperature are initially very low. This is caused by the heat exchanger connected to the heating tanks being at lower part of the tank and that the inlet water flowing into the DHW has a constant temperature of 5 °C. As the heat pump is used to heat up the DHW tank, the outlet temperature is quickly heated up to a maximum of around 62 °C. All results from figure 32 are in accordance with expectations.
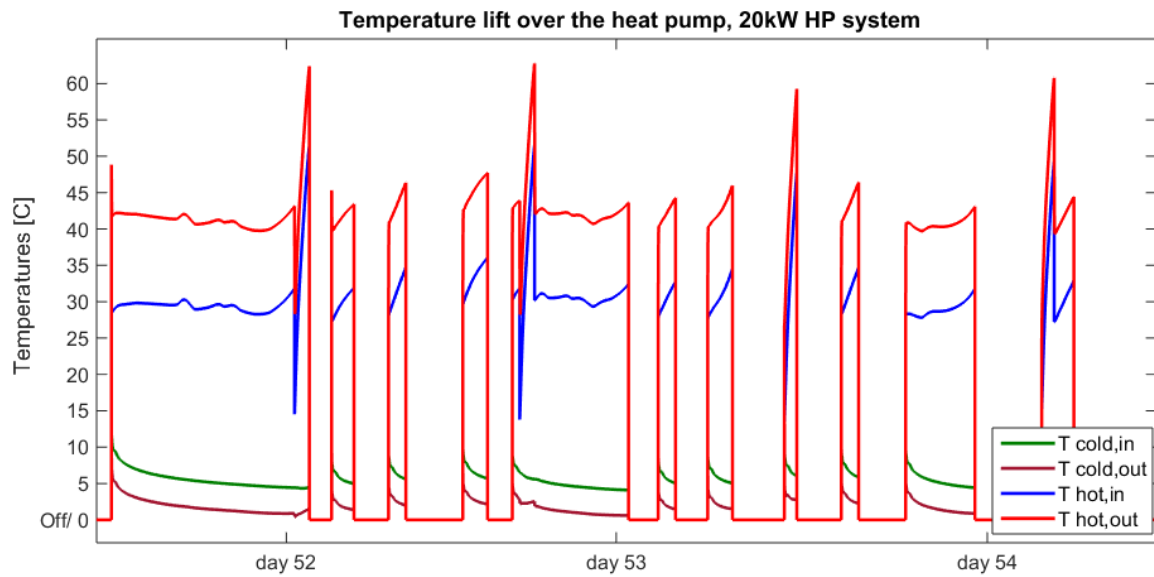
Figure 32 – Inlet and outlet brine/ water temperature of the evaporator/ condenser for a 20kW heat pump system.

The COP and the control of the heat pump for heating up DHW and space heating tank is shown in figure 33. As expected, the COP is lower in DHW mode than in space heating mode. When the heat pump is turned on or switches between space heating and DHW mode, the initial COP is very high. This is caused by a combination of high initial ground temperatures and low initial water temperature (see figure above). When the heat pump is not used, the temperature in the boreholes gradually increases and tank temperatures gradually decreases. As the temperature of the brine decreases and the temperature of the water increases, the COP of the heat pump decreases. At one moment during the simulation shown below, the COP becomes negative. The exact reason for this is not certain.

Coefficient of Performance, 20kW HP system
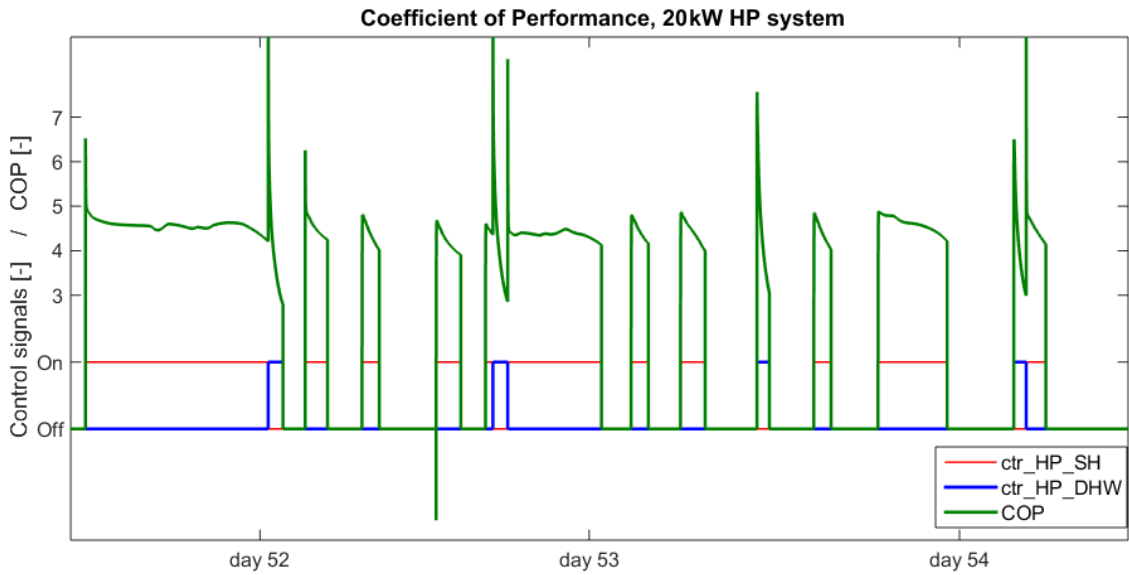
Figure 33 – COP of the heat pump over three days in the winter for the 20kW HP system.

Comparing the performance of the 20kW heat pump system with a 6kW heat pump system shows that the total run time of the heat pump increases and that the peak load unit is used more rapidly for the smaller heat pump size. As a results of the nominal power of the peak load unit being higher for smaller heat pump sizes, the run time of each peak load cycle is reduced and the tank is quickly heated up. The system is able to deliver sufficiently high temperatures to the floor heating system also for the 6kW heat pump case.

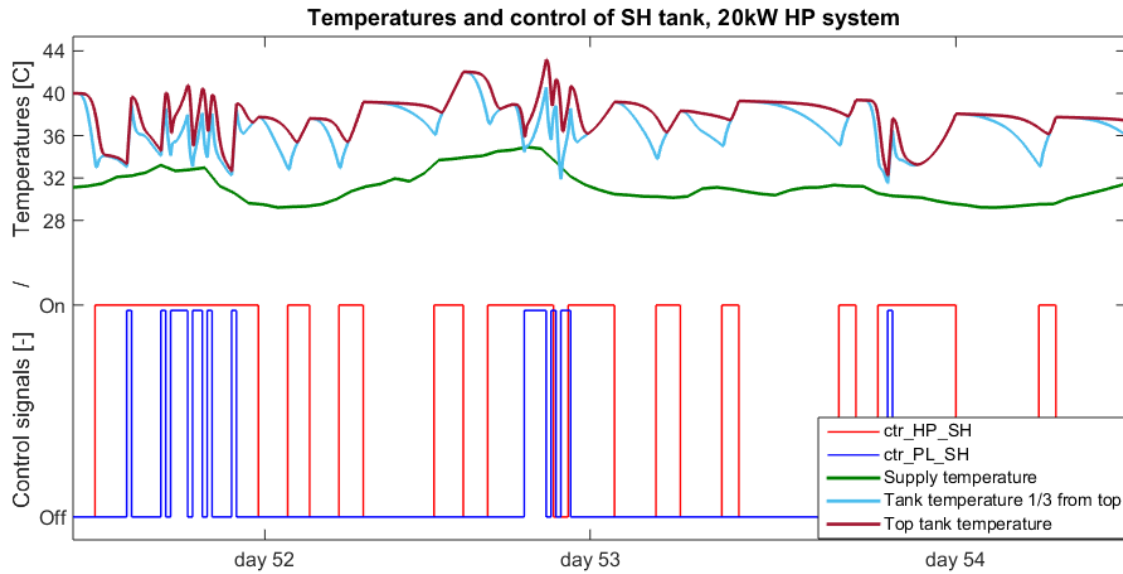**Temperatures and control of SH tank, 6kW HP system**

Figure 34 - Temperatures and control signals of the space heating tank for the 6kW HP system over three days in the winter.

Side 51

Figure 35 shows the same type of graph as in figure 32, but here for the 6kW heat pump system. As a results of the dimensioning described in 4.7.2, the brine temperature is higher for the 6kW heat pump than for the 20kW heat pump. It should however be emphasised that the graphs in this section does not include the cooling down of the ground over longer periods.
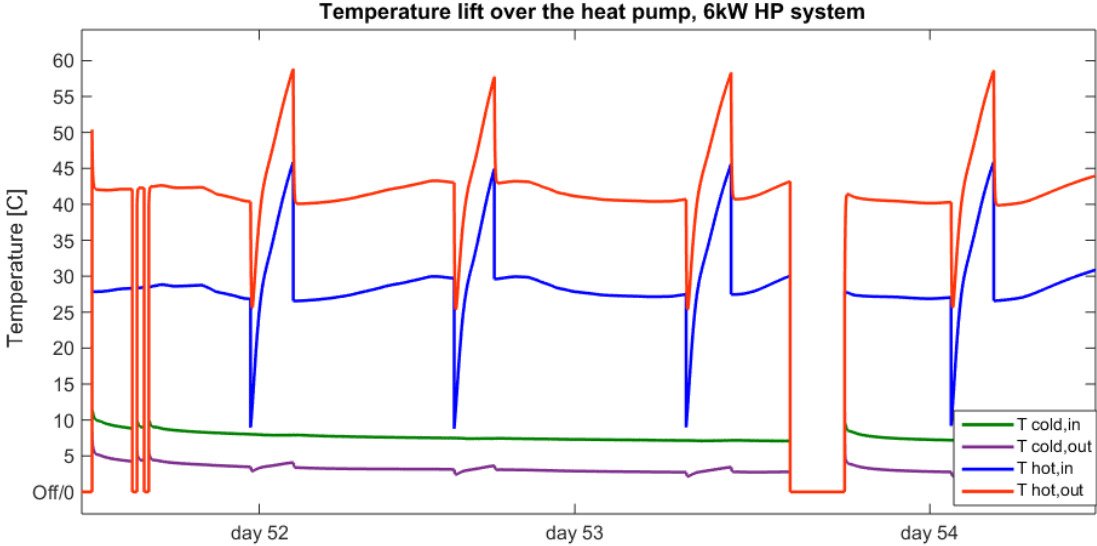
Figure 35 – Inlet and outlet brine/ water temperature of the evaporator/ condenser for a 6kW heat pump system.

5.1.3 Summer simulations

In the same way as the system has been verified over three days in the winter, the operation during summer is evaluated over three days in the summer (day 182- 184). Figure 36 shows the space cooling demand and outdoor temperature over the three days. Day 182 and 183 are particular warm days with day 183 having the highest yearly outdoor temperature of 30 °C. These two days have a long period in which the cooling demand is equal to the maximum cooling demand from the Simien data of 14.4kW.
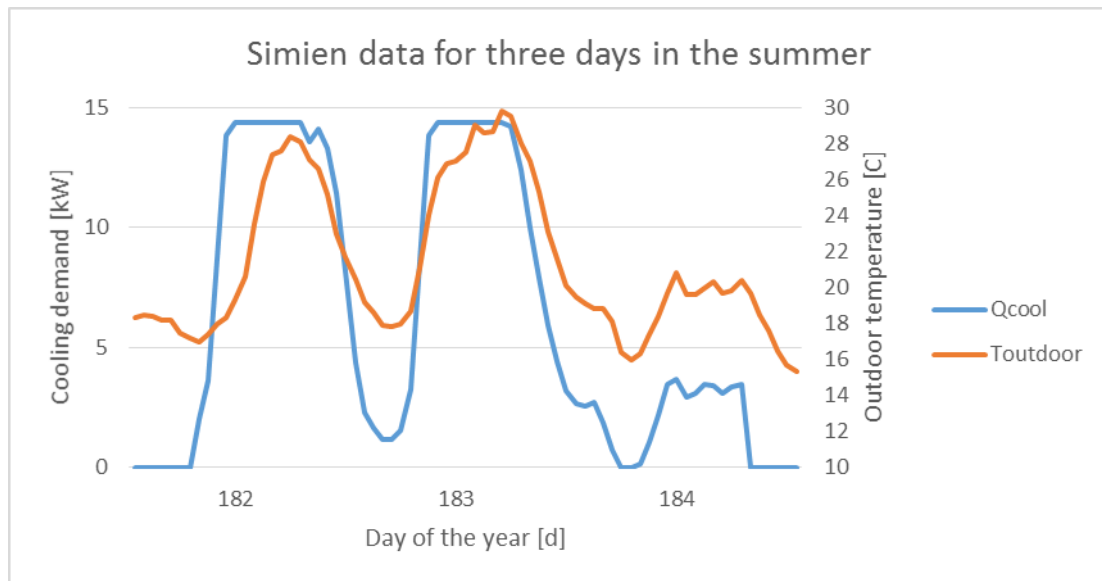
Figure 36 – SIMIEN space heating demand and outdoor temperature over three days in the summer.

For the larger heat pump sizes, the whole cooling demand is delivered by free cooling. The reason for this is that the larger heat pumps also have an increased mass flow rate in the ground and thereby an increased potential for free cooling. Figure 37 shows tank temperatures, cooling supply temperature and control of free cooling for the 40kW heat pump system over the same period as described above. Over this period there is no use of forced cooling. The figure shows that the bottom tank temperature always stays below the supply cooling temperature and the system is thereby able to deliver sufficient cooling to the building.
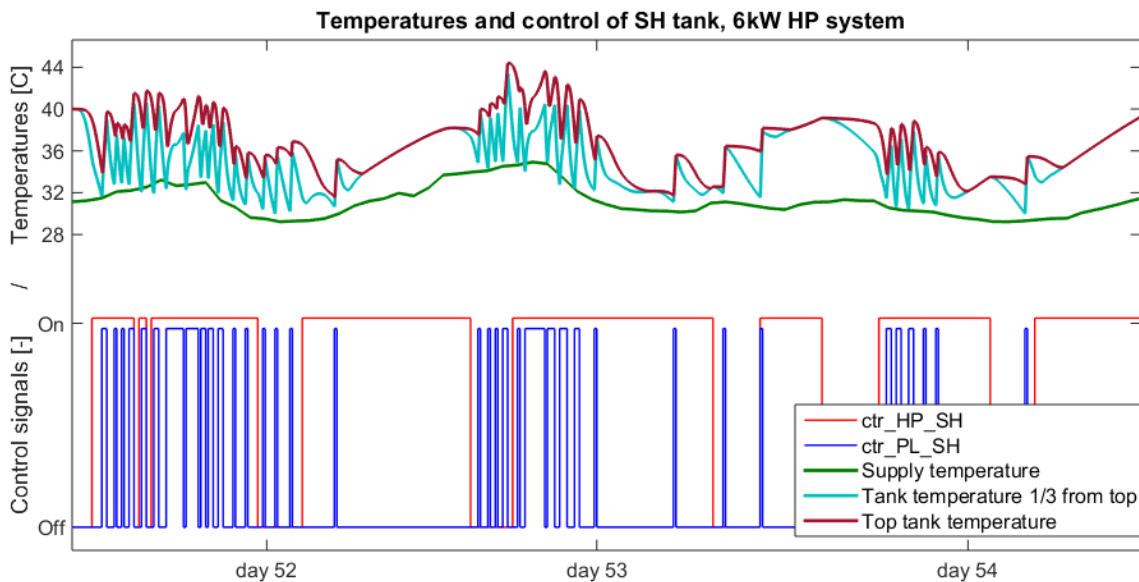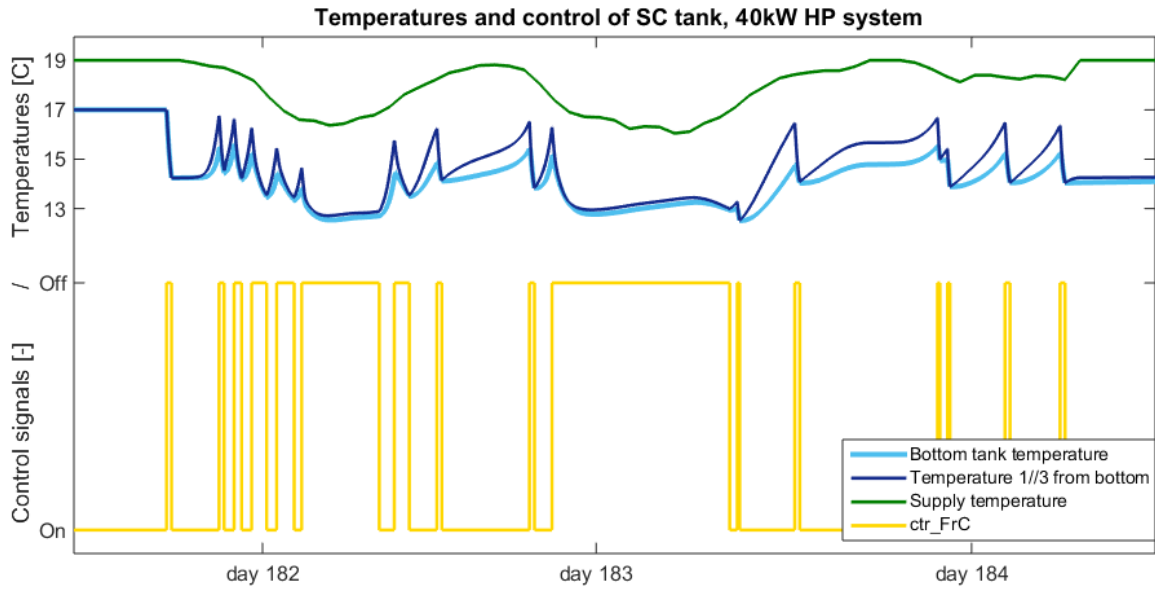
Figure 37 – Temperatures and control signals of the space cooling tank for the 40kW HP system over three days in the winter.

Figure 38 shows the inlet and outlet temperature of the boreholes over one free cooling cycle during the warmest day of the year. After an initial short period where the temperature difference is fluctuating, the temperature difference between inlet and outlet is stabilized to around 1.2 °C. After the start up fluctuations, the brine flowing from the boreholes to the cooling tank stays in the range of 12 to 13 °C.
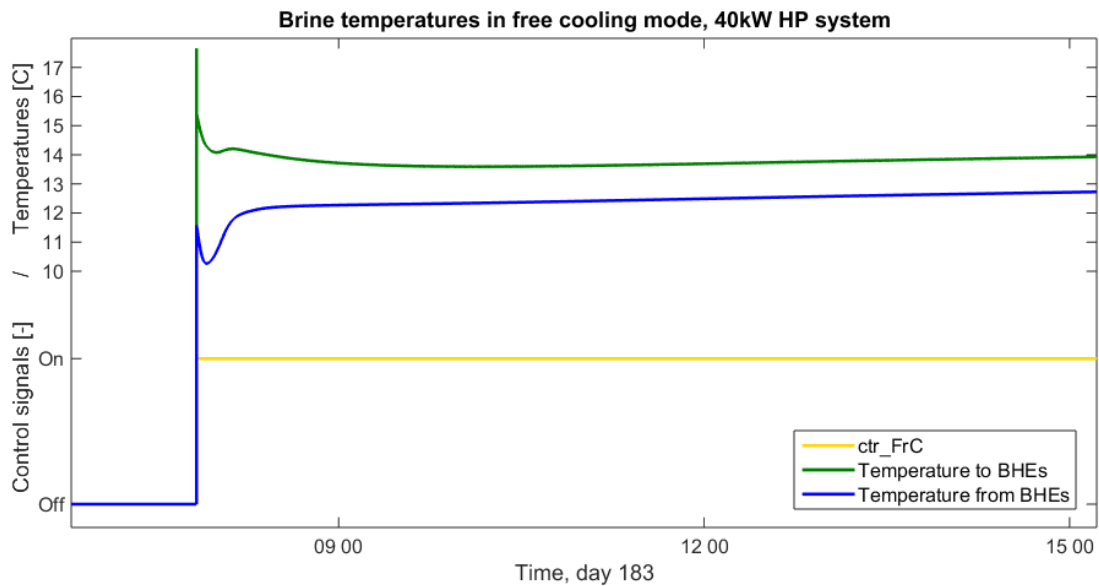
Figure 38 – Brine inlet and outlet temperature during free cooling mode.

Side 54

For the smallest heat pumps, the cooling demand is covered with a combination of free and forced cooling. Figure 39 shows tank temperatures, supply temperature and control for the 6kW heat pump system. In day 182 and 183, forced cooling is extensively used. The heat pump is not to able cover the cooling demand at the coldest periods as the capacity of the heat pump is smaller than the maximum cooling demand. Smaller heat pump sizes also cause longer run times for DHW. The figure shows that in the periods when there is both cooling demand and need for heating of the DHW tank, there is a large gap between the desired supply temperature and the actual supply temperature.
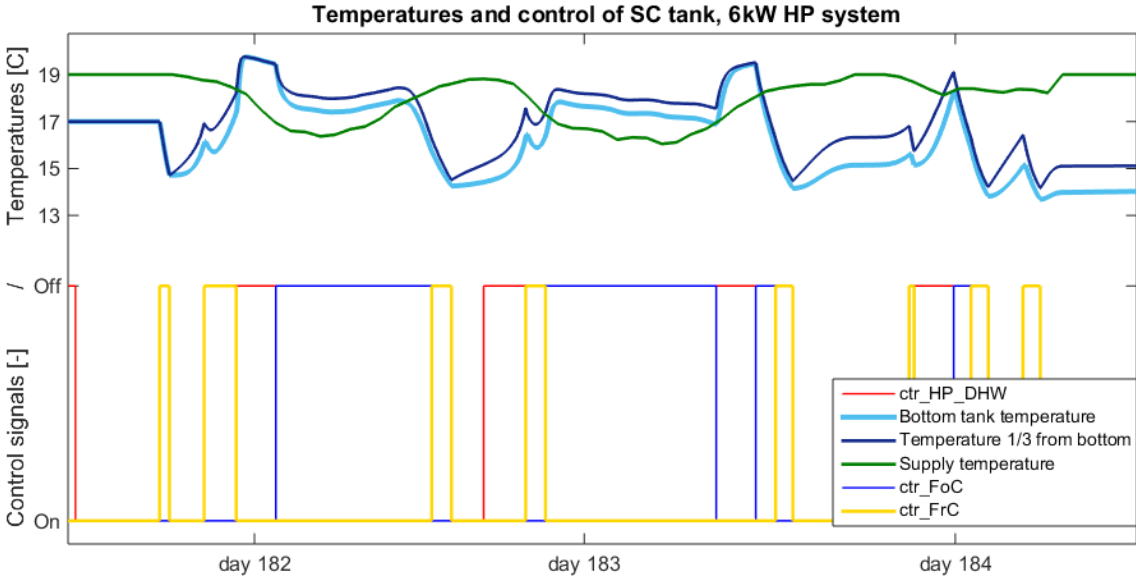
Figure 39 – Temperatures and control signals of the space cooling tank for the 6kW HP system over three days in the winter.

The 6kW heat pump is used to show the performance of the heat pump in forced cooling mode as this is the heat pump with the longest run times for forced cooling. Figure 40 shows the inlet and outlet temperature of the evaporator and condenser for one forced cooling cycle in day 183. Figure 41 shows the COP over the same time period. The temperature lift on the cold side is about 6.5 °C, which is much higher than for the free cooling. As the outlet of the heat exchanger is located at the top of the tank and the heat exchanger efficiency is set the an idealized value, the temperature out of the heat exchanger is close to the return temperature from the cooling circuit (around 19 °C). In forced cooling mode, the inlet temperature to the condenser is lower than the inlet temperature to the evaporator. This cause a very high COP. The COP is above 8.5 for the whole cycle.
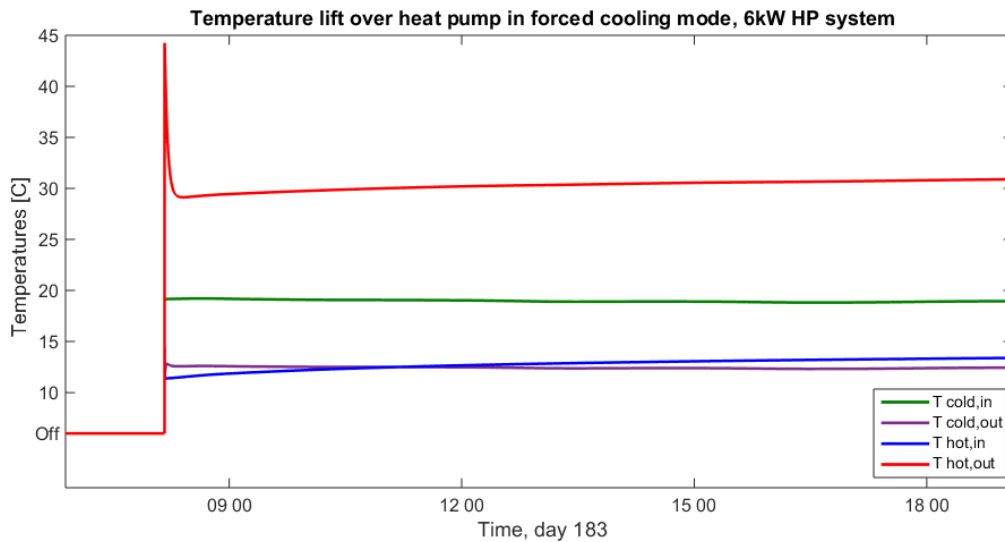
Figure 40 - Temperature lift over the heat pump in forced cooling mode, 6kW heat pump.
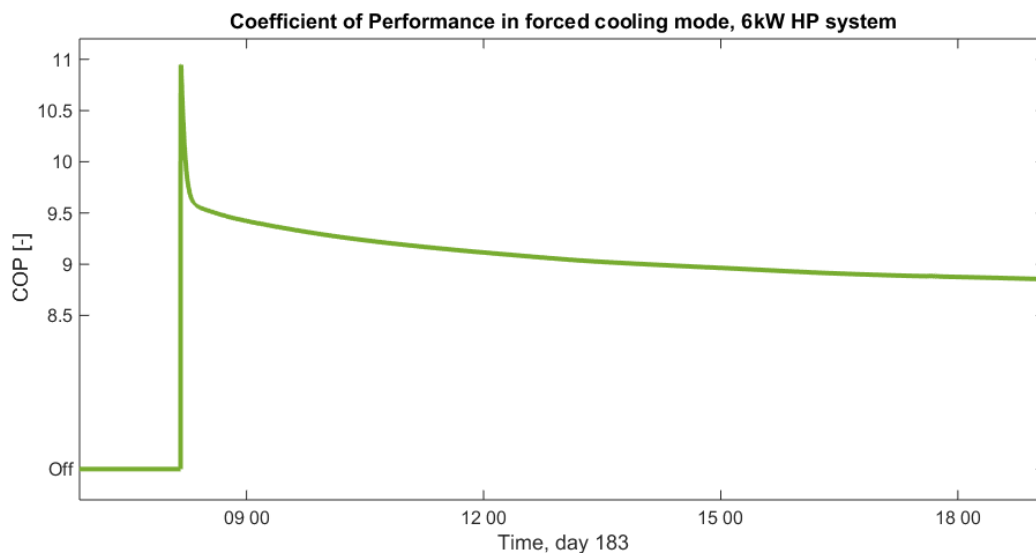
Figure 41 - Coefficient of performance in forced cooling mode, 6kW heat pump system.

5.2 Yearly results

5.2.1 Overall results

Figure 42 shows how the annual energy consumption and total SPF vary with varying heat pump size. In the total SPF, both the energy consumption of the heat pumps and peak loads are included. So are the delivered free cooling and the heat losses from the storage tanks. Energy consumption of pumps are as previously explained not included in the model. The total energy consumption decreases and the SPF increases with increasing heat pump sizes. For the three largest heat pump sizes, the dominant energy consumption comes from electric consumption of

the compressor. For the 6kW and 11kW heat pump, the electric heaters are the most energy consuming components. As the electric heaters have an efficiency lower than one, the high use of electric heaters cause a dramatic reduction in SPF.
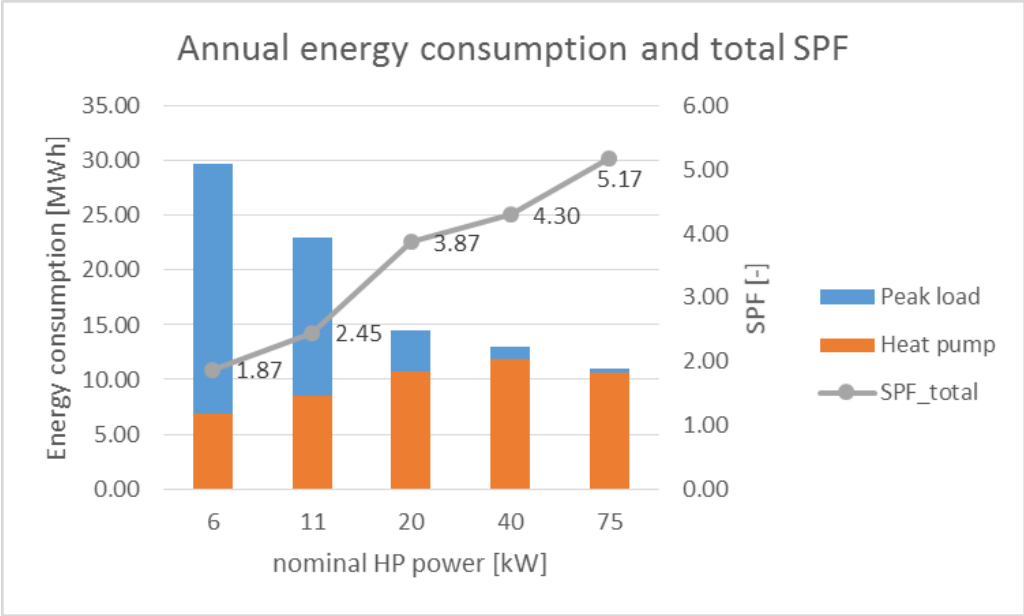
Figure 42 - Annual energy consumption and total SPF for five different heat pump sizes.

The overall performance for the different heat pump sizes can also be evaluated by looked at the annual delivered energy. Figure 43 shows the annual delivered energy from the different heat pump modes, the two peak load units and fom free cooling. The total delivered energy is almost identical for all systems. Virtually all the energy consumption of the peak loads comes from heating up the space heating tank. This is because of the low maximum DHW power demand and that DHW has priority for the heat pump operation. The figure also shows that for the three largest heat pump sizes, almost all of the cooling demand is covered by free cooling. The amount of energy delivered by the heat pump to the space heating tank varies greatly with different heat pump sizes while the amount of energy to the DHW tank stays more or less constant.
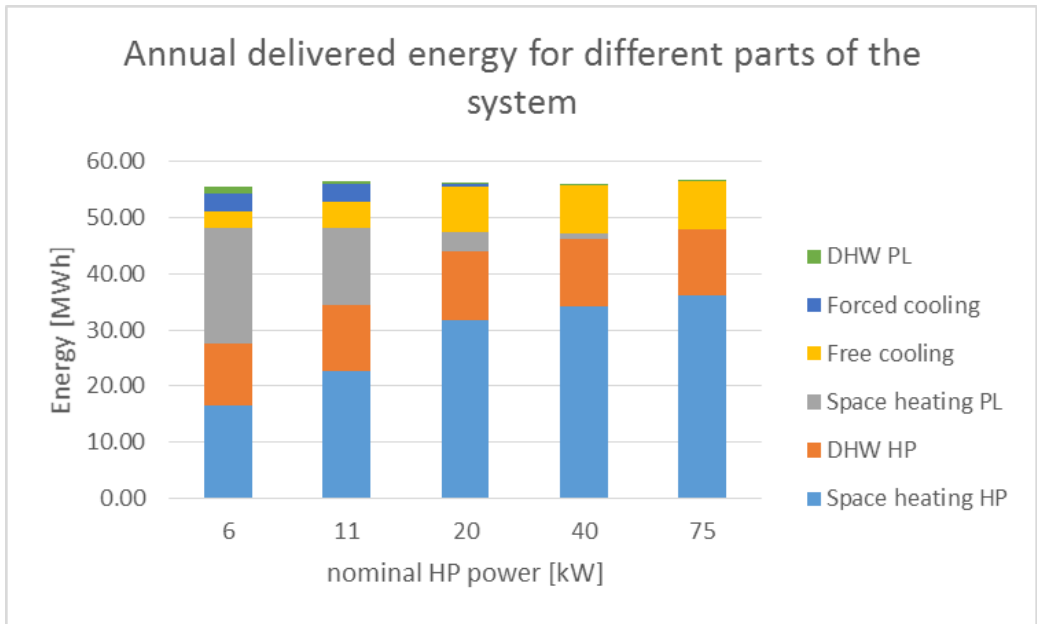
Figure 43 – Total annual delivered energy for the different components for the five heat pump sizes.

The total SPF of the heat pump in different modes is shown for the 20kW heat pump system in figure 44. Results correspond to the results found in section 5.1. The COPs in DHW mode is lower than in space heating mode due to the higher condensation temperature. The SPF of the heat pump is lower than the total SPF of the system (3.87 versus 4.3). About 26% of the total energy consumption for the 20kW system is covered by the electric heaters. Energy delivered by the electric heaters does however only amount to about 6% of the total delivered energy.
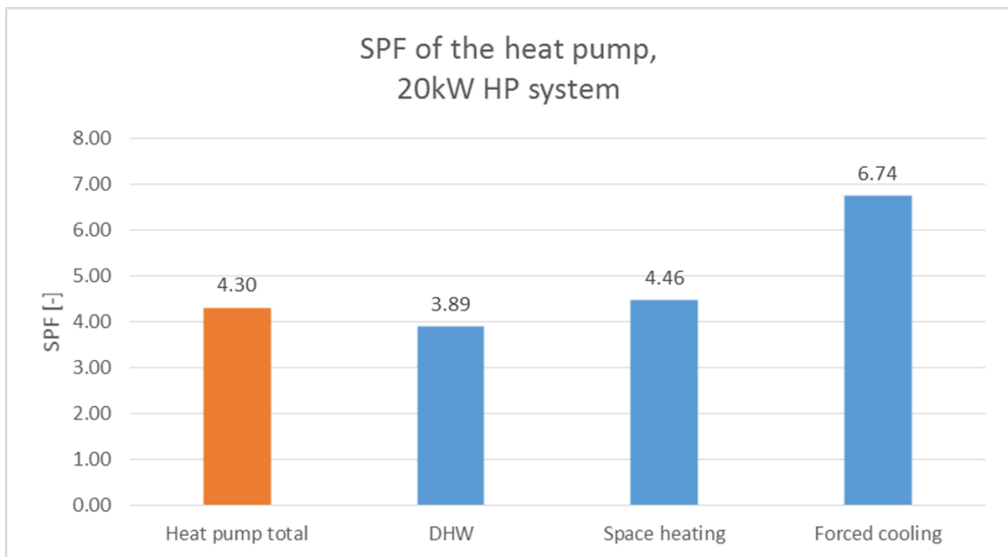
Figure 44 – SPF for the heat pump in different modes, 20kW HP system.

Figure 45 shows the weekly average power consumption for the 20kW system. It shows clearly that the major of the energy consumption is at the beginning and at the end of the year when there is a need for space heating. Most of the energy consumption during summer comes from heating up the DHW tank with the heat pump. As the DHW demand is set to be equal for all weeks throughout the year, the energy consumption is relatively constant in the summer. Week number eight have the highest average power consumption of 7kW, which is about 10% of the maximum power demand for space heating.
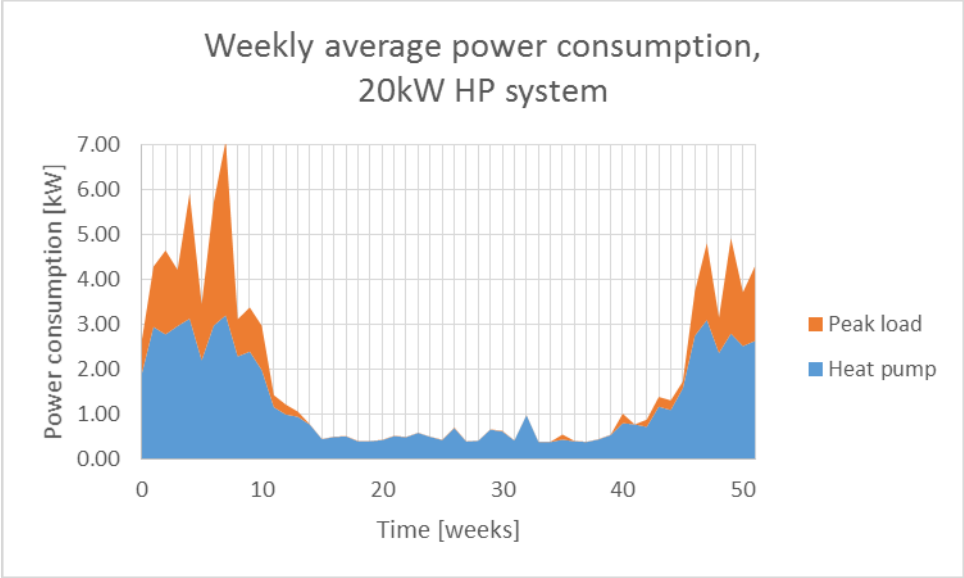
Figure 45 – Weekly average power consumption through the year, 20kW HP system.

Heat losses from the space heating and DHW tank to the ambient over the year for the 20kW heat pump system is shown in figure 46. The figure shows that the total losses increases steadily for the DHW tank, while the losses form the space heating tank are highest during the winter. The annual losses is 0.78MWh for the space heating tank and 0.72MWh for the DHW tank. This means that 2.2% of the heat supplied to the space heating tank and 5.6% of the heat supplied to the DHW tank is lost to the ambient. The heat losses are proportional with the surface area of the tank and the temperature difference between the tank and the ambient. While the temperature difference is highest for the DHW tank, this also has a lower heat transfer area due to the reduced tank size.
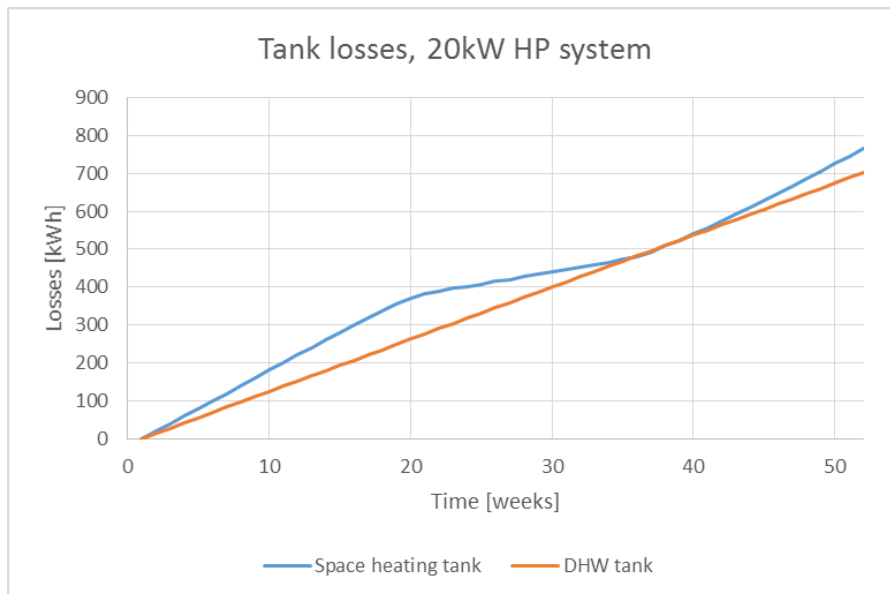
Figure 46 – Heat losses from DHW and space heating tank to ambient.

5.2.2 Demand vs Energy delivered

This section aims to evaluate whether the system is able to cover the buildings demand by comparing the input data to the system with the simulation results. Table 10 shows results for the 20kW heat pump system.

Table 10 – Comparison between input demand and simulation data for 20kW HP system.

	Space cooling	**Space heating**	**DHW**
Simulation [MWh/y]	8.58	35.35	12.2
Demand [MWh/y]	8.66	35.3	12
Deviation [%]	(-) 0.9	(+) 0.2	(+) 1.5

The figure shows that there are small deviations between the energy demands and the delivered energy. This is an indication that the system is functioning correctly. However, for the 11kW and 6kW heat pump systems, the annual delivered cooling is 7.4 % and 28% lower than the cooling demand.

5.2.3 Cost and CO2 analysis

Figure 47 shows how the annual costs for a passive house building vary with different power coverage factors of the heat pump. The curve is fitted between results of the five different heat pump sizes. While energy costs decreases gradually with increasing heat pump sizes, the annual capital costs increases almost linear with increasing heat pump sizes. The 20kW heat pump system has the lowest annual costs of 37 254 NOK. The figure indicates an OCF around 26%. There should here be emphasised that there are many uncertainties regarding the result. This includes both uncertainties of different system parameters and cost parameters.
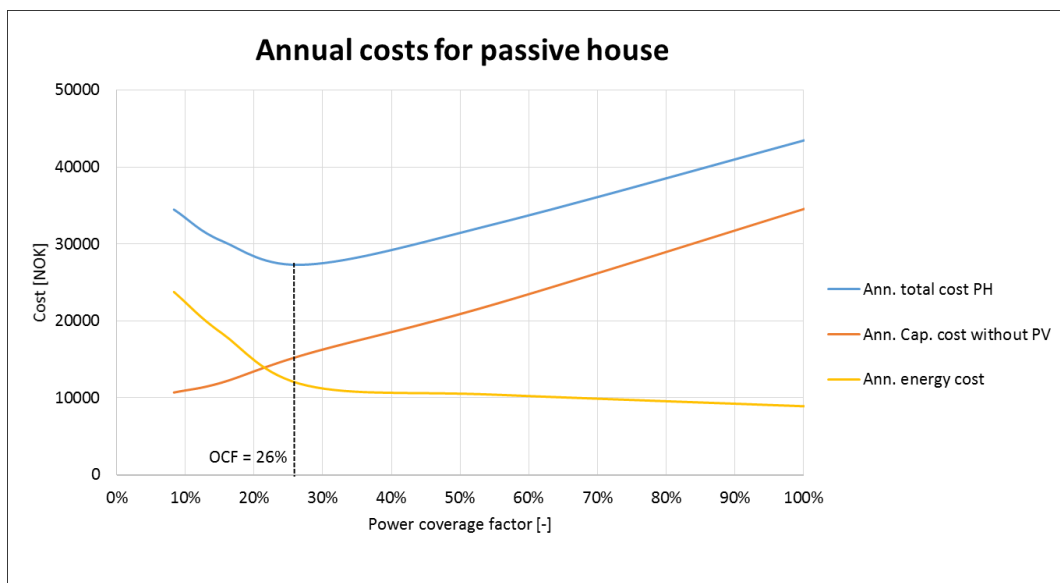
Figure 47 – Annual costs for passive house building.

The annual CO_2 for the heat pump coverage factors are shown in figure 38. The emissions are directly proportional with the annual electricity consumption. The figure below shows that there is a large reduction in emissions when going from the lowest coverage factor of 8% (6kW) to a coverage factor around 28% (20kW). The relative reduction in energy consumption and emission by further increasing the power coverage factor is much lower.
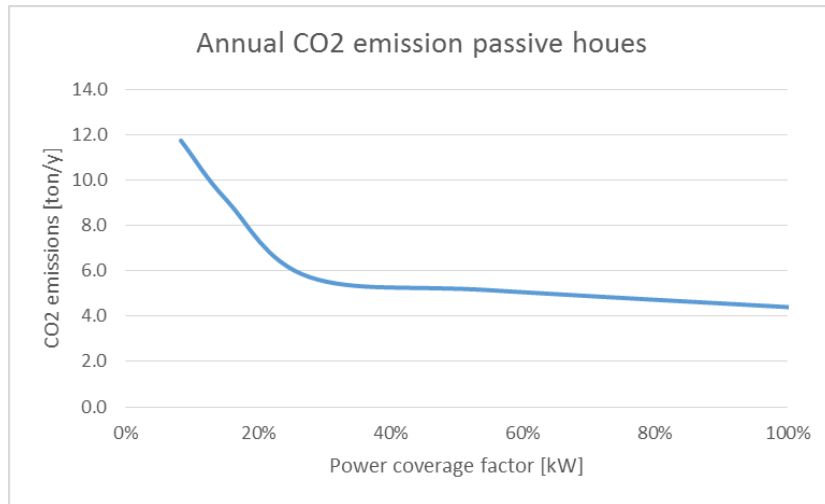
Figure 48 – CO₂ emissions as a function of power coverage factor.

Annual costs for the ZEB is shown in figure 49. As a result of the assumptions described in section 3.5, the annual costs of the ZEB have similar type of curve as for the passive house. The costs of PV are assumed to be directly proportional with the annual energy consumption of the building. As it is assumed that all the power generated by the PV panels can be sold for the same price as power is imported, no energy costs are included in the figure. The 20kW heat pump has the lowest costs also for the ZEB with an annual cost of 26 690 NOK which is slightly lower than for the passive house without PV panels.
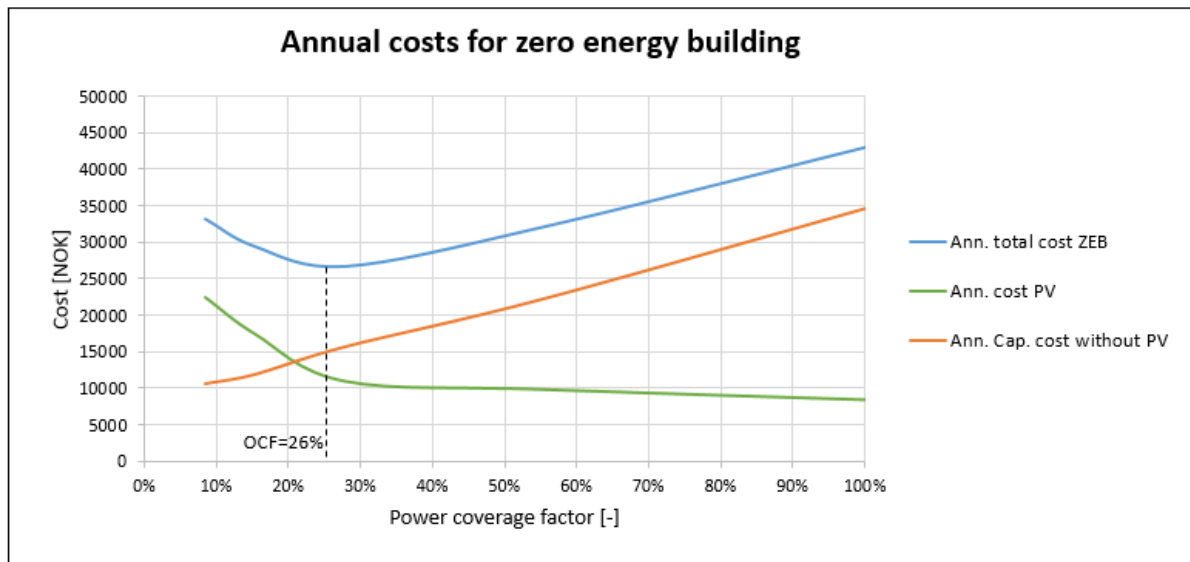
Figure 49 – Annual costs for ZEB.

5.3 Long term simulations

The total annual heat extraction from the ground is sufficiently higher than the annual heat injecting to the ground. Simulations have been performed over a period of four years to investigate how the ground temperatures vary over longer periods. Figure 50 shows the ground temperature at three different radiuses. The outer boundary temperature at a radius of 10 meters fluctuates slowly while the two temperatures closer to the borehole (radius of 1.7 and 4.1 meter) varies much more through the year. All temperatures decreases each year. The reduction is however relatively small. The average outer boundary ground temperature at the fourth year is 9.28 °C, which is 0.22 °C below the undistributed ground temperature. The average temperature at a radius of 1.7 meters from the boreholes is 0.32 °C lower for the fourth year than the first year of simulation. Sensitivity analysis of the number of boreholes and the ground temperature are described in section 5.5.1.
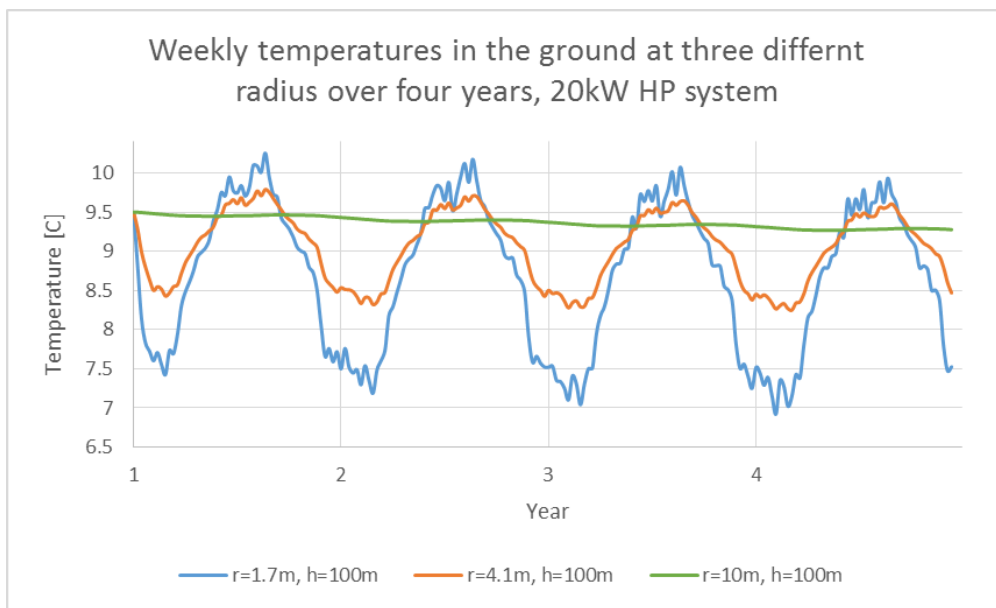
Figure 50 – Ground temperatures at the middle of the borehole at three different radius, 20kW heat pump system.

5.4 Bio boiler

This section investigates the change in results when the peak load unit connected to the space heating tank is replaced with a bio boiler. The bio boiler has significantly different characteristics than the electric heater. The bio fuel has a small reduction in energy prices

compared to electricity. However, the investment cost of the bio boiler is much higher than the electric heater. In figure 51, the annual costs with the two different peak load types are compared. The costs are significantly higher with the use of bio boiler for peak load heating. The difference in cost reduces as the heat pump coverage factor increases. The reason for this is the way the peak load has been dimensioned with decreasing nominal power for increasing heat pump size. The lowest annual costs for the bio boiler system are found with the 40kW heat pump. The costs are however highly flat over a large heat pump power coverage range.
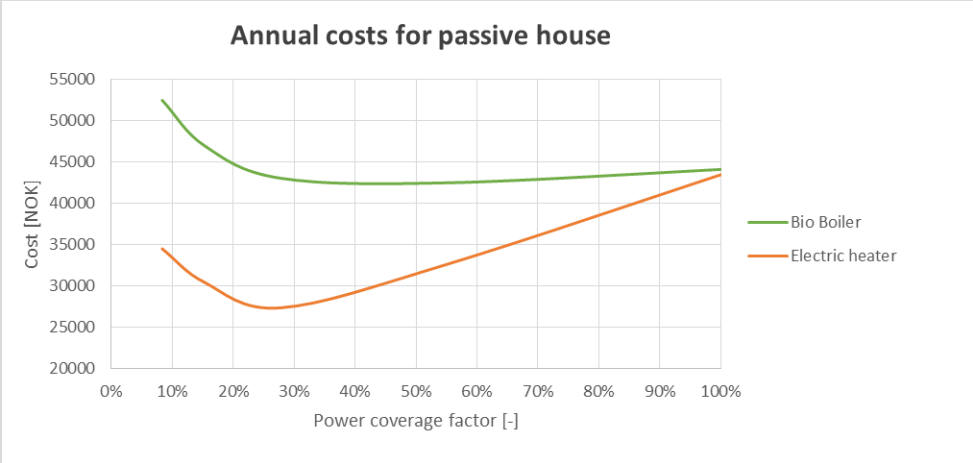
Figure 51 – Annual costs for the passive house with electric heater and bio boiler as peak load unit.

The emissions from bio fuel are significantly lower than for electricity. For this reason, the annual CO_2 emissions are reduced when changing from the use electric heaters to bio boilers. The largest difference in emission are with the lower heat pump coverage factors. For the larger heat pump sizes, the energy consumption of the peak load unit is small and the difference in emissions between the two peak loads are therefore also small.
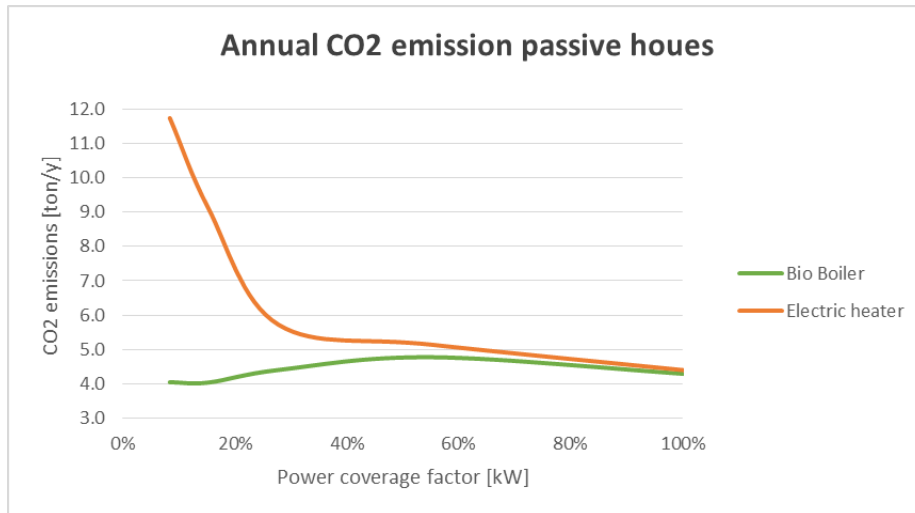
Figure 52 – CO₂ emissions for the passive house with electric heater and bio boiler as peak load unit.

5.5 Sensitivity analysis

5.5.1 Number of boreholes

By changing the number of boreholes for the same heat pump size, the specific heat extraction rate from the ground changes. Increased number of boreholes means a decreased specific heat extraction rate and thereby more stable brine temperatures. This section aim to evaluate what happens to the results when the number of boreholes are changed. All other dimensioning parameters are kept as described in section 4.7. Figure 53 shows the inlet brine temperature to the evaporator over one heat pump cycle used to up the space heating tank. It shows clearly that a decrease in the number of boreholes results in a reduced brine temperature.

Side 65
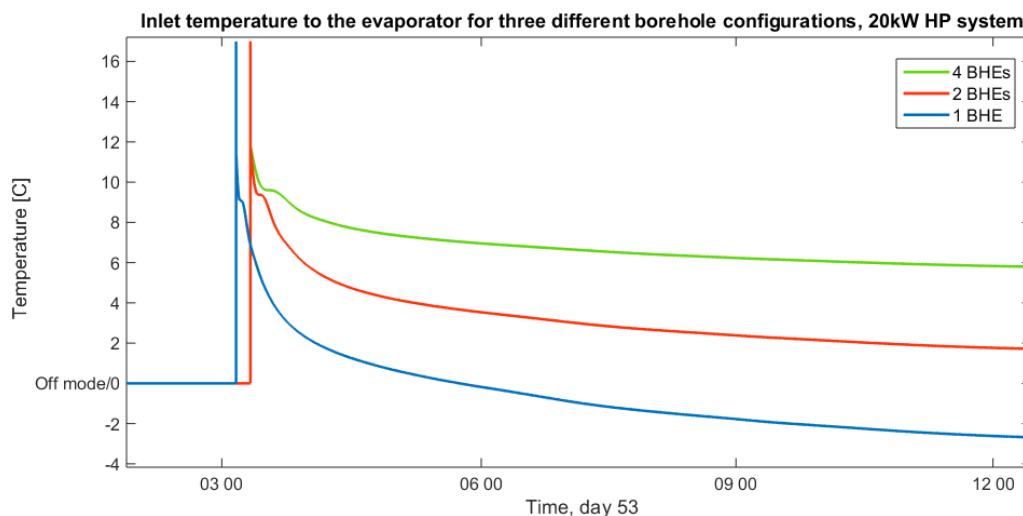
Figure 53 – Inlet temperature to the evaporator for three different borehole configurations, 20kW heat pump system.

Figure 54 shows the total SPF and the SPF of the heat pump for four different borehole configurations. The performance increases with increasing number of boreholes. The reduction in energy consumption per extra borehole is however gradually decreasing. It is also shown that the difference in total SPF and SPF of the heat pump gradually decreases for an increasing number of boreholes. The reason for this is that the energy consumption of the electric heaters are reduced with higher COPs.
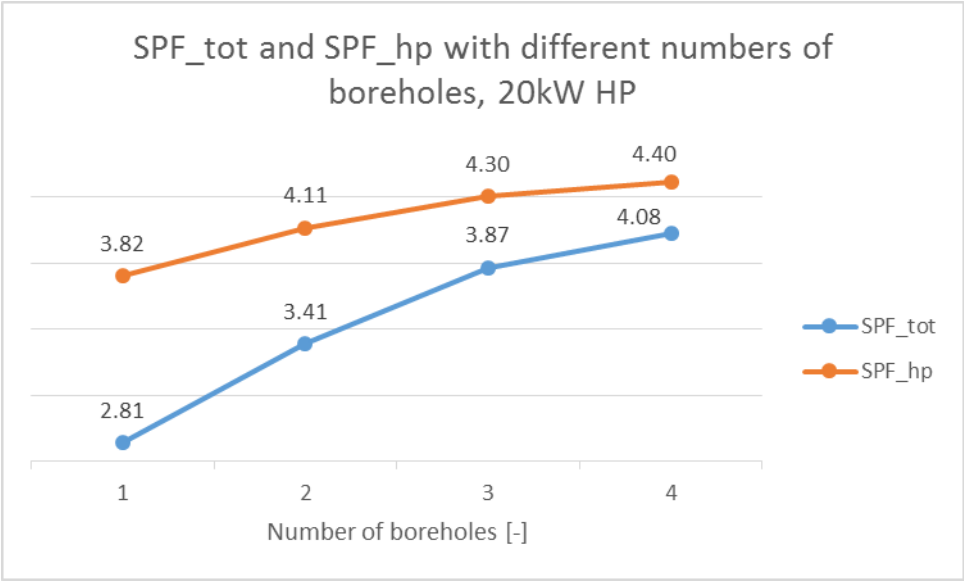
Figure 54 – SPF_tot and SPF_hp for the 20kW heat pump with four different borehole configurations.

While increasing the number of boreholes cause lower energy consumption and thereby reduced energy costs, it also cause increased investment costs. As seen in the figure below, the lowest annual cost is found with three BHEs.
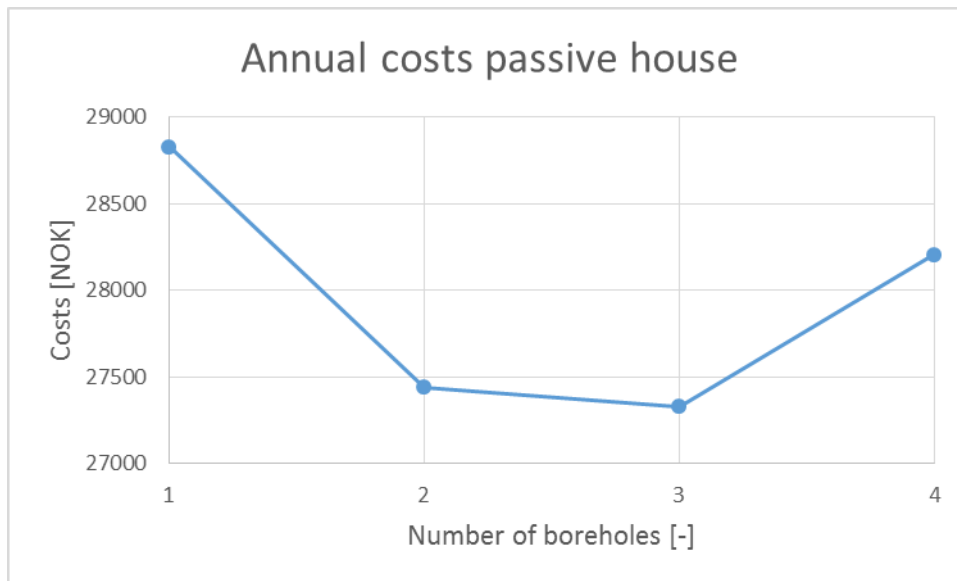
Figure 55 – Annual costs with passive house for 20kW HP system with four different borehole configuration.

The results described above only look at the performance for the first year. Depending on the ground conditions and the dimensioning of the borehole field, the temperature in the ground will decrease over longer periods of heat extraction. As the source temperature decreases, the energy performance of the heating system will also decrease. Figure 56 shows the ground temperature at a radius of 10 meters and depth of 100 meters over four years when the system is dimensioned with two and three boreholes. With a deceased number of boreholes the ground temperature is reduced more rapidly. From this reasoning, it can be concluded that the optimal number of boreholes, from an economical point of view, increases when looking at a longer periods of time.
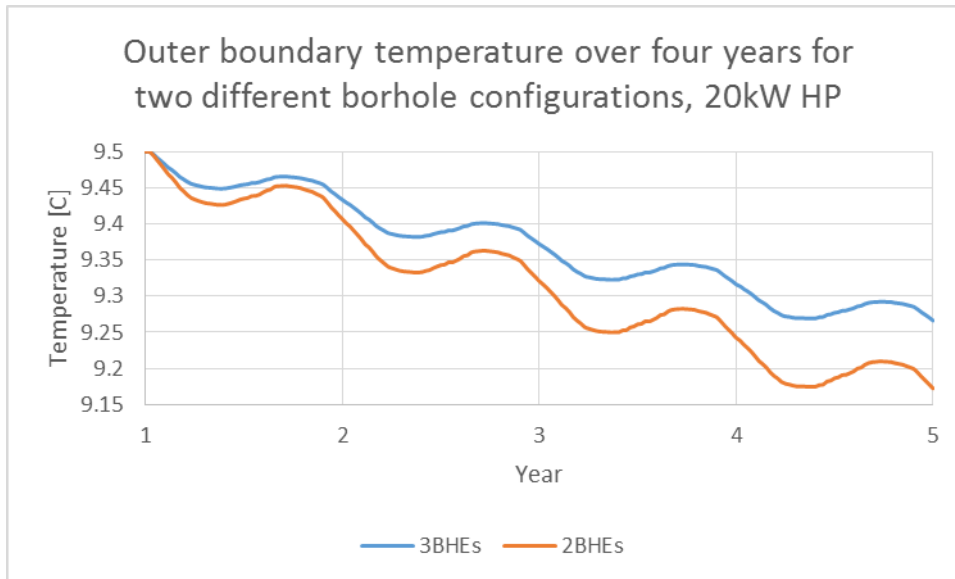
Figure 56 – Outer boundary ground temperature over years with 2 and 3 BHEs, 20kW HP system.

5.5.2 Ground conductivity

Different ground conditions have different thermal conductivity. When the conductivity of the ground increases, the ground temperature will decrease less for the same amount of heat extraction. Figure 57 shows that the ground conductivity has a significant influence on the total SPF and SPF of the heat pump. This shows that is important to get a good overview of the conditions in of the ground.
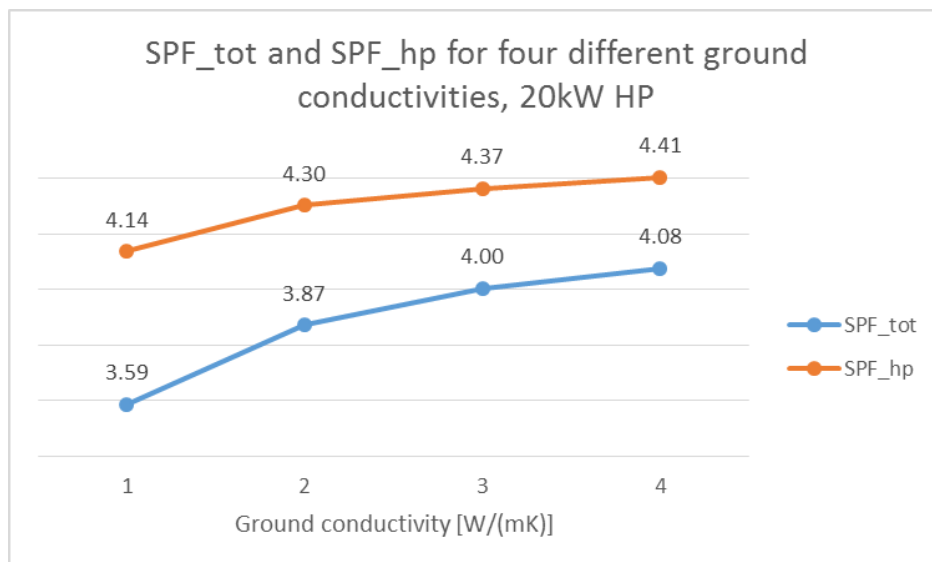
Figure 57 - SPF_tot and SPF_hp for the 20kW heat pump with four different ground conductivities.

5.5.3 Heat exchanger efficiencies

The efficiency of the heat exchangers has been idealized by setting the efficiency to a high value. For the simulations of section 5.1 to 5.4, the heat transfer coefficient of all the heat exchangers in the storage tanks are set to 2000 W/K (kg/s)/ (°C). The figure below shows the effects of changing the efficiency of the heat exchanger between the heat pump and the space heating tank over one heat pump cycle in the winter. When the ua-value is reduced, the required temperature difference between the tank and the circulating water in the heat exchanger will increase. Increasing outlet temperature from the condenser causes a lowered COP. The graph also the cures with an even higher ua values of 2000 W/K (kg/s)/ (°C). The figure indicates the importance of using a correct dimensioning of the heat exchangers. It also shows the potential of the tool to perform sensitivity analysis on specific system parameters.
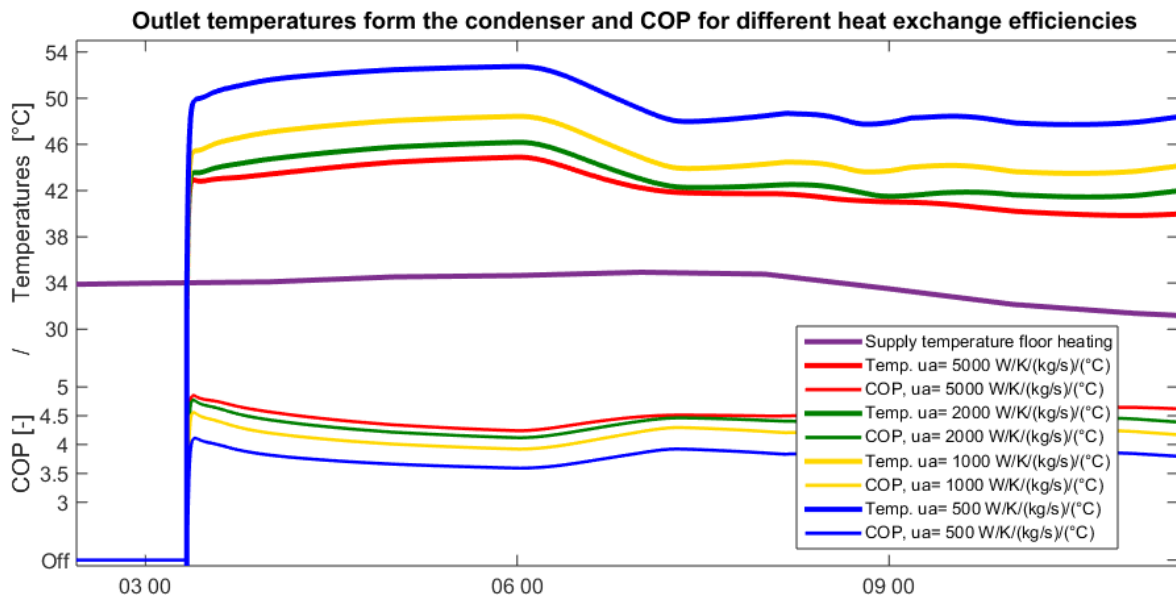
Figure 58 – Outlet temperature from the condenser and COP for different heat exchanger efficiencies.

5.5.4 Cost parameters

As already discussed in the master thesis of Murer, the annual costs and OCF are highly sensitive with changing cost parameters (Murer, 2015). In general, the OCF increase with increasing energy prices and decreases with increasing investment costs. Other parameters of interest for the annual costs are the life time of the different components and the interest rate. Figure 59 investigates what happens to the annual costs and OCF for the ZEB when it no longer assumed that the whole electricity generation of the PV panels can be sold for the same price

as power is imported. In the figure, annual costs are shown when it is assumed that the total energy generated PV panels over the year is sold for 75 % and 50 % of the purchased energy price. This causes both an increase in total annual costs and in OCF.
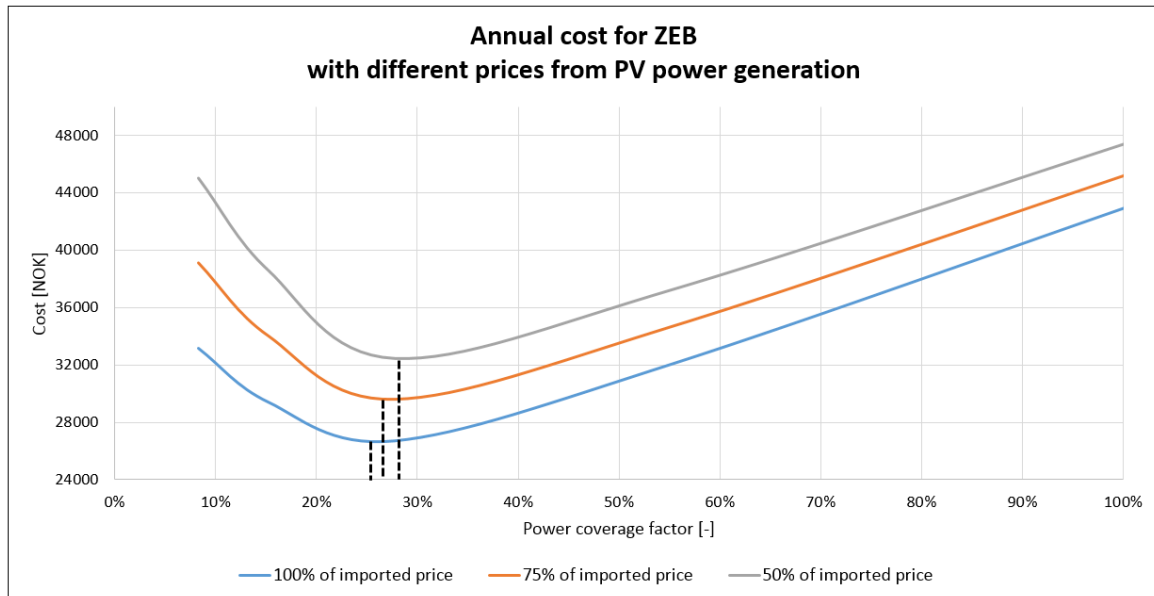
Figure 59 – Annual costs for ZEB with varying prices for power generation of the PV panels.

5.6 Evaluation of results

Due to the large decrease in DHW consumption compared to the previous version, it is natural to expect a decrease also in energy consumption, costs and CO_2 emissions. Murer also assumed a lower specific heat extraction rate of the boreholes for the cost analysis, that resulted in higher investment costs of boreholes. Comparing the lowest annual cost for the passive house with GSHP, electric heaters and a floor heating distribution system, the total cost is reduced by 46 % compared with the results of Murer. The OCF is also reduced from about 39 % to 26%. The SPF of the heat pump, with a nominal power of 20kW, for the same system combination is decreased 4.66 to 4.3. This reduction is likely to be caused by the very high number of boreholes used for simulation in the thesis of Murer (Murer, 2015).

5.7 Computation time

While the computation time have been varying throughout the semester, the final version uses around two to two and a half hours for a one year simulation. Running several systems in

parallel causes only a small increase in computation time. This is a dramatic reduction from the previous version of the tool, where a one-year simulation took about 20 hours (Murer, 2015). The reduction in computation time is a result of several changes, including removing unnecessary and time consuming system blocks, less time consuming ground source model and the use of discrete sample time several places in the model. This section will show some results on how computation time and results change as a result of changing the sample time of the control signals.

In the current simulation, a sample time of 600 seconds is used for all control signals. Monthly simulations have been performed to see the effects of varying the sample time. Both simulations in winter (heating mode) and summer (cooling mode) were conducted. The reference value for the results is the total electric consumption of the heat pump during the 30 days simulation period. Reduction in computation time and deviation in results are compared with inherited sample time the control signals. Simulations are performed with the 20kW heat pump system. Results for simulations over one moth in the winter are shown in table 11 and results over one month in the summer are shown in table 12.

Table 11 - Change in computation time and results for one month simulation during winter for four different sample times of control signals.

Sample time of control signals	Computation time	Relative reduction in computation time	Relative change in electric consumption
Inherited	607 sec	-	-
300 sec	420 sec	- 31 %	0.2 %
600 sec	381 sec	- 37 %	0.3 %
1200 sec	400 sec	- 34 %	2 %

Table 12 - Change in computation time and results for one month simulation during summer for four different sample times of control signals.

Sample time of control signals	Computation time	Relative reduction in computation time	Relative change in electric consumption
Inherited	1165 sec	-	-
300 sec	920 sec	- 21 %	2 %
600 sec	912 sec	- 22 %	1 %
1200 sec	881 sec	- 24 %	4 %

Table 11 and 12 shows that the computation time was significantly reduced by using a discrete sample time. Increasing the discrete sample time from 300 seconds to 1200 seconds had however only a small effect on the computation time. Only small deviations were found in the total energy consumption of the heat pump. Another interesting discovery from the two tables is that the computation time is significantly higher in the winter. With a sample time of 600 seconds for the control signals, the computation time is more than double during summer simulations. It was also found that the yearly simulation took longer time with smaller heat pump sizes. These two results indicates that the system work slowly during forced cooling mode.

6. Future work

Several aspects of the decision tool have been improved during this thesis. The system is however not yet sufficient to be a reliable tool for system design decisions. Several parts of system should be further improved. In addition to the development of the tool, it is also crucial to that the system is properly validated against real measurement data. The following table suggests approaches for future development of the tool.

Table 13 – List of possible future improvements of the tool.

Topic	Description
Valuation of data	For the tool be useful, it is vital that results from simulations are compared with real measurement data from relevant building heating systems. This should be one of the major areas of research before the tool can be finished. The choice of validation cases should be in accordance with the scope of the tool development which focuses on nZEB.
Heat pump	A variable speed heat pump model can be implemented into the tool by introducing coefficients for PLF into the Carnot heat pump block. If the variable speed heat pump was to be implemented to the tool, it will also be necessary to include an appropriate control strategy for the part load operation. As suggested in the master thesis of Murer, an alternative method is to connect the tool to a heat pump model of another simulation environment (e.g. Modelica) using a functional mock-up interface.
Air source	A reversible air source heat model has been implemented into the Carnot heat pump block by fellow student Simon Aldebert. The air source and ground source heat pump systems should be compared.
DHW system	It is not possible to use the heat pump for space heating / cooling and heating of the DHW tank in the current tool. The DHW system can be improved in several different ways. One possibility is to pre-heat the DHW tank using a desuperheater. Alternatively the DHW can be connected to a separate CO_2 heat pump, as it gives high COPs for DHW heating. Both of these methods will require a more advanced heat pump

	model than the one implemented in Carnot and the functional muck-up interface may therefore be used. A third alternative to ensure that the system is able to deliver the given space heating and cooling demand also when there is demand for DHW, is to heat up the DHW tank at periods when there are no space heating or cooling demand.
Cooling system	The cooling tank introduced in this thesis is modelled and controlled in the same way as the heat tanks. As it is not normal to use cooling tanks for cooling of buildings, a better way of accounting for the thermal mass of the building should be implemented.
Pressure drop	The choice made for this thesis is to neglect pressure drops in the system and set the pressure to a constant value of one bar for the whole hydraulic system. The electric consumption of the pumps are depending on the pressure drop in the pipes. It is assumed that the largest power consumption comes from the pump connected to the boreholes. The Carnot GSHE block does not include any pressure calculations. For the future development of the tool, the pressure drop and electric consumption of the pumps should be accounted for.
Distribution and emission system	The distribution and emission system have been highly simplified. The temperatures and mass flow rates are not included in the results from Simien. Ideally, these values should be calculated outside the simulation tool according to the boundary of the tool. It may be considered to couple the decision tool with a different building simulation program so that the distribution and emission system can be kept completely outside of the tool.
Graphical interface	The graphical interface has been made much more user friendly during this thesis. This can however be further improved. For the final version of the tool, the optimal will be to have one executable file that is able to run all the different system combinations. It will also be preferable to have all system parameters defined at one interface.
Computation time	Although the computation time has been dramatically reduced compared with the previous tool, the tool is still quite slow. By further

	looking into the different parts of the Simulink model, the overall computation time can be reduced.
Costs	The total energy costs and thereby the OCF factor are highly sensitive to energy and investment prices. It is therefore very important that these parameters are chosen correctly. The assumption of a fully linear relationship between investment cost and size of the heat pump and other components is also highly simplified and is something that can be further analysed.
PV	The assumption that the electric power produced by the PV panels can be sold for the same price as the imported electricity used by the building is highly simplified. It should be investigated the duration of power production from the PV panels through the year and also price at which it can be sold to the grid.
Alternative program	As suggested by supervisor Laurent Georges, a future version of the decision tool may be implemented in another simulation environment than Matlab/ Simulink. One reason is that the Matlab/ Simulink environment tends to give high computation time.

7. Conclusion

During the work of this thesis, several improvements in the decision tool have been implemented and a variety of simulations has been run, which shows the quality and the potential of the tool in different situations. Results shown from short-term simulations indicates that the system is working according to expectations. Another indication that the system is working properly, is small deviations between the building demands and delivered energy found in the results of simulations. The improvement of the ground source system has caused more realistic brine temperatures. This has also made it possible for a more extensive sensitivity analysis of the ground source design. The thesis shows that the tool has a potential for sensitivity analysis of a large number of the different parameters.

A lot of investigation has also been done on the computation time and the graphical interface. The computation time has been reduced so that it now takes about 2 hours for a one year simulation. With the new layout of the Simulink-files, it has become easier for the user to understand the functionality of the system. The reduced computation time and a more user friendly interface will be of good help for the further development of the tool.

Even though the tool has been significantly improved, there still exists weaknesses. Results from simulations during this thesis are associated with many uncertainties and should therefore mostly be seen as a proof of concept. One of the major tasks for the tool to become more useful and reliable, is the work of validation. It is suggested that in the further development of the tool, extensive work should be put into the validation of simulation data with real measurement data from relevant building system. With sufficient validation, in addition to new improvements of the simulation tool, it may become a powerful tool for both consulting and research purposes.

This thesis strengthen the believed that simulation tools will play a significant role in the future development of energy efficient heating and cooling systems of buildings. Hopefully, this master thesis will be a positive contribution in the important area of reducing energy consumption.

Bibliography

Carnot Version 6.0 beta. 2014. Extension to Simulink/Matlab. © Solar-Institut Jülich. Available for free at University of Applied Sciences Düsseldorf.

Filliard, B., Guiavarch, A. and Peuportier, B. (2009). *Performance evaluation of an air-to-air heat pump coupled with temperate air-sources integrated into a dwelling.* Paper. Glasgow UK: Performance Simulation Association conference 2009.

He, M. (2012). *Numerical Modelling of Geothermal Borehole Heat Exchanger Systems.* PhD Thesis. Leicester UK: Institute of Energy and Sustainable Development, De Montfort University.

Incropera, F. P., Bergman, T. L., Lavine, A. S. and DeWitt, D. P. (2006). *Fundamentals of Heat and Mass Transfer.* New Jersey USA: John Wiley & Sons Inc.

Karlsson, F. and Fahlèn, P. (2006). *Capacity-controlled ground source heat pumps in hydronic heating systems.* Report. Gøteborg Sweden: Swedish National Testing and Research Institute, Department of Energy, Chalmers University of Technology.

Magnussen, I. H., Spilde, D. and Killingland, M. (2011). *Energibruk - Energibruk i Fastlands-Norge.* (Energy use – Energy consumption in mainland Norway). Report number 9/2011. Oslo: Norges Vassdrags- og Energidirektorat.

Maldonado, E, (2013) Executive editor: *Concerted Action - Energy Performance of Buildings.* EU Report, electronic version. Porto: University of Porto on behalf of the Portuguese Energy Agency (AGENE)

Murer, T. (2015). *Analysis of change in design procedures for heat pump systems in nZEB.* Master thesis. Rapperswil Switzerland: MRU Environmental Engineering, University of Applied Science.

NS 3031:2014. (2014). *Beregninger av bygningers energiytelse – Metode og data.* (Calculation of energy performance of buildings – Method and data). Version 2014. Standard Norge.

Ochs, F. (2012). *CARNOT EWS model. Modelling for vertical ground heat exchanger*. Manual. Aachen Germany: Solar-Institut Jülich.

Ramstad, R. (2015). E-mail correspondence with the author.

Pérez-Lombarda, L., Ortizb, J. and Poutb, C. (2007). *A review on buildings energy consumption information.* Available at Elsevier.

Smedegård, O. (2012). *Modeling and Analysis of Heat Pumps for Zero Emission Buildings.* Master Thesis. NTNU Trondheim: Department of Energy and Process Engineering, Norwegian University of Science and Technology

Småland, L. (2013). *Analyse av forenklede vannbårne varmedistribusjonssystemer for større bygninger.* NTNU Master Thesis. Trondheim: Department of Energy and Process Engineering, Norwegian University of Science and Technology

Stene, J. (1997). *Grunnleggende varmepumpteknikk.* Trondheim: SINTEF Energiforskning.

Stene, J. (2014 A). *Components*. Presentation in the course TEP4260. Trondheim: Department of Energy and Process Engineering, Norwegian University of Science and Technology.

Stene, J. (2014 B). *Heat Sources*. Presentation in the course TEP4260. Trondheim: Department of Energy and Process Engineering, Norwegian University of Science and Technology.

Stene, J. (2014 C). *Thermodynamics*. Presentation in the course TEP4260. Trondheim: Department of Energy and Process Engineering, Norwegian University of Science and Technology.

Stene, J. and Smedegård, O. (2013). *Hensiktsmessige varme- og kjøleløsninger i bygninger*. (Adequate Heating and Cooling systems in Buildings). Written by COWI AS on behalf of Enova SF. Document number A.

Tobler Haustechnik AG (2012). *Planungsunterlagen – Sixmadun Sole-Wasser Wärmepumpen*.

Wemhöner, C. (2010). *Field monitoring. Results of field tests of heat pump systems in low energy houses*. Final report Annex 32 part 3 IEA HPP. Muttenz Switzerland: Institute of Energy in Building, University of Applied Sciences Northwestern Switzerland.

Ytterhus, M. (2014). *Modelling the ground during the early-phase design of heat pump systems in nZEB*. Project report. NTNU Trondheim: Department of Energy and Process Engineering, Norwegian University of Science and Technology.

Appendix 1 – Control signals

Table 14 Control signals.

Nr	Control signal	Turns on when	Turns off when	Additional constrains
1	ctr_FrC	Demand for cooling. AND Temperature in cooling tank* increase to 2 °C below supply temperature cooling.	Temperature in cooling tank decrease to 4 °C below supply temperature cooling.	Turned off when ctr_HP_DHW is turned on. Turned off when ctr_FoC is turned on.
2	ctr_FoC	Demand for cooling above 2kW. AND Temperature in cooling tank increase to same temperature as the supply temperature for cooling.	Temperature in cooling tank is cooled down to 2 °C below supply temperature cooling.	Turned off when ctr_HP_DHW is turned on.
3	ctr_HP_SH	Demand for space heating. AND Temperature in heating tank** decrease to less 4 °C above supply temperature.	Temperature in heating tank increase to 8 °C above supply temperature	Turned off when ctr_HP_DHW is turned on.
4	ctr_PL_SH	Demand for space heating. AND Temperature in heating tank decrease 1 °C above supply temperature	Temperature in heating tank increase to 5 °C above supply temperature.	
5	ctr_HP_DHW	DHW tank temperature decrease to 48 °C.	DHW tank temperature increase to 53 °C.	Set temperature increased by 10 °C one day of the week.
6	ctr_PL_DHW	DHW tank temperature decrease to 45 °C.	DHW tank temperature increase to 50 °C.	Set temperature increased by 10 °C one day of the week.
7	ctr_HP	ctr_HP_SH or ctr_HP_DHW or ctr_FoC is on		Heat pump turned off when output temperature of condenser is above 70 °C or inlet temperature to evaporator is below -5 °C.

*cooling tank measured one third from bottom.

**space heating and DHW tank measured at one third from top.

Appendix 2 – Data of the 20kW Heat Pump

Table 15 – Heating power data at different temperature levels for the 20kW heat pump (Murer, 2015).

Heating power [W]			
	Water outlet temperature [°C]		
Brine inlet temperature [°C]	**35**	**50**	**65**
- 5	18 500	18 010	17 610
15	32 650	32 230	31 430
25	40 550	40 250	39 300

Table 16 – Source power data at different temperature levels for the 20kW heat pump (Murer, 2015).

Source power [W]			
	Water outlet temperature [°C]		
Brine inlet temperature [°C]	**35**	**50**	**65**
- 5	13 790	11 630	8 830
15	27 450	25 330	22 130
25	35 100	33 070	29 700

Table 17 – Electric power data at different temperature levels for the 20kW heat pump (Murer, 2015).

Electric power [W]			
	Water outlet temperature [°C]		
Brine inlet temperature [°C]	**35**	**50**	**65**
- 5	4 710	6 380	8 780
15	5 200	6 900	9 300
25	5 450	7 180	9 600

The source matrix is based on the assumption of zero losses in the heat pump
(source power = heating power – electric power by the compressor).

Appendix 3 – System parameters

Sources:

A: idealized value based on simulation testing, assumptions by the author or from discussions with supervisors (or combination of these)

C: default value in Carnot

L: found in literature

M: kept same value as in previous version (Murer, 2015)

S: value found from Simien inputs

Table 18 – List of system parameters.

Description	Value	Unit	Source
Bio Boiler			
Heat loss coefficient	3	W/K	C
Volume of the boiler	0.02	m³	C
Relative power in 0..1	[0.25 1]	-	C
Temperature	[40 70]	°C	C
Efficiency data in 0..1	[0.73 0.73; 0.73 0.73]	-	M
Electric power	[20 120]	W	C
Number of nodes	1	-	C
Stoichiometric air demand	4.07		
Heat without/with condensation	[18 20] *1000	kJ/kg	M
Massfraction [H C O S N H2O]	[0.062 0.50 0.43 0.0005 0.003 0.0045]	-	M
Condensation temperature	47	°C	M
Building input			
Heated space area	2400	m^2	S
Annual DHW demand	5	$kWh/m^2/$ yr	L1
Annual space heating	14.7	$kWh/m^2/$ yr	S

Side iii

Annual space cooling demand	5	kWh/m^2/ yr	S
DOT winter	- 25	°C	S
DOT summer	30	°C	S
Ambient temperature in machinery rom	17	°C	A
Ground Source Heat Exchanger block			
Average annual outdoor temperature	6	°C	S
Temperature gradient	0.025	K/m	C
Thermal conductivity in the ground	2.0	W/m	C
Heat capacity of the ground	800	J/kg/K	C
Density of the ground	2500	kg/m^3	C
Thermal conductivity in the filling	2.0	W/m	L2
Heat capacity of the filling	1000	J/kg/K	C
Density of the filling	2000	kg/m^3	C
Length of each probe	200	m	L3
Probe distance	20	m	L3
Diameter of tube	0.032	m	C
Diameter of drilled hole	0.32	m	C
No. of nodes in axial direction	10	-	C
No. of nodes in radial direction	10	-	C
Heat Exchanger between the Ground and the hot side of the Heat Pump			
Type of flow(0=parallel,0.5 =cross, 1=counter)	1	-	M
Constant heat transfer ua0	5000	W/m	A
[mdot_nom_hot (>0) , ua_exp_hot (>=0)]	[0.04 0]	[kg/s, -]	C
[mdot_nom_cold (>0) , ua_exp_cold (>=0)]	[0.04 0]	[kg/s, -]	C
Heat losses to ambient	3	W/K	C
Capacity	10e3	J/K	C
Heat Exchangers inside Tanks			

uac: heat transfer coefficient	2000	W/K/(kg/s)/(°C)	A
uam: mass flow dependent heat transfer	0.2	-	C
uat: temperature difference dependent heat transfer	0.5	-	C
Heat Exchangers from Heat Pump to Heating Tanks			
Relative height of inlet	0.5	-	A
Relative height of outlet	0	-	A
Heat Exchangers from Peak Load Units to Heating Tanks			
Relative height of inlet	0.8	-	A
Relative height of outlet	0.5	-	A
Heat Exchanger from Heat Pump to Cooling Tank			
Relative height of inlet	0	-	A
Relative height of outlet	1	-	A
Heat Pump			
Thermal capacity hot loop	80000	J/K	C
Thermal capacity cold loop	50000	J/K	C
Heat loss coefficient	7	W/K	C
Tanks			
Heat loss coefficient cylinder wall	0.5	W/(m²K)	C
Heat loss coefficient bottom	0.5	W/(m²K)	C
Heat loss coefficient top cover	0.5	W/(m²K)	C
Effective (wall and fluid) vertical conductivity	0.05	W/(m*K)	C
Number of nodes	10	-	C
Number of measurement points	10	-	C

L1: (NS 3031, 2014).

L2: (Stene, 2014).

L3: (Ochs, 2012).

Appendix 4 – Cost and emission parameters

Table 19 - List of cost emission parameters.

Description	Value	Unit	Source
Capital cost			
Interest rate	%	7	M
Emissions			
Emissions of electricity	390	kgCO$_2$/MWh	M
Emissions of bio fuel	42	kgCO$_2$/MWh	M
Energy cost			
Electricity	0.8	NOK/kWh	M
Bio fuel	0.74	NOK/kWh	M
Investment cost and lift time			
Heat pump, investment cost	6000	NOK/kW	M
Heat pump, lift time	18	years	M
BHEs, investment cost	500	NOK/m	M
BHEs, lift time	18	years	M
Electric heaters, investment cost	500	NOK/kW	M
Electric heaters, lift time	15	years	M
Floor heating/ cooling, investment cost	400	NOK/m^2	M
Floor heating/ cooling, life time	40	years	M
Tanks, investment cost	40 000	NOK	A
Tanks, lifetime	20	years	M
PV, investment cost	25 000	NOK/kWp	M
PV, lifetime	20	years	M
Maintenance and running costs			
Maintenance cost heat pump	0.02	NOK/InvCost	M
Maintenance cost electric heaters	0.005	NOK/InvCost	M
Maintenance cost bio heater	0.02	NOK/InvCost	M
Maintenance cost PV	55	NOK/kWp	M

Appendix 5 – g-functions

Table 20 – g-functions in the new Carnot EWS block.

Nr	Number of boreholes	Configuration	New*
1	1	1 BHE	No
2	2	2 BHEs, B/H = 0.1	No
3	2	2 BHEs, B/H = 0.05	No
4	4	2x2 BHEs, B/H = 0.1	Yes
5	4	2x2 BHEs, B/H = 0.05	Yes
6	8	8 BHEs, B/H = 0.1	Yes
7	8	8 BHEs, B/H = 0.05	Yes
8	16	2x8 BHEs, B/H = 0.1	Yes
9	16	2x8 BHEs, B/H = 0.05	Yes
10	18	3x6 BHEs, B/H = 0.1	No
11	50	5x10 BHEs, B/H = 0.05	No

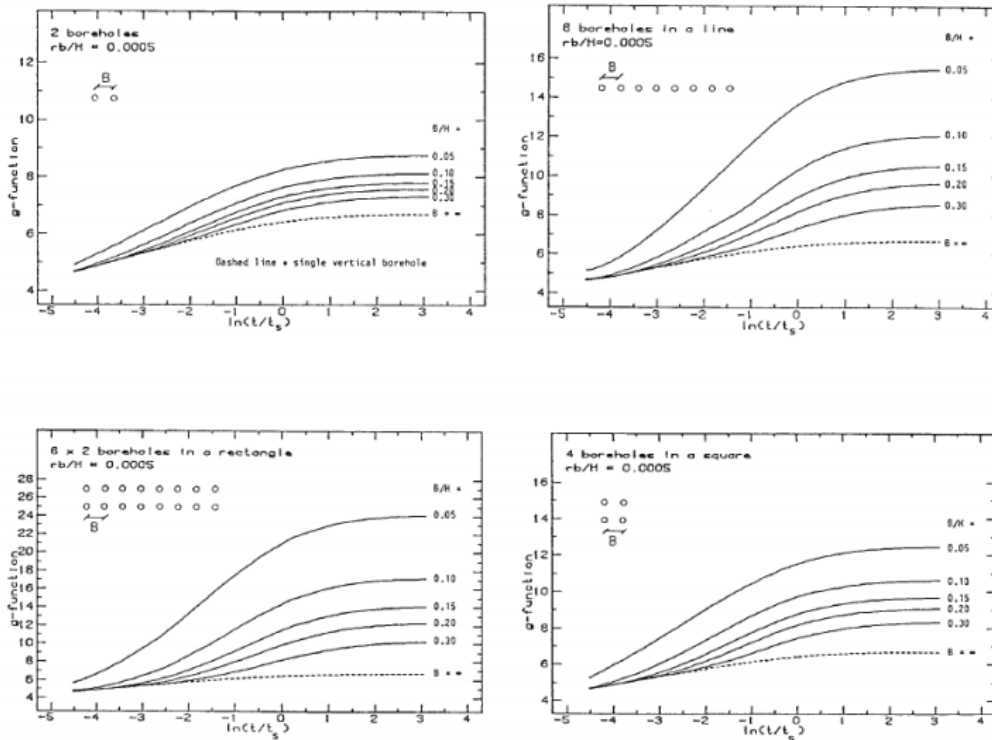* Six new g-functions have been implemented during this master thesis.

Figure 60 – Eskilson g-functions for four different configurations (He, 2012).